Isotopic Studies of Ice Core Nitrate and Atmospheric Nitrogen Oxides in Polar Regions

Julia C. Jarvis

A dissertation
submitted in partial fulfillment of the
requirements for the degree of

Doctor of Philosophy

University of Washington

2008

Program Authorized to Offer Degree:
Department of Earth and Space Sciences

University of Washington
Graduate School

This is to certify that I have examined this copy of a doctoral dissertation by

Julia C. Jarvis

and have found that it is complete and satisfactory in all respects,
and that any and all revisions required by the final
examining committee have been made.

Chair of the Supervisory Committee:

_____
Eric J. Steig

Reading Committee:

_____
Eric J. Steig

_____
Lyatt Jaeglé

_____
Becky Alexander Suess

Date: _____

In presenting this dissertation in partial fulfillment of the requirements for the doctoral degree at the University of Washington, I agree that the Library shall make its copies freely available for inspection. I further agree that extensive copying of the dissertation is allowable only for scholarly purposes, consistent with “fair use” as prescribed in the U.S. Copyright Law. Requests for copying or reproduction of this dissertation may be referred to ProQuest Information and Learning, 300 North Zeeb Road, Ann Arbor, MI 48106-1346, 1-800-521-0600, to whom the author has granted “the right to reproduce and sell (a) copies of the manuscript in microform and/or (b) printed copies of the manuscript made from microform.”

Signature _____

Date _____

University of Washington

Abstract

Isotopic Studies of Ice Core Nitrate and Atmospheric Nitrogen Oxides in Polar Regions

Julia C. Jarvis

Chair of the Supervisory Committee:
Associate Professor Eric J. Steig
Department of Earth and Space Sciences

Atmospheric nitrogen oxides regulate concentrations of natural and anthropogenic trace gases through interactions with tropospheric oxidants. Understanding past and present changes in atmospheric NO_x ($NO + NO_2$) is possible through measurements of nitrate (NO_3^- or nitric acid, HNO_3) in polar ice cores. This dissertation is comprised of four studies which contribute towards understanding the controls on nitrate isotopes preserved in polar ice.

Box modeling of local photochemistry at Summit, Greenland show that the $\delta^{15}N$ and $\delta^{18}O$ of HNO_3 are influenced by several factors, including isotope fractionation associated with NO-NO_2 cycling and seasonal changes in HNO_3 formation chemistry and in NO_x sources. A technique for the capture of atmospheric NO_2 in remote regions for later isotopic analysis is described. First measurements of the $\delta^{15}N$ of NO_2 at Summit show little difference with the $\delta^{15}N$ of HNO_3, indicating that isotope fractionation associated with the oxidation of NO_2 to HNO_3 is small.

The role of post-depositional processing on nitrate isotopes in the Summit snowpack is explored through isotopic measurements of gas-phase HNO_3, surface snow nitrate, and snowpit nitrate. These measurements indicate that NO_x emitted from the snow following nitrate photolysis quickly recombines with local oxidants to produce HNO_3 prior to recycling back to the snow. This photolytic loss and recycling has a small influence on nitrate isotopes preserved in ice at Summit.

Measurements of nitrate isotopes in an ice core from South Pole, Antarctica show evidence of active post-depositional recycling and loss of nitrate. A large near-surface trend in the $\delta^{15}N$ of nitrate is attributed to post-depositional losses, while the $\delta^{18}O$ of nitrate indicates that oxygen isotope fractionation associated with post-depositional loss is overwhelmed by the influence of local oxidants on nitrate recycling.

The concentration and $\delta^{15}N$ of nitrate in an ice core from Summit, Greenland exhibit trends which are strongly correlated with recent changes in global NO_x emissions. The Greenland $\delta^{15}N$ record indicates that the $\delta^{15}N$ of recent NO_x emissions must be isotopically light, which is consistent with the combustion of fossil fuels. This shows that the Greenland $\delta^{15}N$ record preserves changes in source emissions of atmospheric NO_x.

TABLE OF CONTENTS

LIST OF FIGURES

LIST OF TABLES

ACKNOWLEDGEMENTS

It's difficult to put into words my appreciation for the many people who have supported me and this work.

My advisor, Eric Steig, has been an unflagging source of encouragement for this project and my role in it. I feel fortunate to have an advisor and mentor who exudes both a boundless enthusiasm for science and an obvious devotion to his family. I will always be grateful to Eric for his support of me as a person, not just as a graduate student. This couldn't be more clearly demonstrated than by his support and understanding of my decision to finish my Ph.D. remotely.

Meredith Hastings has been a colleague, advisor, mentor, and good friend, all rolled into one. I am indebted to her for many great scientific discussions, her time spent reading countless drafts of chapters and papers, her willingness to help tackle a problem with Brave Irene, and, above all, her encouragement of me every step of the way.

The nature of this work, and of much scientific work today, requires the help of many people. Lyatt Jaeglé, Becky Alexander, Ed Waddington, and Shelley Kunasek have offered valuable input which has greatly benefited this work. Peter Neff, Dan Gleason, Joe Flaherty, Chris Yarnes, and Andy Schauer are undeniable superstars for their help with running samples, growing bacteria, cutting ice, washing bottles, and fixing machines. The collection of so many field samples would not have been possible without Kat Huybers, Joe Flaherty, Mike Town, Shelley Kunasek, Aaron Donohoe, Lora Koenig, Justin Wettstein, Dan Gleason, Peter Neff, and the Summit science techs. The good folks at Veco Polar Resources and the 109th ANG got all of us (and so many breakable mist chambers and bubblers!) safely to Greenland and back, many times over.

I owe volumes of thanks to a tow-truck driving, James Dean-looking fellow from Fox Towing in Ann Arbor, who unlocked a returned moving truck so I could retrieve my laptop full of data, which I had so carefully hidden away for safekeeping that it was safe even from me.

There are many people who have enriched and inspired my six years in graduate school. Claire Todd provided the soundtrack to many a day working in lab and writing at home. My most enjoyable two months of grad school are thanks to the Summit 2006 Phase III crew (Andrea, Dan, Kat, Kathy, Paul, and Jake), who know how to throw a great dance party. My family –the Jarvises, Muellers, and Burton-Robinson-Trouts– are special, wonderful, supportive people who I love dearly. My husband, Andrew, has patiently listened to endless discussions of failing bacteria and a malfunctioning mass spectrometer, encouraged me across thousands of miles, and has fed my mind, my soul, and my stomach. Andrew and our dog, Olive, never cease to remind me of the important things in life: love, laughter, and family.

Finally, I'd like to offer heartfelt thanks to my fellow graduate students, in particular Summer Rupper, Joe MacGregor, Michelle Koutnik, Laura Certain, Kat Huybers, Claire Todd, and Lora Koenig, as well as Gerard Roe and Liila Woods, who have been bottomless sources of friendship, support, laughter, boosts in confidence, and sage advice. I can't imagine what graduate school would have been like without them. They are true friends.

Chapter 1

Introduction

1.1. Motivation and Background

Concentrations of atmospheric NO_x ($NO + NO_2$) have increased significantly in the last 50-100 years (e.g., Galloway et al., 2003). This change has an impact on the biogeochemistry of ecosystems through an increase in atmospheric nitrogen deposition (Wolfe et al., 2006). Furthermore, NO_x is closely tied to cycles of OH and ozone (O_3), which in turn regulate atmospheric concentrations of greenhouse gases such as methane. Understanding past and present changes in NO_x concentration thus plays a key role in predicting future atmospheric changes and in determining mitigation strategies.

One of our best resources for exploring and examining recent changes in the atmosphere is polar ice sheets, which preserve atmospheric particulates and gases deposited to the ice surface and trapped in air bubbles within the ice. In particular, ice cores from Greenland and Antarctica provide us with records of past changes in gas-phase nitric acid (HNO_3) and particulate nitrate ($p\text{-}NO_3^-$), which are major sinks of atmospheric NO_x. Previous studies have found that the concentration of nitrate in Greenland ice sharply increases around the mid-20^{th} century (e.g., Mayewski et al., 1990), which has been attributed to increasing anthropogenic emissions of NO_x.

The interpretation of these records is not straightforward, as nitrate in surface snow undergoes post-depositional change before it is fully buried. Photolysis and volatilization of nitrate in the snowpack results in emissions of nitrogen oxides from the snow, which means that the amount of nitrate preserved in ice may not directly reflect atmospheric concentrations of NO_x. However, the isotopes of nitrate ($^{15}N/^{14}N$ and $^{18}O/^{16}O$) are influenced by these changes, which allow us to assess the degree to which post-depositional loss and recycling has altered records of ice nitrate.

This thesis seeks to examine and quantify the controls on nitrate isotopes in polar ice, which will aid in our interpretation of past changes in ice nitrate and contribute to our understanding of present and future changes in atmospheric NO_x.

1.1.1. Nitrate in Polar Ice

The deposition of nitric acid and particulate nitrate is a major sink for atmospheric nitrogen oxides such as NO and NO_2. NO and NO_2 cycle quickly in the atmosphere in the presence of sunlight and O_3 (Figure 1.1),

$$NO + O_3 \rightarrow NO_2 + O_2 \qquad (R1.1)$$

$$NO_2 + h\nu \rightarrow NO + O(^3P) \qquad (R1.2)$$

$$O(^3P) + O_2 + M \rightarrow O_3 + M \qquad (R1.3)$$

where M represents an unreactive third body. In addition to oxidation via O_3 (*R1.1*), NO can also be oxidized via HO_2 (*R1.4*) and RO_2 (*R1.5*), where R represents a hydrocarbon chain:

$$NO + HO_2 \rightarrow NO_2 + OH \qquad (R1.4)$$

$$NO + RO_2 \rightarrow NO_2 + RO \qquad (R1.5)$$

During the day, NO_2 is primarily oxidized by OH to form HNO_3:

$$NO_2 + OH \rightarrow HNO_3 \qquad (R1.6)$$

At night, NO_2 reacts with O_3 to form N_2O_5, followed by hydrolysis to HNO_3:

$$NO_2 + O_3 \rightarrow NO_3 + O_2 \qquad (R1.7)$$

$$NO_3 + NO_2 + M \leftrightarrow N_2O_5 + M \qquad (R1.8)$$

$$N_2O_5 + H_2O_{(surface,\ aerosol)} \rightarrow 2HNO_3 \qquad (R1.9)$$

Nitric acid can also be produced through reaction of NO_3 with dimethylsulfide (DMS) or hydrocarbons (HC):

$$NO_3 + DMS,\ HC \rightarrow HNO_3 + products \qquad (R1.10)$$

During the polar winter, the production of HNO_3 proceeds primarily via the nighttime reaction mechanism, while HNO_3 production during summer follows the daytime pathway. While the lifetime of NO_x in the troposphere is on the order of days, long-

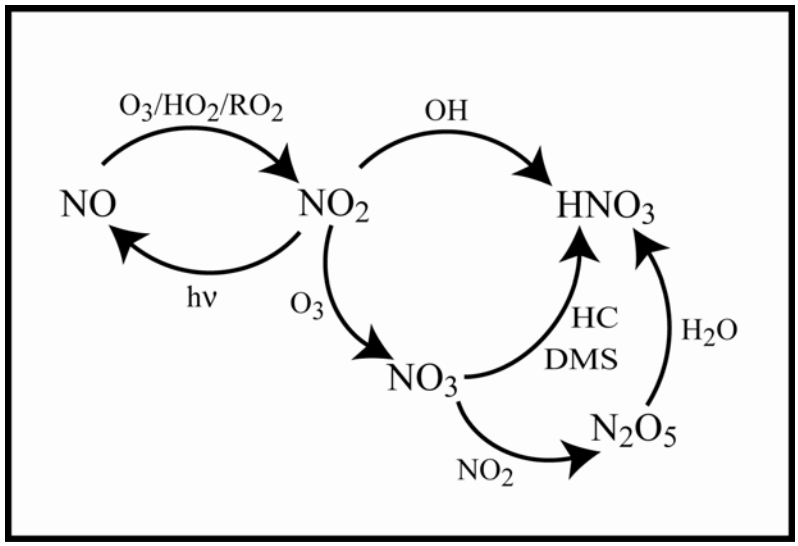

Figure 1.1. A simple schematic of NO_x and HNO_3 cycling in the atmosphere.

range transport of NO_x is possible through the formation of organic nitrates, such as peroxyacetyl nitrate (PAN). These organic nitrates form through the reaction of NO_2 with volatile organic compounds. Following the thermal decomposition of PAN, which produces NO_2, transported nitrogen oxides form HNO_3 via *R1.6-R1.10*.

After deposition to the surface of ice sheets through snow, fog, or dry deposition, snow nitrate is influenced by post-depositional changes. The photolysis of nitrate from the top tens of centimeters of surface snow can lead to emissions of NO_x from the snow. Nitrate can also evaporate or sublimate from the surface of snow crystals and be wind swept from the snowpack. Once released from the snowpack, these nitrogen oxides either are transported to other locations or are redeposited to the snow as nitric acid following reaction with local oxidants.

1.1.2. Nitrate Isotopes

The $^{15}N/^{14}N$ and $^{18}O/^{16}O$ isotope ratios of atmospheric nitric acid contain information regarding the chemical and source history of NO_x. These isotope ratios are presented in delta (δ) notation, $\delta = (R_{sample} / R_{standard} - 1) * 1000‰$, where $R = {}^{15}N/{}^{14}N$ or $^{18}O/^{16}O$. Previous work has suggested that the $\delta^{18}O$ of nitrate is influenced by the $\delta^{18}O$ of oxidants involved in the chemical formation of HNO_3 (*R6-R10*) (e.g., Hastings et al., 2003; Michalski et al., 2003). Additional studies have suggested that the $\delta^{15}N$ of nitrate is influenced by the $\delta^{15}N$ of precursor NO_x, which has both anthropogenic and natural sources to the atmosphere (Elliott et al., 2007; Heaton et al., 2004; Hastings et al., 2003; Yeatman et al., 2001; Russell et al., 1998; Freyer, 1991; Heaton, 1990). Anthropogenic sources include fossil fuel combustion, biomass burning, and fertilizer use, while natural sources of NO_x include lightning, stratospheric injection, and natural biogenic soil emissions.

1.2. Dissertation Goals and Organization

The goal of this dissertation is to examine and quantify the controls on nitrate isotopes preserved in polar ice. Specifically, this work aims to (1) model the impact of local photochemistry on isotopes of atmospheric HNO_3 at Summit, Greenland, (2) analyze the air-to-snow transfer of HNO_3 at Summit, (3) develop a technique to capture and measure the isotopes of atmospheric NO_2 in remote regions, and (4) examine the influence of post-depositional processing and NO_x source emissions on nitrate isotopes in polar ice from Greenland and Antarctica.

Several chapters in this dissertation are written as manuscripts, and therefore some of the introductory information is duplicated. Chapter 2 has been submitted to *Geophysical Research Letters.* Chapters 3 and 5 are in preparation for submission to the *Journal of Geophysical Research*.

1.3. Synopsis

This dissertation explores the local air chemistry and air-to-snow transfer of nitrogen oxides in Greenland to assist in the interpretation of ice nitrate records from Greenland and Antarctica. In Chapter 2, a framework is developed for discussing local air chemistry at Summit, Greenland. A box model approach is used to understand how seasonal changes in oxidant concentrations and the isotopic fractionation associated with NO-NO_2 cycling lead to changes in the isotopes of HNO_3 deposited to snow. The air-to-snow transfer of HNO_3 is explored in Chapter 3, which describes isotopic measurements of gas-phase HNO_3 and snow nitrate collected at Summit during 2005-07. Chapter 4 details a technique developed to capture and analyze atmospheric NO_2 in remote regions. First measurements of the $\delta^{15}N$ of NO_2 collected at Summit are presented and discussed in the context of the gas-phase HNO_3 measurements from Chapter 3. These studies culminate in Chapter 5, which is an analysis of long-term records of nitrate isotopes in polar ice from Summit, Greenland and South Pole, Antarctica. Differences in the magnitude of the trends in $\delta^{15}N$ and $\delta^{18}O$ of nitrate from

these locations are discussed in light of the very different depositional environments at Summit and South Pole and with regard to the influence of increasing anthropogenic NO_x emissions. Finally, a summary of the findings of this dissertation and suggestions for future work are presented in Chapter 6.

Chapter 2

The Influence of Local Photochemistry on Isotopes of Nitrate in Greenland Snow

[Jarvis, J.C., E.J. Steig, M.G. Hastings, S.A. Kunasek, The influence of local photochemistry on isotopes of nitrate in Greenland snow, submitted to *Geophysical Research Letters*, 2008]

2.1. Summary

To explore the seasonality in $\delta^{15}N$ and $\delta^{18}O$ of nitrate in Greenland snow, we describe a simple box model of local photochemistry. Isotope ratios of HNO_3 are controlled by the nitrogen isotope fractionation between NO and NO_2, the ratio of NO_2 to NO, and seasonal variations in HNO_3 production. We find that the observed seasonal range in $\delta^{15}N$ requires either a large net fractionation (~70‰) associated with NO_x cycling or a significant seasonal change in the $\delta^{15}N$ of NO_x sources. The observed range in $\delta^{18}O$ of nitrate is smaller than that calculated from HNO_3 production pathways, suggesting that seasonal transport is also required to explain the seasonality in nitrate $\delta^{18}O$. Additional influences, such as post-depositional processing of nitrate, fractionations associated with NO_x oxidation, and halogen chemistry at Summit, may also impact nitrate isotopes but are not yet quantified.

2.2. Introduction

Reactive nitrogen oxides (primarily $NO_x = NO + NO_2$) play a fundamental role in tropospheric photochemistry. Through interactions with tropospheric oxidants, these compounds affect the lifetimes of volatile organic compounds, methane, and other natural and anthropogenic trace gases. Because the dominant sink for NO_x is the deposition of nitric acid (HNO_3 or nitrate, NO_3^-), there has been considerable interest in

using measurements of nitrate concentration in polar ice cores to examine the past variability of atmospheric NO_x. However, interpretation of ice core nitrate is complicated by various processes, including post-depositional losses of nitrate by photolysis and evaporation (Dominé and Shepson, 2002). Measurements of the isotope ratios of nitrate ($^{15}N/^{14}N$ and $^{18}O/^{16}O$) have the potential to constrain the relationship between ice core nitrate and atmospheric NO_x. Recent measurements show a strong seasonality in $\delta^{15}N$ and $\delta^{18}O$ of nitrate in snowpits at Summit, Greenland (Hastings et al., 2004), which, to date, have been explained only qualitatively.

Seasonal variations in the isotopes of nitrate and its precursors have also been observed in other regions. The seasonality in $\delta^{15}N$ has been attributed either to variations in the source of NO_x to a region (e.g., soil emissions, fossil fuel combustion) or to variations in chemical processes prior to the formation of nitrate (e.g., Elliott et al., 2007; Hastings et al., 2003; Yeatman et al., 2001; Freyer, 1991; Heaton, 1987). The isotopic fractionation between NO and NO_2 and seasonal variations in the ratio of NO_x to O_3 have also been proposed as explanations for seasonality in $\delta^{15}N$ of atmospheric NO_2 and particulate and rain nitrate sampled in urban Germany (Freyer et al., 1993; Freyer, 1991). Seasonal variations in $\delta^{18}O$ of nitrate have been primarily attributed to seasonal variations in oxidation chemistry preceding nitrate formation (Hastings et al., 2003; Michalski et al., 2003).

The seasonality in $\delta^{15}N$ and $\delta^{18}O$ and its implications for the interpretation of the ice core record of nitrate motivate the development of a quantitative understanding of controls on the isotopic variability of nitrate and NO_x in polar regions. We use a simple photochemical box model to evaluate the impact of local photochemistry on $\delta^{15}N$ and $\delta^{18}O$ of HNO_3 and we compare our model predictions to observations of nitrate isotopes in Greenland snow. While complete characterization of the isotopes of nitrate precursor species will eventually be necessary, such measurements are extremely challenging. Our model represents a first step using the limited information currently available.

2.3. Model Development

2.3.1. Nitrate Chemistry in Polar Regions

Atmospheric NO and NO_2 cycle rapidly in the presence of O_3 and sunlight (where *M* represents an unreactive third body):

$$NO + O_3 \longrightarrow NO_2 + O_2 \qquad (R2.1)$$

$$NO_2 + h\nu \longrightarrow NO + O(^3P) \qquad (R2.2)$$

$$O(^3P) + O_2 \xrightarrow{M} O_3 \qquad (R2.3)$$

During the polar summer, HNO_3 formation primarily follows a "daytime" reaction:

$$NO_2 + OH \xrightarrow{M} HNO_3 \qquad (R2.4)$$

During the polar winter, HNO_3 formation follows "nighttime" pathways through N_2O_5, dimethylsulfide (DMS) or hydrocarbons (HC):

$$NO_2 + O_3 \rightarrow NO_3 + O_2 \qquad (R2.5)$$

$$NO_3 + NO_2 \xleftrightarrow{M} N_2O_5 \xrightarrow{H_2O} 2HNO_3 \qquad (R2.6)$$

$$NO_3 + DMS, HC \rightarrow HNO_3 + products \qquad (R2.7)$$

We focus on these seasonal differences in local HNO_3 production, which we expect will influence the seasonality of $\delta^{18}O$ of atmospheric HNO_3 because of large differences in $\delta^{18}O$ of the various reactants. We additionally explore the influence of the fractionation between NO and NO_2 on the range in $\delta^{15}N$ of atmospheric HNO_3.

The flux of HNO_3 through each pathway can be determined from known reaction rates and atmospheric concentrations of NO, NO_2, O_3, and OH. Because year-round measurements of these compounds at Summit are unavailable, we utilize monthly mean concentrations from GEOS-Chem, a global chemistry and transport model that uses assimilated meteorological observations (e.g., Bey et al., 2001; http://www.as.harvard.edu/ctm/geos/index.html). The GEOS-Chem mean summertime concentrations of NO and NO_2, shown in Table 2.1, are within the large ranges

Table 2.1. Box model input concentrations obtained from the GEOS-Chem model for Summit, Greenland. Values represent monthly averages for 2001.

Month	**NO** (pptv)	**NO_2** (pptv)	**O_3** (ppbv)	**OH** (molecules cm^{-3})
January	<<0.1	15.6	28.8	8.2×10^{-2}
February	0.4	25.4	31.7	5.2×10^{-3}
March	1	6.9	36.7	4.3×10^{-4}
April	2.3	6.3	40.7	2.2×10^{-5}
May	4.2	6.7	41.3	5.9×10^{-5}
June	5.5	6.5	38.4	1.2×10^{-6}
July	4.8	6.4	33.3	1.1×10^{-6}
August	4.1	8.4	33.7	7.0×10^{-5}
September	1.5	6.9	29.4	1.6×10^{-5}
October	0.7	9.2	33.1	3.0×10^{-4}
November	<<0.1	8.1	32.4	9.8×10^{-2}
December	<<0.1	33.5	30.0	4.3×10^{-2}

observed at Summit (0-60 pptv; see Yang et al., 2002). O_3 concentrations are 20-54% lower than year-round surface O_3 measurements at Summit, which are typically between ~45 and 60 pbbv (www.cmdl.noaa.gov). The GEOS-Chem OH concentrations are a factor of four to six lower than the monthly averages of 1 x 10^6 molecules cm^{-3} in April and ~4-6 x 10^6 molecules cm^{-3} in June and July predicted by measurement and modeling studies at Summit (Sjostedt et al., 2007; Yang et al., 2002; Zhou et al., 2001). The implications of these differences are discussed in Section 2.5.

The output from our simple box model represents atmospheric HNO_3 isotopes prior to deposition to the snow surface. While it is well known that post-depositional photolysis of nitrate leads to the emission of nitrogen oxides from snow surfaces (e.g., Dibb et al., 2002; Honrath et al., 2002), existing evidence suggests that this does not play a significant role in determining the final isotopic ratios in HNO_3 in snow, if snow accumulation rates are sufficiently high (Grannas et al., 2007). In particular, Hastings et al. (2004) found no evidence of significant post-depositional losses at Summit based on snow samples collected six months apart. Thus we do not include post-depositional loss processes in our model.

Isotopic fractionations associated with HNO_3 production from NO_y species (NO_y = total reactive nitrogen = NO_x + PAN (peroxyacetyl nitrate) + HNO_3 + N_2O_5 + particulate nitrate, etc.) are not yet quantified, requiring us to make several assumptions. We assume that the deposition of HNO_3 does not influence the isotopic composition of NO_y, because HNO_3 is a small component of the overall NO_y budget at Summit (e.g., Munger et al., 1999). Measurements and model simulations suggest that the NO_y budget at Summit is dominated by PAN, which is transported to the Arctic from northern midlatitudes and thermally decomposes to NO_2 (Ford et al., 2002; Munger et al., 1999; Wang et al., 1998). While PAN is known to be a major source of NO_x to the Arctic troposphere and is seasonally variable (Moxim et al., 1996 and Bottenheim et al., 1993 and references therein), any fractionation associated with PAN decomposition is currently unknown. We assume that NO_x at Summit is continually replenished by the NO_y reservoir, and that there is no significant fractionation between NO_x and NO_y.

2.3.2. $\delta^{15}N$

Our $\delta^{15}N$ model focuses on the isotope fractionation factor (α) associated with NO-NO_2 cycling:

$$\alpha = \frac{\left[^{15}NO_2\right] / \left[^{14}NO_2\right]}{\left[^{15}NO\right] / \left[^{14}NO\right]} \qquad (2.1)$$

Mass balance requires that

$$[^{15}NO_x] = [^{15}NO_2] + [^{15}NO] \text{ and } [^{14}NO_x] = [^{14}NO_2] + [^{14}NO]. \qquad (2.2)$$

Combining (2.1) and (2.2), and approximating the total N as ^{14}N due to the low natural abundance of ^{15}N (~0.4%), we obtain:

$$\left[^{15}NO_2\right] = \left[^{15}NO_x\right] - \frac{\left[^{15}NO_x\right]}{1 + \alpha\left(\left[NO_2\right] / \left[NO\right]\right)} \qquad (2.3)$$

Equation 2.3 predicts a linear inverse relationship between the ratio of NO_2 to NO and $\delta^{15}N$-NO_2. Since the lifetime of NO_2 against conversion to gas-phase HNO_3 is relatively short, we expect that $\delta^{15}N$-HNO_3 should closely follow $\delta^{15}N$-NO_2. We thus use Equation 2.3 to model $\delta^{15}N$ of HNO_3 as a function of $\delta^{15}N$-NO_x, α, and the ratio of NO_2 to NO.

In the model, α is varied to explore the extent to which observations can be explained by the NO-NO_2 fractionation alone, as Freyer et al. (1993) argued was the case for the urban environment. Although conditions at Summit are very different, we emphasize that α is an effective fractionation that combines photochemical and thermodynamic effects. While kinetic isotope effects during photochemical NO-NO_2 cycling will likely minimize isotopic differences between the two species, there may nevertheless be an effective α in this situation that is different from 1.00.

We set $\delta^{15}N$ of NO_x to be a constant value, which allows us to isolate the effect of local photochemistry on the seasonality in HNO_3 isotopes. Potential isotope effects associated with long range transport, such as the production and destruction of PAN, are ignored as they have not yet been characterized. Should the seasonal variability of PAN

decomposition or changes in other NO_x sources significantly influence the isotopic composition of NO_x, this will appear as a mismatch between modeled and observed $\delta^{15}N$-HNO_3.

2.3.3. $\delta^{18}O$

Unlike $\delta^{15}N$, variations in $\delta^{18}O$ of HNO_3 are not expected to directly track those in NO_2, but will depend instead on the $\delta^{18}O$ of oxidants in *R2.4-R2.7*. Given that O_3 concentrations are several orders of magnitude higher than NO_x at Summit and that NO-NO_2 cycling is rapid, $\delta^{18}O$-NO_x is expected to be strongly influenced by $\delta^{18}O$-O_3. For simplicity, we set $\delta^{18}O$-NO_x equal to that of O_3, and assume that $\delta^{18}O$-O_3 is constant. Existing measurements suggest that the $\delta^{18}O$ of tropospheric O_3 ranges from 90-120‰ versus VSMOW (Johnston and Thiemens, 1997; Krankowsky et al., 1995). The isotopic composition of tropospheric OH is largely determined by that of water vapor (Dubey et al., 1997; Lyons, 2001), therefore we set $\delta^{18}O$-OH equal to that of water vapor at Summit, which varies sinusoidally between -60‰ in winter and -25‰ in summer (Grootes and Stuiver, 1997; E.J. Steig, unpublished data).

Because $\delta^{18}O$-O_3 is much greater than $\delta^{18}O$-OH, NO_2 reacts with isotopically distinct oxidants in summer (OH) and in winter (O_3). A simple mixing model is therefore a good approximation of the expected isotope variations, and we assume that $\delta^{18}O$ from O_3 and OH is transferred directly to NO_x and HNO_3. For example, HNO_3 produced via *R2.4* is composed of two oxygen atoms from NO_2 and one from OH:

$$\delta^{18}O_{HNO3(fromNO2+OH)} = (2\,\delta^{18}O_{NO2} + \delta^{18}O_{OH})/3 \qquad (2.4)$$

We derive similar equations for each formation pathway of HNO_3 and calculate the fractional contribution of each pathway based on reactant concentrations from GEOS-Chem (Table 2.2; details on these calculations are presented separately in Kunasek et al., 2008). Combining the isotopic signature of each pathway (e.g., Equation 2.4) with its fractional contribution results in a prediction of $\delta^{18}O$-HNO_3 throughout the year. An important implication of this model is that oxygen isotope ratios of HNO_3 are

Table 2.2. The percentage of total HNO_3 production via individual pathways at Summit, Greenland, 2001, calculated using monthly mean concentrations from the GEOS-Chem model and known reaction rates.

Month	**NO_2 pathway** (*R2.4*)	**N_2O_5 pathway** (*R2.6*)	**DMS pathway** (*R2.7*)	**HC pathway** (*R2.7*)
January	0.2	34.6	65.2	0.0
February	1.9	19.5	78.7	0.0
March	14.2	12.0	73.8	0.0
April	38.4	22.3	39.3	0.1
May	94.5	1.3	4.2	0.0
June	99.7	0.1	0.2	0.0
July	99.9	0.1	0.0	0.0
August	83.3	12.8	3.9	0.0
September	24.1	6.4	69.5	0.0
October	5.0	26.9	68.0	0.1
November	0.3	20.9	78.8	0.1
December	0.1	55.9	44.0	0.0

diagnostic of the production pathway, as has been suggested by Alexander et al. (2004), Hastings et al. (2003), and Michalski et al. (2003).

2.4. Nitrate Isotope Data from Greenland Snowpits

We compare our model predictions of atmospheric HNO_3 isotope variations with measured nitrate isotopes in snow from Summit, Greenland. Hastings et al. (2004) measured $\delta^{15}N$ and $\delta^{18}O$ of nitrate from two one-meter snowpits at Summit. The $\delta^{15}N$ of nitrate ranges ~30‰, from -15‰ (vs. N_2) in winter to +17‰ in summer. The range in the $\delta^{18}O$ of nitrate is 15‰, from +80‰ vs. VSMOW in winter to +65‰ in summer. Samples collected six months apart show no indication of post-depositional losses from this site and no consistent seasonal cycle is observed in nitrate concentration, suggesting that the observed isotopic variations of nitrate are unrelated to concentration or post-depositional losses.

2.5. Model and Measurement Comparison

2.5.1. Controls on the $\delta^{15}N$ of HNO_3

The range in $\delta^{15}N$ of atmospheric HNO_3 predicted by the model is controlled by the fractionation between NO and NO_2 and the ratio of NO_2 to NO. Using a previously reported α value of 1.018 (Freyer et al., 1993), the model predicts a ~8‰ range in $\delta^{15}N$-HNO_3 (Figure 2.1). The magnitude of this change is less than a third of the overall observed 30‰ range in $\delta^{15}N$ of snow nitrate. The mismatch in the seasonal $\delta^{15}N$ range between measurements and model suggests that (1) α may be larger than 1.018, (2) seasonal changes in NO_x sources affect $\delta^{15}N$-NO_x, or (3) additional fractionations, such as that associated with PAN decomposition, need to be measured and considered. We achieve the best match with the range in $\delta^{15}N$ of snow nitrate with α equal to 1.07. This is significantly larger than the effective α calculated by Freyer et al. (1993), which was composed of photochemical and thermodynamic isotope exchange

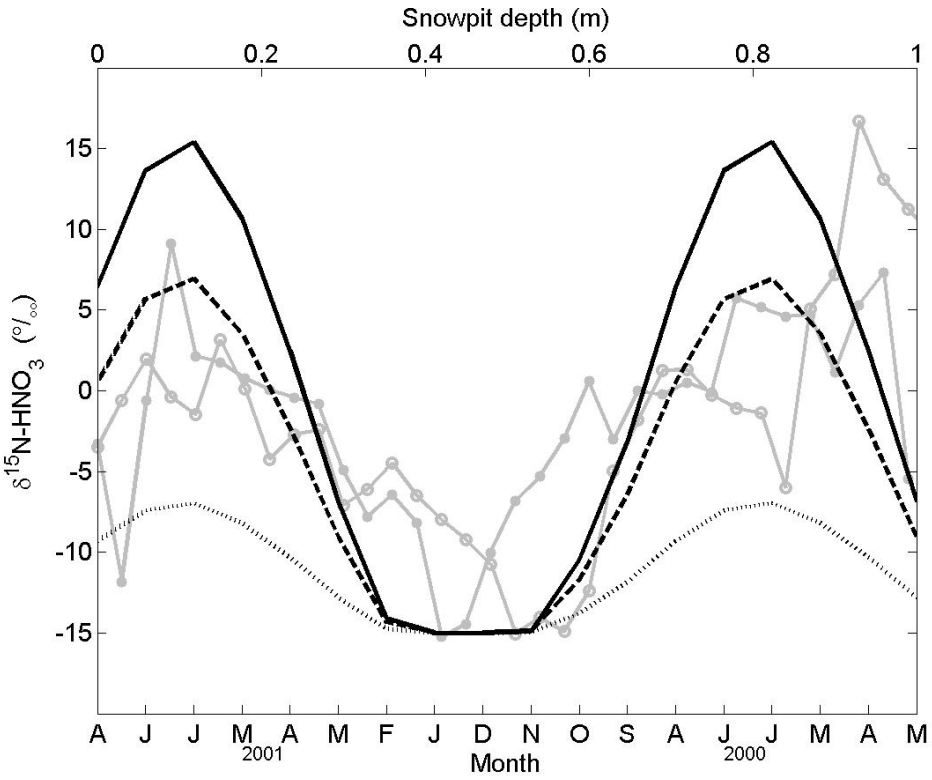

Figure 2.1. Observed $\delta^{15}N$ of NO_3^- vs. snowpit depth from two snowpits at Summit, Greenland (solid gray lines, vs. top axis) and modeled seasonal changes in $\delta^{15}N$ of HNO_3 vs. month at Summit (black lines, vs. bottom axis). The modeled $\delta^{15}N$ of NO_x is held constant (-15‰) and the fractionation between NO and NO_2 (α) varies from 1.018 (dotted line) to 1.05 (dashed line) and 1.07 (solid black line). Note that model output for 2001 is repeated for 2000.

in an urban atmosphere. At Summit, where NO_x concentrations are significantly lower than O_3, the contribution to α by thermodynamic exchange is dwarfed by photochemical exchange. Thermodynamic exchange only becomes significant when the concentration of NO_x approaches or exceeds the concentration of O_3 (i.e., urban locations). Thus under conditions at Summit, α represents primarily photochemical exchange, which, to our knowledge, has never been measured directly. It is unlikely that this fractionation is as large as 1.07 because such a large photochemical fractionation would require Freyer et al.'s estimate of thermodynamic exchange to be significantly lower than previous measurements and theory suggest (e.g., Begun and Melton, 1956).

If the α associated with $NO\text{-}NO_2$ cycling is smaller than 1.07, then the $\delta^{15}N$ of snow nitrate at Summit contains additional information, such as changes in $\delta^{15}N\text{-}NO_x$. Several previous studies have suggested that the $\delta^{15}N$ of nitrate contains a NO_x source signal (e.g., Elliott et al., 2007; Heaton et al., 2004; Yeatman et al., 2001; Russell et al., 1998). In fact, Hastings et al. (2003) found that seasonal variations in the $\delta^{15}N$ of rain nitrate at Bermuda cannot be explained without changes in the source of NO_x. Thus it is very likely that our model-measurement discrepancy in $\delta^{15}N$ is largely explained by seasonal variations in NO_x sources.

Finally, it is possible that additional fractionations play a role in determining the seasonality in $\delta^{15}N\text{-}HNO_3$ at Summit. For example, the unquantified fractionation associated with PAN decomposition may influence the range in $\delta^{15}N\text{-}HNO_3$. We note that the maximum values of $\delta^{15}N$ of nitrate observed in the snowpits occur in spring, not in summer as predicted by our model. Since the contribution of PAN thermal decomposition to the NO_x budget over Greenland also peaks in the spring (Beine et al., 1997; Moxim et al., 1996), it is possible that this influences the $\delta^{15}N$ of nitrate. Direct measurements of the isotopic composition of PAN and NO_2 will be required to test this hypothesis.

2.5.2. Controls on the $\delta^{18}O$ of HNO_3

Modeled monthly values of $\delta^{18}O\text{-}HNO_3$ are primarily controlled by $\delta^{18}O\text{-}O_3$. Figure 2.2 shows modeled $\delta^{18}O\text{-}HNO_3$ values obtained with varying $\delta^{18}O\text{-}OH$ (-60‰ in winter to -25‰ in summer) and with $\delta^{18}O\text{-}O_3$ equal to +110‰. The calculated $\delta^{18}O\text{-}HNO_3$ ranges from +65‰ to +104‰. Decreasing the $\delta^{18}O$ of O_3 (or of NO_x) shifts $\delta^{18}O\text{-}HNO_3$ down while maintaining the overall range of 40‰, which is more than twice that observed at Summit. The overall range is also maintained when $\delta^{18}O\text{-}HNO_3$ is calculated using observed O_3 concentrations and a six-fold increase in GEOS-Chem OH concentrations to match summertime measurements at Summit.

The modeled range in $\delta^{18}O\text{-}HNO_3$ is determined largely by the varying ratio of HNO_3 production pathways, and is only weakly sensitive to the choice of $\delta^{18}O\text{-}OH$. Given the potential influence of chemical losses on $\delta^{18}O\text{-}OH$ (Morin et al., 2007), Kunasek et al. (2008) estimate that under summer conditions at Summit, OH likely retains 10% of the isotopic signature from OH sources (e.g., $O(^1D)$ from O_3 photolysis) due to incomplete equilibration with water vapor. Considering an enriched $\delta^{18}O$ source for OH from O_3, it is a good approximation that the maximum $\delta^{18}O\text{-}OH$ in the summer at Summit is -11‰. We find that summer $\delta^{18}O\text{-}OH$ could be as high as 0‰ and the model would still predict a larger range (30‰) in $\delta^{18}O\text{-}HNO_3$ than observed. This over-prediction of $\delta^{18}O\text{-}HNO_3$ may be due to (1) seasonal changes in transport, (2) isotope fractionations associated with NO_2 (and HNO_3) production, or (3) effects of halogen chemistry on HNO_3 production.

Seasonal changes in the transport of air masses to Summit could influence $\delta^{18}O\text{-}HNO_3$ in two ways. First, $\Delta^{17}O$ measurements of snow nitrate at Summit suggest that snow nitrate may originate not from local NO_2 oxidation, but from regional transport of HNO_3 ($\Delta^{17}O = \delta^{17}O - 0.52*\delta^{18}O$; Kunasek et al., 2008). Depending on its isotopic value, this transported HNO_3 could account for the model-measurement discrepancy in $\delta^{18}O\text{-}HNO_3$. Second, air masses transported from different regions may contain NO_x with differing isotopic signatures. While $\delta^{18}O\text{-}NO_x$ is constant in our

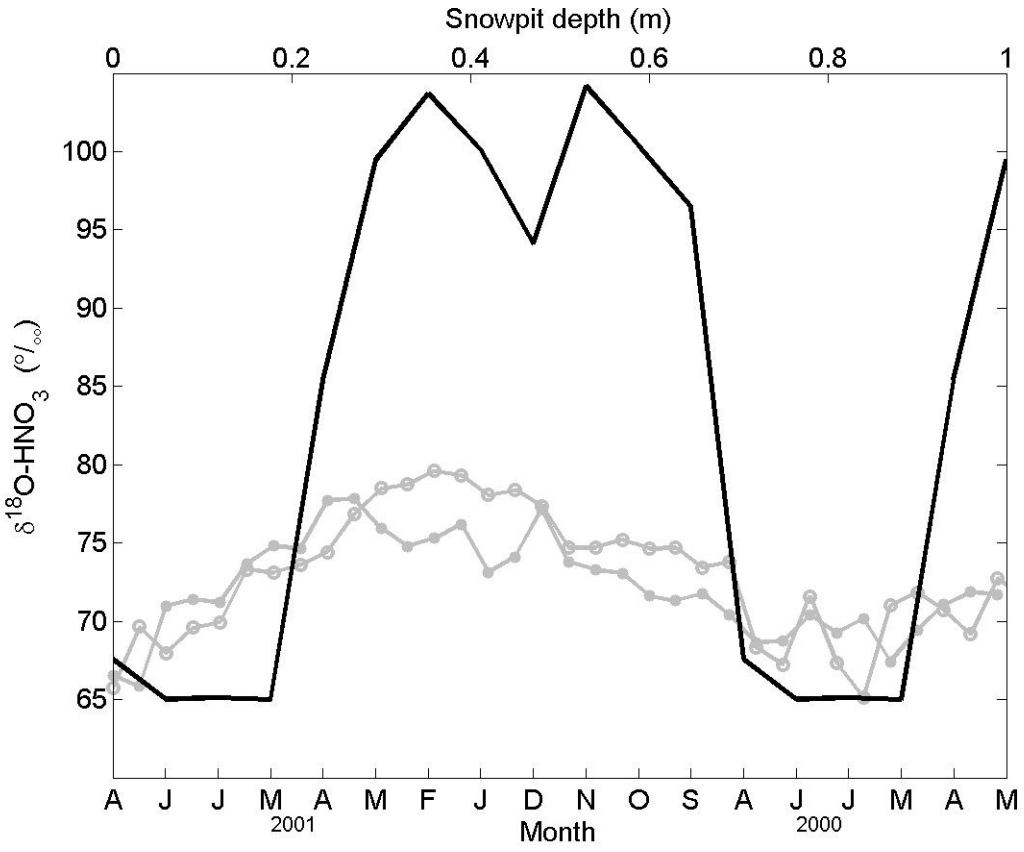

Figure 2.2. Observed $\delta^{18}O$ of NO_3^- vs. snowpit depth from two snowpits at Summit, Greenland (gray solid lines, vs. top axis) and modeled seasonal changes in $\delta^{18}O$ of HNO_3 vs. month at Summit (black line, vs. bottom axis). Our model uses GEOS-Chem predicted O_3 and OH concentrations for 2001 as input.

model, a supply of seasonally varying $\delta^{18}O\text{-}NO_x$ would modify the modeled seasonal range in $\delta^{18}O\text{-}HNO_3$. For example, under model conditions described for Figure 2.2, an increase in winter transport from regions dominated by OH would result in a lowering of the modeled winter $\delta^{18}O\text{-}HNO_3$ at Summit, thereby decreasing the seasonal $\delta^{18}O$ range. If seasonal changes in NO_x sources also control $\delta^{15}N\text{-}HNO_3$, a possibility explored in Section 2.5.1, the model-measurement discrepancy will disappear if seasonally transported NO_x contains depleted $\delta^{18}O$ and depleted $\delta^{15}N$ in winter as compared to summer.

Seasonal variations in $\delta^{18}O\text{-}NO_x$ may also be possible given potential isotope fractionations associated with the reaction of O_3 with NO or NO_2. Since recent work suggests that the transfer of O atoms during R1 favors the terminal oxygen in O_3 (Savarino et al., 2008), the degree to which $NO\text{-}NO_2$ equilibrium is reached may influence the $\delta^{18}O\text{-}NO_x$ such that it is seasonally variable. However, we note that the net effect of forward and reverse reactions between O_3 and NO_x is likely smaller than the very large difference between $\delta^{18}O\text{-}O_3$ and $\delta^{18}O\text{-}OH$. Further isotopic studies of these reactions are needed to clarify the effect on HNO_3.

Finally, halogen chemistry may have an isotopic impact on nitrate formation in polar regions (Morin et al., 2007). HNO_3 formation through $BrONO_2$ would serve to increase the influence of O_3 on $\delta^{18}O\text{-}HNO_3$, and could potentially decrease the seasonal range of modeled $\delta^{18}O\text{-}HNO_3$. However, incorporation of halogen chemistry into our model requires measurements of the concentrations and seasonality of bromine compounds at Summit, which are not yet available.

2.5.3. Influence of HO_2 and RO_2 Oxidation of NO on the $\delta^{18}O$ of HNO_3

The model calculations presented in Section 2.5.2. do not include the contribution to $\delta^{18}O\text{-}NO_x$ of alternate summertime oxidation pathways of NO at Summit. In addition to oxidation via O_3 (*R2.1*), NO can also be oxidized via HO_2 (*R2.8*) and RO_2 (*R2.9*), where R represents a hydrocarbon chain:

$$NO + HO_2 \rightarrow NO_2 + OH \qquad (R2.8)$$

$$NO + RO_2 \rightarrow NO_2 + RO \qquad (R2.9)$$

These NO oxidation pathways can account for up to 25% of the summertime production of NO_2 (Table 2.3), which, depending on the $\delta^{18}O$ of HO_2 and RO_2, can cause the $\delta^{18}O$ of NO_x to vary throughout the year.

To incorporate these reactions into the model calculations, we utilize monthly mean GEOS-Chem concentrations of HO_2 and we assume that production via RO_2 is ½ the production via HO_2. Because the $\delta^{18}O$ values of HO_2 and RO_2 have not been quantified, we estimate them to be equal to the $\delta^{18}O$ of atmospheric O_2 (+23.5‰). We then calculate a monthly varying $\delta^{18}O$ of NO_x as a function of the NO_2 production pathway and the $\delta^{18}O$ of the respective oxidant. Accounting for the influence of NO_2 formation pathways on $\delta^{18}O$-NO_x results in an even larger seasonal range in $\delta^{18}O$-HNO_3 than previously calculated (Figure 2.3). Furthermore, increasing the $\delta^{18}O$ of HO_2 and RO_2 to levels typical of O_3 (e.g., to +100‰), also produces an over-estimate (a modeled 40‰ range) of the seasonal range of $\delta^{18}O$-HNO_3. These findings further support our conclusion that local photochemistry at Summit is not sufficient to explain the seasonal range in observed $\delta^{18}O$ of snow nitrate.

Table 2.3. The calculated percentage of total NO_2 production via individual pathways at Summit, Greenland, 2001, using monthly mean concentrations from the GEOS-Chem model and known reaction rates. Production via RO_2 is estimated to be ½ the production via HO_2.

Month	**O_3 pathway** (*R2.1*)	**HO_2 pathway** (*R2.8*)	**RO_2 pathway** (*R2.9*)
January	99.5	0.4	0.2
February	98.6	0.9	0.5
March	94.1	3.9	2.0
April	87.3	8.5	4.2
May	81.2	12.6	6.3
June	76.7	15.6	7.8
July	76.9	15.4	7.7
August	81.5	12.3	6.2
September	89.5	7.0	3.5
October	97.0	2.0	1.0
November	99.7	0.2	0.1
December	99.8	0.1	0.1

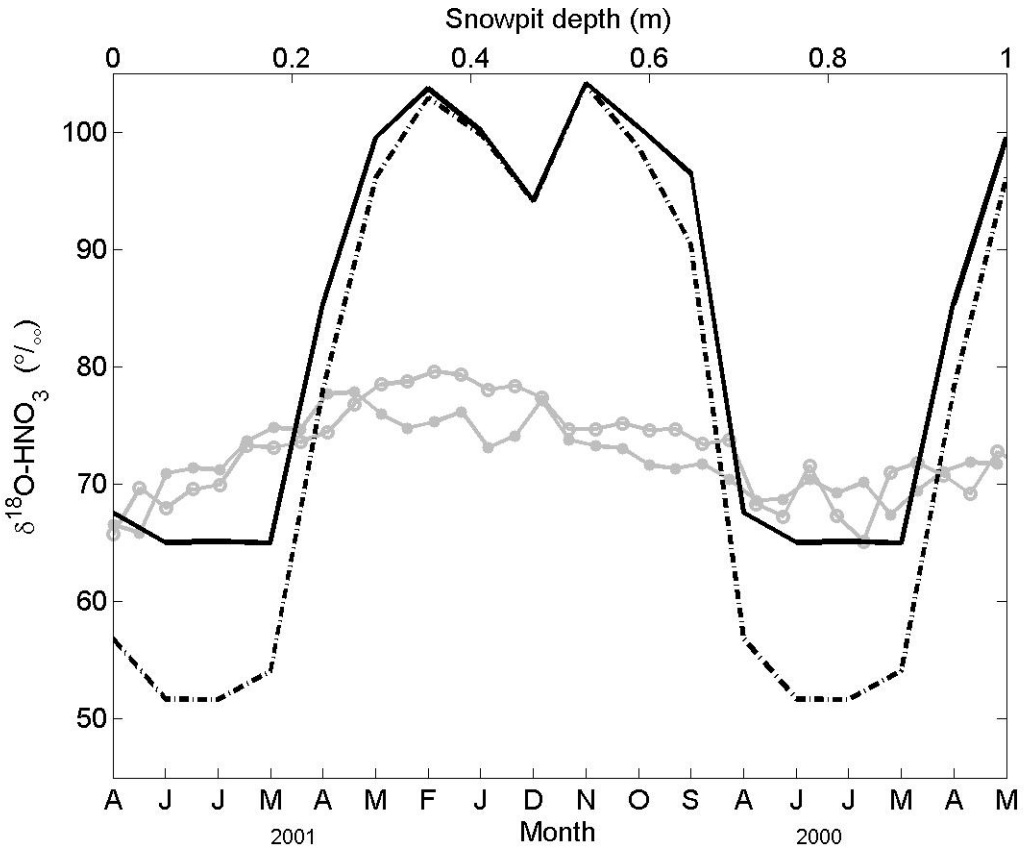

Figure 2.3. Observed $\delta^{18}O$ of NO_3^- vs. snowpit depth from two snowpits at Summit, Greenland (gray lines, vs. top axis). The modeled seasonal changes in $\delta^{18}O$ of HNO_3 vs. month at Summit using $\delta^{18}O\text{-}NO_x = \delta^{18}O\text{-}O_3$ are represented by the solid black line (vs. bottom axis). The dashed black line (vs. bottom axis) represents modeled seasonal changes in $\delta^{18}O$ of HNO_3 vs. month at Summit using a fluctuating $\delta^{18}O\text{-}NO_x$, which is based on the fractional NO_2 formation pathway and the isotopic value of each oxidant (O_3, HO_2 or RO_2). Our model uses GEOS-Chem predicted NO, NO_2, O_3, HO_2, and OH concentrations for 2001 as input.

2.6. Conclusions

We compare measurements of nitrate isotopes from Greenland snowpits to the $\delta^{18}O$ and $\delta^{15}N$ of HNO_3 determined with a simple model of local photochemistry. Less than a third of the variation in $\delta^{15}N$ of nitrate observed at Summit can be explained by our simple model, which incorporates isotope fractionation associated with NO-NO_2 cycling and seasonal changes in the local ratio of NO_2 to NO. An explanation of the full range in observed $\delta^{15}N$ of nitrate requires either implausibly large NO-NO_2 fractionation, additional fractionations not currently quantified, and/or additional sources of variation in $\delta^{15}N$-NO_x. Seasonal changes in $\delta^{15}N$-NO_x are likely given seasonal variability in NO_x source emissions and transport. Ongoing, coordinated measurements of the isotopic composition of both NO_2 and HNO_3 at Summit should help reduce the uncertainty in our assumption that $\delta^{15}N$-HNO_3 directly reflects $\delta^{15}N$-NO_2. Clearly, better quantification of isotopic fractionations associated with NO_y cycling is also needed.

The large seasonality and very different isotopic compositions of OH and O_3, in the absence of other processes, would result in a much larger range in $\delta^{18}O$-HNO_3 than observed at Summit. The discrepancy between the modeled seasonal range and that which is observed at Summit may be accounted for by seasonal variations in the isotopic composition of NO_x and/or HNO_3 transported to Summit. The quantification of post-depositional processing of nitrate, fractionations associated with NO_x oxidation, and halogen chemistry at Summit is needed to establish the impacts of these processes on nitrate isotopes.

Chapter 3

Surface Snow and Gas-phase Nitrate Isotopes at Summit, Greenland: Implications for Post-depositional Recycling

[Jarvis, J.C., M.G. Hastings, E.J. Steig, S.A. Kunasek, to be submitted to *Journal of Geophysical Research*]

3.1. Summary

While the post-depositional release of nitrate from polar snowpacks is known to occur, the lack of quantitative constraints on the post-depositional processing of snow nitrate limits our understanding of the effects this has on the polar atmosphere and the interpretation of ice cores. We present the first simultaneous measurements of nitrate isotopes ($^{15}N/^{14}N$ and $^{18}O/^{16}O$) in air and snow from Summit, Greenland, providing new observational constraints on post-depositional processing of snowpack nitrate. The $\delta^{15}N$ of HNO_3 is similar in surface snow and in air sampled 1.5 meters above the snow surface during Spring and Summer 2006, ranging between -15 and + 6‰ versus N_2. The $\delta^{18}O$ of HNO_3 is ~40‰ enriched in the surface snow relative to the air samples. Comparisons with photochemical box modeling of HNO_3 chemistry at Summit suggest that the $\delta^{18}O$ measurements are consistent with gas-phase HNO_3 that originated from photolyzed snow nitrate. Using these measurements, we estimate the isotopic impact of photolytic recycling and photolytic loss of snow nitrate at Summit. Additional isotopic measurements of labeled nitrate in surface snow confirm the role of photolytic recycling of snowpack nitrate. A comparison of surface snow and snowpit samples demonstrates the preservation of the seasonal cycle of nitrate isotopes in snow and highlights the need for further studies of the spatial variability in nitrate isotopes at Summit.

3.2. Introduction

The transfer to and preservation of atmospheric compounds in snow in polar regions is a dynamic area of research. Recent studies point to the influence of snowpack chemistry on the composition of the overlying atmosphere (Grannas et al., 2007; Dominé and Shepson, 2002). Flux measurements of nitrogen oxides above and within surface snow in the Arctic and Antarctic show that NO_x ($NO + NO_2$) is emitted from the snowpack (Beine et al., 2002; Honrath et al., 2002; 1999; Jones et al., 2001; 2000). This NO_x is produced from the photolysis of nitrate (NO_3^-, or nitric acid, HNO_3) in the upper few tens of centimeters of snow (Galbavy et al., 2007; Qiu et al., 2002; King and Simpson, 2001). Combined with the concurrent release of OH, the release of NO_x from surface snow may have both local and regional impacts on air chemistry (e.g., Cotter et al., 2003). Because they are closely linked to cycles of tropospheric oxidants, nitrogen oxides influence the lifetimes of atmospheric gases such as methane and volatile organic compounds.

The release of NO_x from surface snow may also have implications for the interpretation of ice cores. If the photolysis of snowpack nitrate alters the amount of nitrate preserved in ice, the nitrate concentration record derived from ice cores no longer directly reflects the amount of nitrate originally deposited to the snow surface. Additional processes, such as volatilization and diffusion of nitrate, may also influence the preservation of nitrate in snow (e.g., Röthlisberger et al., 2002). In the absence of constraints on these post-depositional changes, ice core nitrate concentrations cannot be used as a quantitative indicator of past NO_x concentrations. Quantifying the air-to-snow transfer and preservation of nitrogen oxides is thus a fundamental step in the interpretation of the nitrate ice record.

Several studies have sought to quantify the post-depositional release of snowpack nitrate and the preservation of nitrate in snow at Summit, Greenland. Measurements of nitrate concentrations in surface snow and snowpits at Summit suggest that 7% of nitrate, at most, is lost from snow after deposition (Burkhart et al., 2004). A more recent study by Dibb et al. (2007) found that up to 25% of freshly

deposited nitrate may be lost from the surface snow at Summit over 1-2 years after deposition. Measurements of nitrate isotopes ($^{15}N/^{14}N$ and $^{18}O/^{16}O$ isotope ratios) in snow offer the opportunity to constrain and track these changes over time. From measurements of nitrate concentration and $\delta^{15}N$ and $\delta^{18}O$ of nitrate in surface snow and snowpits at Summit, Hastings et al. (2004) found no indication of post-depositional losses of snow nitrate based on samples collected six months apart. These contrasting findings warrant further investigation of nitrate isotopes both in Summit snow and in the air above the snow to provide a more complete characterization of post-depositional change and air-to-snow transfer of nitrate at Summit.

We present isotopic measurements of atmospheric gas-phase HNO_3 and snow nitrate at Summit, Greenland and analyze the observed differences in the context of nitrate photolysis in snow. We define post-depositional or photolytic *loss* of nitrate as the loss of nitrate from the snowpack followed by the export of loss products from the region, whereas post-depositional or photolytic *recycling* of nitrate refers to the loss of nitrate from the snowpack followed by redeposition to the snow surface in the immediate vicinity. Distinguishing between loss and recycling has implications for temporal changes in the isotopes of snowpack nitrate at Summit, discussed in Section 3.5.6.

3.3. Methods

3.3.1. Field Sampling

Field sampling of surface snow and atmospheric HNO_3 took place at Summit, Greenland (72ºN, 38ºW) from March through July of 2006. Atmospheric HNO_3 was collected with mist chambers, in which gas-phase HNO_3 is dissolved in water misting over a stream of sampled air (Dibb et al., 1998; 1994). A hydrophobic filter (Millipore Fluoropore Membrane Filter, 1.0 μm) on the inlet of the mist chamber, which was placed approximately 1.5 m above the snow surface, prevented snow and particulates from entering the sampling chamber. Due to the low mixing ratios of HNO_3 at Summit

(pptv level), air was sampled continuously for at least 48 hours to collect enough HNO_3 for later laboratory analysis. Average flow rates through the mist chambers were recorded every two minutes and ranged from 10 to 40 LPM STP. At the end of each sampling period, mist chamber samples and filters were placed in individual amber HDPE containers and frozen immediately. Each mist chamber was rinsed thoroughly with deionized water between sampling periods. Filter blanks and mist chamber water blanks were collected weekly.

To test the reproducibility of gas-phase HNO_3 collection and analysis, samples were collected from multiple mist chambers. Measurements presented here include samples from two mist chambers operating independently from March 24 to April 20 and from May 24 to July 6. An additional mist chamber was used to sample air exiting the second mist chamber between May 24 and June 18. Four sets of samples represent 3- or 4-day sampling periods (May 8-11, June 24-28, June 28-July 2, July 2-6) while the majority of samples represent 2-day sampling periods.

Surface snow was collected 4-6 times daily for several multi-day periods each month during March-July, 2006. Surface snow samples were also collected regularly from July 2005 to March 2007. Care was taken to sample only the loose, unpacked top layer of snow using a clean glass scraper. Each sample represents previously undisturbed snow; no snow was collected in the exact same spot as a previous sample. At the beginning of August 2007, a 1-meter snowpit was sampled at 3 and 6-cm resolution. In Section 3.5.6., we additionally display isotopic measurements from a 2-meter snowpit sampled at 5-cm resolution in May 2006 (see Kunasek et al., 2008).

Experiments involving labeled nitrate were used to further explore the influence of photolysis on the isotopes of surface snow nitrate. In July 2007, a 15μM solution of nitrate enriched in ^{15}N ($\delta^{15}N \sim +8000‰$) was sprayed over a 13.5 m^2 area of snow at Summit. Surface snow was collected from this area and from an adjacent, untouched area of snow every 6 hours for three days. Fresh snow fell on the last day of surface sampling. Two weeks after the end of surface snow sampling, two 10-cm snowpits were sampled at 2-cm intervals in the labeled nitrate area and the unaltered control area.

3.3.2. Laboratory Analysis

Samples were transported frozen to the University of Washington (UW), where they remained frozen until the day of analysis. For filter samples, 30 mL of our laboratory milliQ deionized water was added to each container while in a cold room (maintained at -10ºC). These samples were shaken and sonicated for 30 minutes prior to analysis.

All samples were analyzed at UW for major anion (Cl^-, NO_2^-, NO_3^-, SO_4^{2-}) concentrations using a Dionex ion chromatograph with a IonPac AS11-HC column (2x250mm) and an eluent concentration (KOH) of 20 mM (loop size and injection size = 100 μL). The error in concentration is typically less than ± 0.1μM for nitrate and less than ± 0.05μM for nitrite. Concentration measurements were used to determine the volume of sample required to achieve 10nmol N (nitrate and nitrite) for isotopic analysis. Samples were then analyzed for $^{15}N/^{14}N$ and $^{18}O/^{16}O$ isotope ratios using the denitrifier method, in which bacteria convert nitrate and nitrite to N_2O, which is isotopically analyzed with a continuous flow mass spectrometer (Sigman et al., 2001; Casciotti et al., 2002). The denitrifier method, which utilizes denitrifying bacteria lacking N_2O-reductase (*Pseudomonas aureofaciens*), allows for the analysis of samples with concentrations as low as 1μM nitrate.

Samples analyzed with the denitrifier method were calibrated to internationally recognized reference materials IAEA-NO-3 and USGS35 following corrections outlined in Kaiser et al. (2007), Hastings et al. (2004), and Casciotti et al. (2002). The $\delta^{15}N$ of each sample was calibrated to measurements of IAEA-NO-3 ($\delta^{15}N$ of +4.7‰, Böhlke and Coplen, 1995; Gonfiantini et al., 1995) made during the same sample batch. Because some exchange with water is expected for oxygen atoms during denitrification (Casciotti et al., 2002), the $\delta^{18}O$ of each sample was corrected using both IAEA-NO-3 ($\delta^{18}O$ of +25.6‰, Böhlke et al., 2003) and USGS35 ($\delta^{18}O$ of +57.5‰, Böhlke et al., 2003). Throughout this text, reported values of $\delta^{15}N$ and $\delta^{18}O$ are referenced to N_2 in air and Vienna Standard Mean Ocean Water (VSMOW), respectively.

We initially assign the 1σ error in $\delta^{15}N$ and $\delta^{18}O$ of nitrate for each batch to be equal to the standard deviation among IAEA-NO-3 standards analyzed in that batch. With our current measurement capabilities, this translates to an overall average 2σ error of 3‰ for $\delta^{15}N$ and 7‰ for $\delta^{18}O$. However, the reproducibility of duplicate samples within a given batch is sometimes outside of the 2σ error for that batch. We therefore additionally calculate the standard deviation among replicate samples (for $\delta^{15}N$ and $\delta^{18}O$) and for USGS35 standards (for $\delta^{18}O$) within each batch. We report the largest of these to be the 2σ error for samples within that batch. Of the 107 surface snow samples presented here, 42 were analyzed two or more times for $\delta^{15}N$ and $\delta^{18}O$. For these replicate samples, as many as 47% are outside the 2σ error for $\delta^{18}O$ of nitrate. However, for $\delta^{15}N$, the 2σ error accurately represents the true error derived from replicate samples. The replicate samples are reported as averages ±1 standard error of the mean (i.e., standard error (S.E.) = (standard deviation of samples)*(number of samples)$^{-1/2}$).

3.4. Results

3.4.1. Gas-phase HNO_3 and HONO

The gas-phase HNO_3 concentrations determined from mist chamber sampling 1.5 m above the snow at Summit are several nmol m^{-3} STP (1nmol m^{-3} = 22.4 pptv), averaging 3.6 nmol m^{-3} in April and 3.1 nmol m^{-3} in May/June 2006 (Figure 3.1a). These values are similar to the range of previous measurements of gas-phase HNO_3 at Summit (Honrath et al., 2002; Dibb et al., 1998; 1994). Due to our long (48-hour) sampling periods, we do not observe sharp spikes in HNO_3 concentrations such as those reported by Dibb et al. (1998), with the exception of a peak in gas-phase HNO_3 in mid-April.

Small amounts of gas-phase HONO are detected in the mist chamber samples in the form of nitrite (NO_2^-) (Dibb et al., 2004; 2002). On average, nitrite represents 11% of the total N (where total N = $[NO_2^-]$ + $[NO_3^-]$) in each sample, ranging from 0

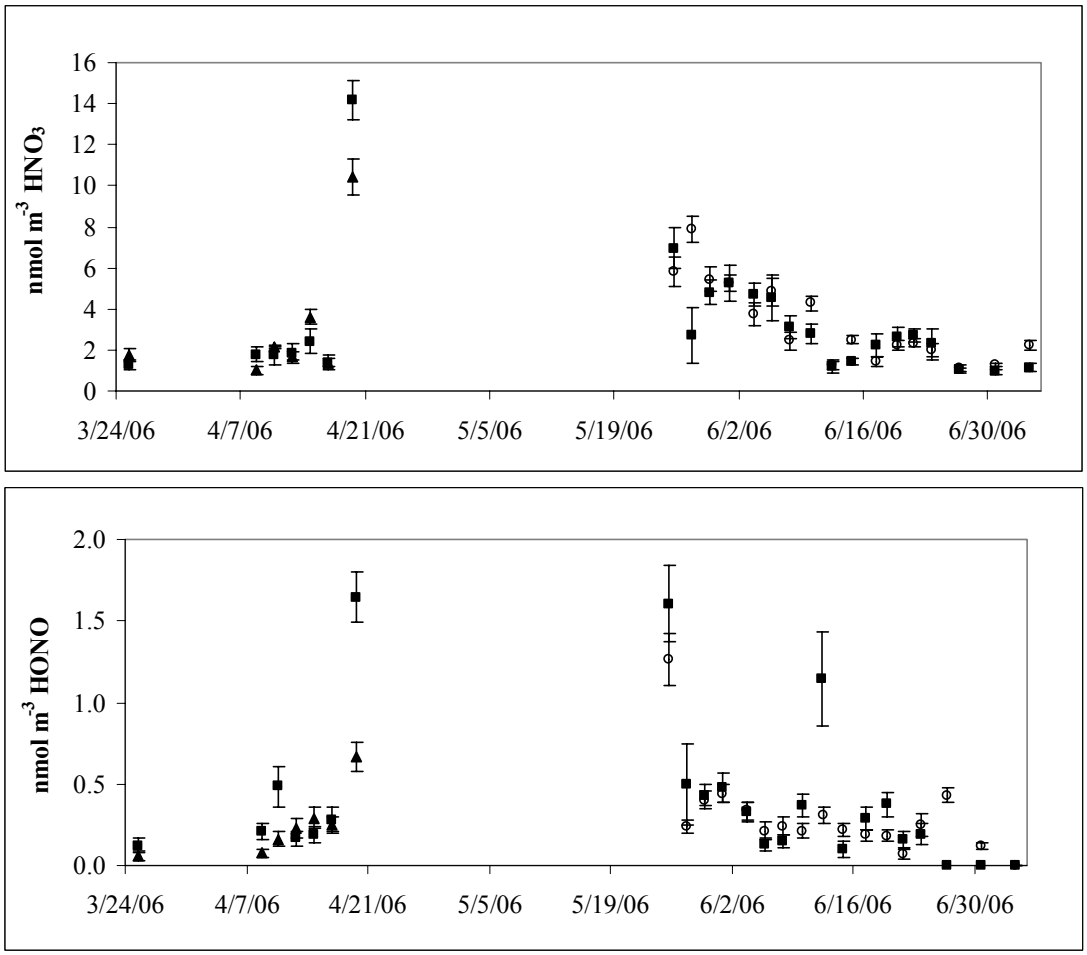

Figure 3.1. Concentrations of (a) gas-phase HNO_3 and (b) HONO sampled 1.5 m above the snow at Summit, Greenland in 2006. The open and closed symbols represent two different mist chamber setups. Data points represent samples from a single mist chamber (filled squares and triangles) and two mist chambers sampling inline (open circles). Error bars represent the propagation of errors associated with gas-phase collection of HNO_3 and HONO, including uncertainties in the volume of air sampled, in the final volume of mist chamber water, and in concentration measurements. No mixing ratio data are available for samples between March 26th and April 7th.

to as much as 50% of total N. HONO concentrations, determined from the NO_2^- concentrations, were less than 1.6 nmol m^{-3} STP (Figure 3.1b), similar to previous measurements of HONO at Summit (Dibb et al., 2002).

We find good agreement in gas-phase HNO_3 and HONO collection between the different mist chamber setups. For the dual mist chamber setup, nitrate (or nitrite) concentrations from both mist chambers were added to determine the total HNO_3 (or HONO) collected for that setup. The use of two mist chambers inline, which lowered the overall flow rate of sampled air, resulted in an uneven distribution of nitrate and nitrite between the two mist chambers: ~2/3 of the total nitrate or nitrite was collected in the first mist chamber while 1/3 of the total was collected in the second mist chamber. The gas-phase HNO_3 and HONO concentrations derived from nitrate and nitrite collected in the dual mist chamber setup match the concentrations derived from the single mist chamber setup (Figure 3.1). The propagation of uncertainties associated with gas-phase HNO_3 and HONO collection (e.g., error in volume of air sampled, error in concentration measurements, etc.) produces an average error of ±17% HNO_3. This is comparable to the difference in measured concentration of gas-phase HNO_3 between the mist chamber setups, which agree within 33 (±41)%. Slight differences in the amount of HNO_3 collected by the various mist chambers may be due to occasional freezing in the mist chambers that impaired the collection of nitric acid. Because each mist chamber setup sampled a unique volume of air, the good agreement in HNO_3 concentrations suggests that the mist chambers efficiently collect HNO_3 from sampled air. This implies that any isotopic fractionation of HNO_3 during sampling should be minimized.

Since the mist chambers were constantly monitored during sampling, water in the mist chambers was maintained at a level high enough to produce vigorous misting. However, for the May 28-30 sampling period, the volume of water in the single mist chamber decreased rapidly to an extremely low level near the end of the sampling period. We suspect this concentrated nitric acid in the water, lowering the pH of the solution and resulting in the evaporation of HNO_3 along with water. We consider this

to be a unique event, as mist chamber water levels were generally quite high and the final concentration of HNO_3 in mist chamber samples is on the order of 1-10 μM, which roughly translates to a pH of ~5-6. We additionally note that for the sampling period of June 9-11, the disagreement in HNO_3 concentration measured by the different mist chamber setups is likely a result of different sampling times for the single and dual mist chambers, which rarely occurred.

We find variable amounts of nitrate and nitrite on the inlet filters, which are expected to collect particulate nitrate and nitrate while allowing gas-phase HNO_3 to pass through. Total N (= nitrate + nitrite) concentrations on the filters range from 1.26 to 20.74μM, while filter blanks show considerable amounts of total N (between 1 and 2.5μM). Nitrite dominates the total N on the filter samples and filter blanks, accounting for approximately 74% of the total N on the filter samples and ~78% of total N on the filter blanks. We address the influence of particulate nitrate on the mist chamber results and the potential contamination of inlet filters in Section 3.5.3.

3.4.2. Surface Snow Nitrate

The concentration of nitrate in surface snow collected between March and July 2006 at Summit ranges from 0.74 to 9.82μM (average of 3.16μM), reaching a maximum concentration in early April (Figure 3.2). Additional surface snow samples collected weekly from July 2005 through March of 2007 have a similar range in nitrate concentration (not shown). Nitrate concentration is slightly increased in spring and fall, which is consistent with previous observations (Dibb et al., 2007). The range of nitrate concentration in surface snow observed in this study is comparable to prior measurements of snowpack nitrate at Summit (e.g., Dibb et al., 2007; Burkhart et al., 2004; Hastings et al., 2004).

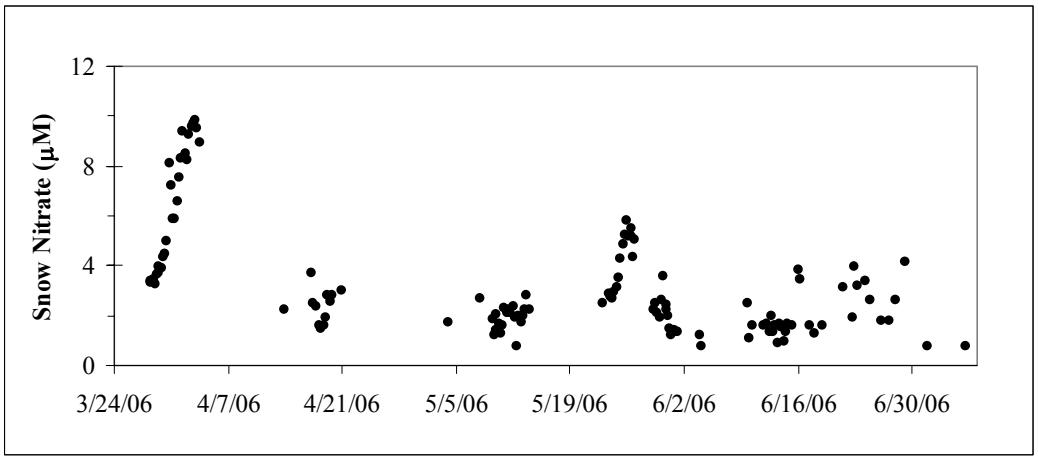

Figure 3.2. The concentration of nitrate (μM) in surface snow at Summit, Greenland during Spring and Summer 2006.

3.4.3. $\delta^{15}N$ and $\delta^{18}O$ of Gas-phase HNO_3 and Snow Nitrate

We find good agreement in isotopic measurements of gas-phase HNO_3 collected with single and dual mist chambers (Figure 3.3). This further suggests that any isotope fractionation associated with mist chamber sampling of HNO_3 is minimal, given that the mist chamber setups differed in the flow rate and volume of air sampled.

The $\delta^{15}N$ of snow nitrate and of gas-phase HNO_3 1.5 m above the surface snow at Summit both range between -15 and +6‰ versus N_2 during Spring/Summer 2006 (Figure 3.4). This range in $\delta^{15}N$ of snow nitrate is within the ranges previously reported in Arctic snow by Hastings et al. (2004) and Heaton et al. (2004). The average $\delta^{15}N$ of gas-phase HNO_3 in March-April 2006 (-4.0‰ ± 0.9) and May-June 2006 (-3.8‰ ± 0.7) is comparable to the average $\delta^{15}N$ of snow nitrate over the same time periods (-5.3‰ ± 0.4 and -5.5‰ ± 0.7) (Table 3.1).

The average measured $\delta^{18}O$ of gas-phase HNO_3 and of snow nitrate differ by over 40‰ (Figure 3.5 and Table 3.1). The $\delta^{18}O$ of gas-phase HNO_3 ranges between +25 and +47‰ versus VSMOW, while the $\delta^{18}O$ of surface snow nitrate ranges between +45 and +108‰. Hastings et al. (2004) and Heaton et al. (2004) both reported a smaller range and lower average $\delta^{18}O$ of nitrate for measurements of summertime surface snow at Summit and springtime fresh snow at Svalbard, respectively. We discuss the implications of the differences in $\delta^{15}N$ and $\delta^{18}O$ between snow nitrate and gas-phase HNO_3 in Section 3.5.

Table 3.1. The average $\delta^{15}N$ (‰ vs. N_2) and $\delta^{18}O$ (‰ vs. VSMOW) of gas-phase HNO_3 and surface snow nitrate at Summit, Greenland in 2006. Data are reported as averages ±1 standard error of the mean.

Sampling period	Gas-phase HNO_3		Surface snow nitrate	
	$\delta^{15}N$	$\delta^{18}O$	$\delta^{15}N$	$\delta^{18}O$
3/24/2006 – 4/21/2006	-4.0 ± 0.9	34.3 ± 1.4	-5.3 ± 0.4	80.6 ± 1.7
5/24/2006 – 7/6/2006	-3.8 ± 0.7	34.2 ± 0.7	-5.5 ± 0.7	80.9 ± 1.6

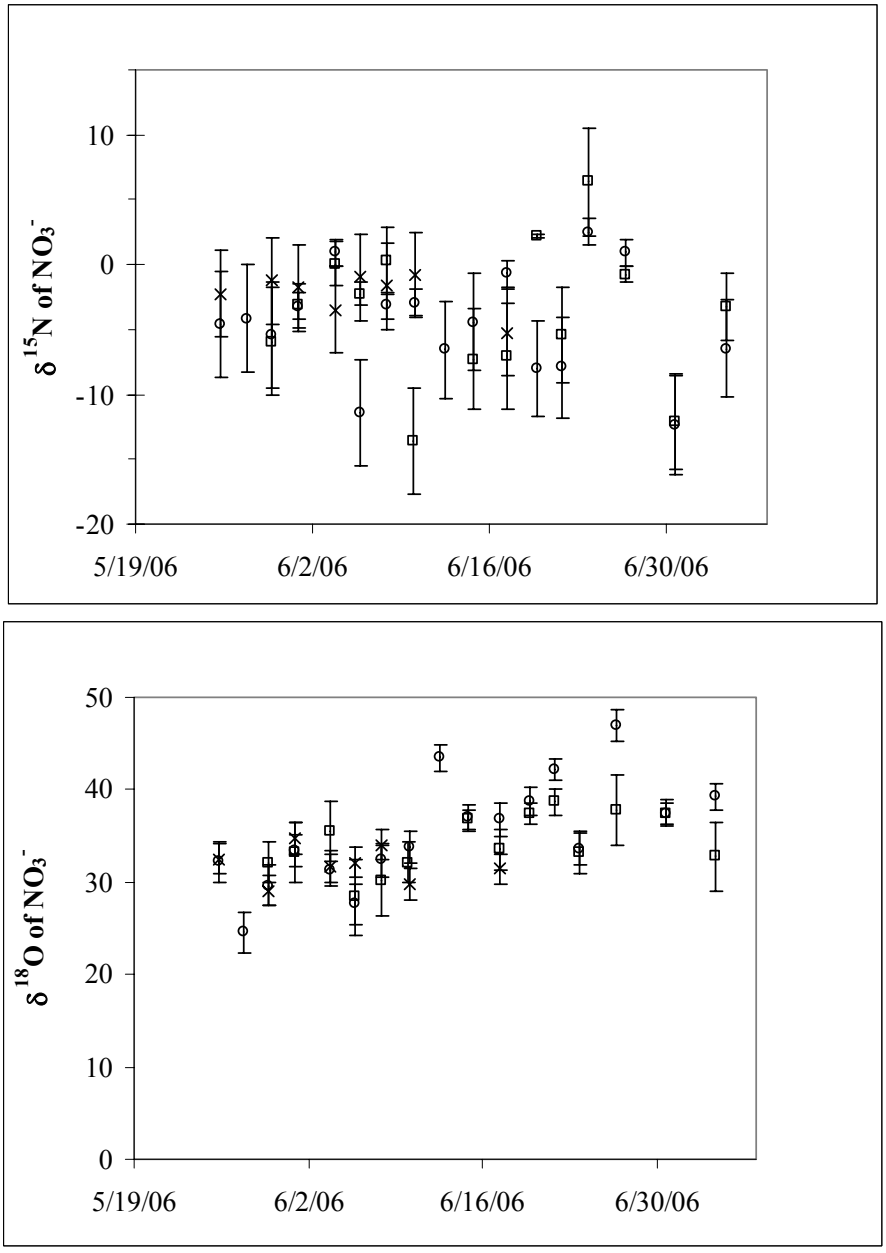

Figure 3.3. The (a) $\delta^{15}N$ (‰ vs. N_2) and (b) $\delta^{18}O$ (‰ vs. VSMOW) of gas-phase HNO_3 collected using a single mist chamber (open squares) and two mist chambers sampling inline (open circles represent the first mist chamber and x-marks represent the second mist chamber).

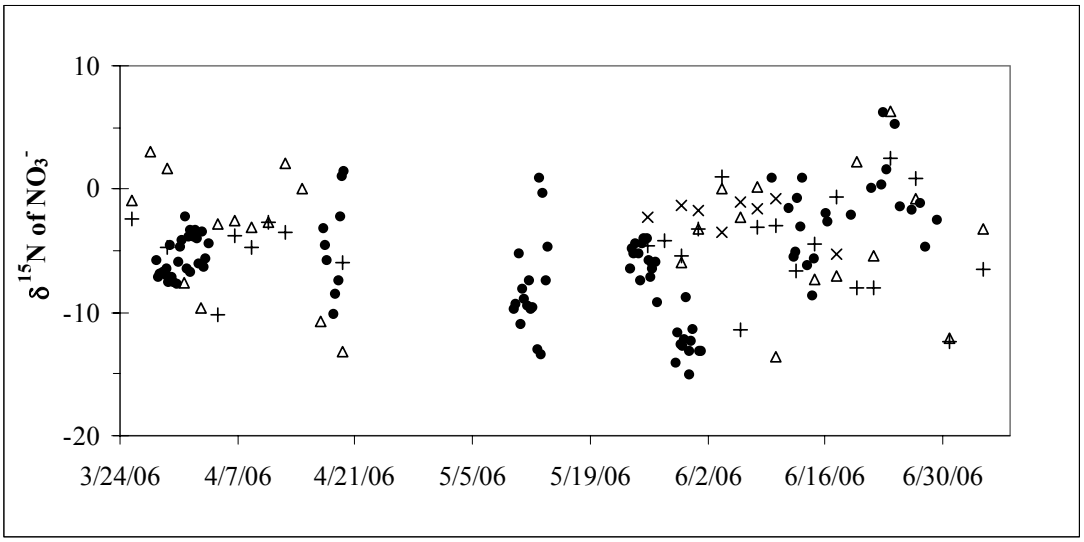

Figure 3.4. The $\delta^{15}N$ (‰ vs. N_2) of surface snow nitrate (filled circles) and gas-phase HNO_3 (open triangles, +-marks, and x-marks represent different mist chambers). The average 2σ error of $\delta^{15}N$ measurements is 3‰.

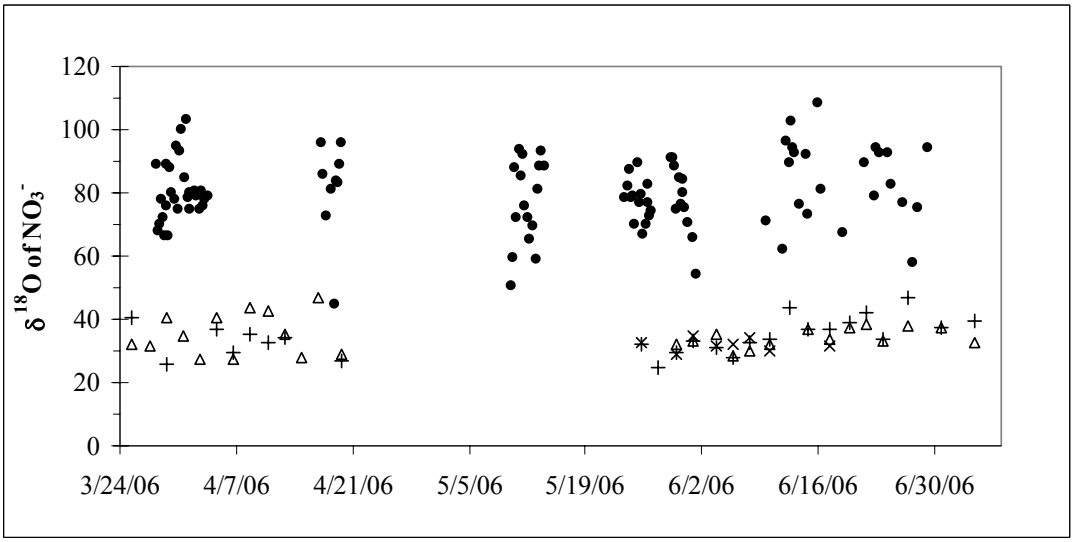

Figure 3.5. The $\delta^{18}O$ (‰ vs. VSMOW) of surface snow nitrate (filled circles) and gas-phase HNO_3 (open triangles, +-marks, and x-marks represent different mist chambers). The average 2σ error of $\delta^{18}O$ measurements is 7‰.

We observe no diurnal cycle in the concentration or isotopes of nitrate in surface snow, although this may in part reflect our relatively large measurement error. Previous reports of a diurnal cycle in nitrate isotopes measured over two days at Summit indicate a diurnal range (~5‰ in $\delta^{15}N$ and ~4‰ in $\delta^{18}O$, Hastings et al., 2004). We also do not observe a clear relationship between nitrate concentration and isotopes and the timing of snow and/or fog events at Summit. However, no attempt was made to collect fresh snow or fog drops separately from the snow surface, making an examination of this relationship difficult.

Surface snow samples were grouped into seasonal bins based on the date of sample collection (e.g., Summer = June, July, and August). We observe a seasonal cycle in surface snow nitrate isotopes (Table 3.2). Over 7.5 seasons at Summit (Summer 2005 through early Spring 2007; note that for the Summer 2005 and the Spring 2007 surface snow bins, only two samples from August and March, respectively, were analyzed for isotopes, thus these bins are not representative of an entire season), the $\delta^{15}N$ of snow nitrate clearly cycles between depleted values in the winter (e.g., -13‰ in Winter 2007) and enriched values in the summer (e.g., -2.7‰ in Summer 2006). The magnitude and direction of this seasonal cycle is similar to previous observations at Summit (Hastings et al., 2004). In contrast, the seasonal trend in $\delta^{18}O$ of surface snow nitrate is not as clear, nor is it similar to previous observations. The seasonal range in $\delta^{18}O$ of snow nitrate in this study is 34‰, which is 26‰ greater than the seasonally binned range found from nitrate analysis of snowpits at Summit in 2001 (Hastings et al., 2004). In addition, Hastings et al. (2004) observed a seasonal cycle in $\delta^{18}O$ of nitrate with higher values in winter, whereas in this study we find maxima in $\delta^{18}O$ in Fall 2005, Spring/Summer 2006, and Winter 2007. The observed seasonal cycle of nitrate isotopes in surface snow is also shown in Figure 3.10 and discussed in Section 3.5.6.

Table 3.2. Seasonally averaged $\delta^{15}N$ (‰ vs. N_2) and $\delta^{18}O$ (‰ vs. VSMOW) of nitrate in surface snow at Summit, Greenland. Data are reported as the seasonal average ±1 standard error of the mean. Note that the Spring 2007 surface snow bin only contains two samples from March and the Summer 2005 surface snow bin only contains two samples from August, therefore these bins do not represent average surface snow for an entire season.

Season	**2005**		**2006**		**2007**	
	$\delta^{15}N$	**$\delta^{18}O$**	**$\delta^{15}N$**	**$\delta^{18}O$**	**$\delta^{15}N$**	**$\delta^{18}O$**
Winter (DJF)	-	-	-10.9 ± 1.5 *n=7*	69.5 ± 5.0 *n=7*	-13.0 ± 3.2 *n=4*	101.6 ± 7.9 *n=4*
Spring (MAM)	-	-	-6.7 ± 0.4 *n=82*	79.3 ± 1.1 *n=82*	-11.7 ± 1.7 *n=2 (March)*	103.8 ± 33 *n=2 (March)*
Summer (JJA)	1.3 ± 2.1 *n=2 (August)*	71.7 ± 6.8 *n=2 (August)*	-2.8 ± 0.9 *n=26*	82.0 ± 2.8 *n=26*	-	-
Fall (SON)	-0.1 ± 2.9 *n=5*	77.3 ± 4.1 *n=5*	-10.2 ± 1.8 *n=4*	72.9 ± 5.2 *n=4*	-	-

3.4.4. $\delta^{15}N$ and $\delta^{18}O$ of Snowpit Nitrate

In August 2007, a 1-meter snowpit was sampled at 3-cm and 6-cm resolution at Summit. Measurements of nitrate concentration, $\delta^{15}N$ and $\delta^{18}O$ of nitrate, and $\delta^{18}O$ of snow are shown in Figure 3.6. The $\delta^{18}O$ of snow, which increases during warmer months and decreases during cooler months at Summit (Grootes and Stuiver, 1997), was used to identify approximate seasonal bins (Table 3.3). These seasonal bins indicate that the snowpit samples include snow deposited from Spring 2006 through Summer 2007. The $\delta^{15}N$ of nitrate reaches maxima in Summer 2006 and Spring 2007, which is comparable to seasonal patterns at Summit observed by Hastings et al. (2004). The $\delta^{18}O$ of nitrate shows no clear seasonal cycle, reaching relative maxima in Summer 2007, Winter 2007, and Spring 2006.

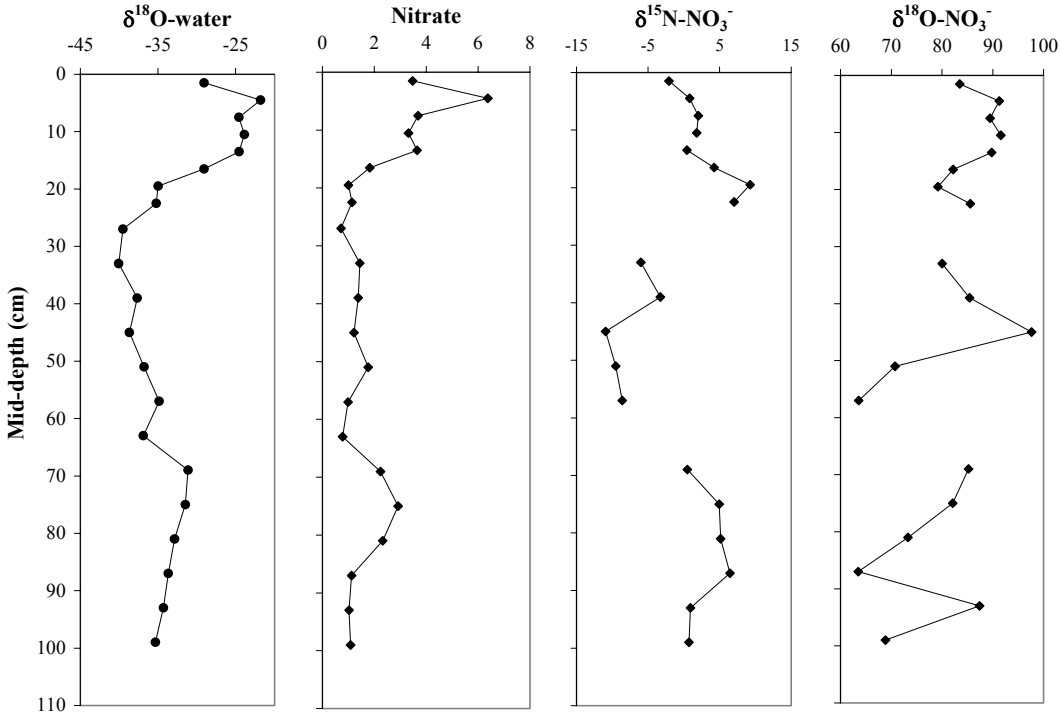

Figure 3.6. The $\delta^{18}O$ of snow, nitrate concentration (μM), $\delta^{15}N$ of nitrate (‰ vs. N_2), and $\delta^{18}O$ of nitrate (‰ vs. VSMOW) from a 1-m snowpit sampled at Summit in August 2007. For three samples (at 24, 54, and 60 cm depth), the nitrate concentration was too low for isotopic analysis.

Table 3.3. Seasonal bins of a 1-m snowpit sampled at Summit in August 2007. Data are reported as the bin average ±1 standard deviation. Only one sample in the Fall 2006 bin contained enough nitrate for isotopic analysis; therefore no standard deviation is reported for $\delta^{15}N$ and $\delta^{18}O$ of nitrate for that season.

Snowpit Depth (m)	**Season**	**$\delta^{18}O$-snow (‰ vs. SMOW)**	**$[NO_3^-]$ (μM)**	**$\delta^{15}N$-NO_3^- (‰ vs. N_2)**	**$\delta^{18}O$-NO_3^- (‰ vs. VSMOW)**
0.0 – 0.15	Summer (JJA) 2007 *n = 5*	-24.8 ±2.7	4.1 ±1.3	0.6 ±1.6	89.1 ±3.3
0.15 – 0.24	Spring (MAM) 2007 *n = 3*	-33.1 ±3.5	1.3 ±0.4	6.8 ±2.5	82.3 ±3.2
0.24 – 0.54	Winter (DJF) 2007 *n = 5*	-38.5 ±1.3	1.3 ±0.4	-7.4 ±3.5	83.5 ±11.2
0.54 – 0.66	Fall (SON) 2006 *n = 2*	-35.9 ±1.4	0.9 ±0.2	-8.6	63.6
0.66 – 0.90	Summer (JJA) 2006 *n = 4*	-32.3 ±1.2	2.2 ±0.8	4.3 ±2.6	76.0 ±9.8
0.90 – 0.99	Spring (MAM) 2006 *n = 2*	-34.8 ±0.7	1.1 ±0.04	0.8 ±0.1	78.1 ±13.1

3.5. Discussion

Of note in our measurements is the difference in $\delta^{18}O$ between gas-phase HNO_3 and surface snow nitrate at Summit. The $\delta^{18}O$ of gas-phase HNO_3 samples is consistently ~40‰ lower than the $\delta^{18}O$ of surface snow nitrate, while the average $\delta^{15}N$ of gas-phase HNO_3 is comparable to that of snow nitrate (Table 3.1; Figures 3.4 and 3.5). Possible reasons for this disparity in $\delta^{18}O$ include isotopic fractionation during the collection of gas-phase HNO_3, interference from filters, and influences of photolytic cycling of nitrate between the snow and atmosphere. In the discussion that follows, we examine these explanations with regard to the $\delta^{18}O$ measurements and we determine whether each explanation is also consistent with $\delta^{15}N$ and nitrate concentration observations. We then explore the implications of photolytic cycling for nitrate isotopes in snow (Section 3.5.5) on a seasonal to annual scale (Section 3.5.6).

3.5.1. Controls on Nitrate Isotopes

Studies of nitrate isotopes in rain and snow have suggested that the $\delta^{15}N$ of nitrate is determined primarily by the $\delta^{15}N$ of precursor NO_x, which may vary considerably from different sources. In contrast, the $\delta^{18}O$ of nitrate is influenced by the different pathways of formation of atmospheric HNO_3 prior to deposition (Elliott et al., 2007; Heaton et al., 2004; Hastings et al., 2003; Yeatman et al., 2001; Russell et al., 1998; Freyer, 1991; Heaton, 1990; 1987). Atmospheric HNO_3 is formed primarily through two different oxidation pathways. In the polar summer, NO_2 reacts with OH,

$$NO_2 + OH \rightarrow HNO_3 \qquad (R3.1)$$

while during the polar winter, NO_2 reacts with ozone,

$$NO_2 + O3 \rightarrow NO_3 + O_2 \qquad (R3.2)$$

$$NO_3 + NO_2 + M \leftrightarrow N_2O_5 + M \qquad (R3.3)$$

$$N_2O_5 + H_2O_{(surface,\ aerosol)} \rightarrow 2HNO_3 \qquad (R3.4)$$

$$NO_3 + DMS,\ HC \rightarrow HNO_3 + products \qquad (R3.5)$$

where M refers to an unreactive third body, DMS is dimethylsulfide, and HC is hydrocarbons.

This seasonal difference in the formation pathways of HNO_3 constituted the framework for box modeling of HNO_3 air chemistry at Summit, described in detail in Jarvis et al. (submitted, 2008; see Chapter 2) and Kunasek et al. (2008). Briefly, the $\delta^{18}O$ of gas-phase HNO_3 formed locally at Summit is determined by the reaction rates of HNO_3 formation and seasonally varying concentrations and unique $\delta^{18}O$ values of OH and O_3. The $\delta^{18}O$ of tropospheric O_3 is 90-120‰ versus VSMOW (Johnston and Thiemens, 1997; Krankowsky et al., 1995), while the $\delta^{18}O$ of tropospheric OH is influenced by the $\delta^{18}O$ of water vapor, which ranges between about -60‰ and -25‰ at Summit (Grootes and Stuiver, 1997). The $\delta^{18}O$ of tropospheric OH is also influenced by sink reactions involving CO and CH_4 (e.g., Morin et al., 2007), which prevent 100% equilibration of OH with water vapor. Under summertime conditions at Summit, Kunasek et al. (2008) estimated that these competing reactions result in the equilibration of 90% of OH with water vapor, while 10% of OH retains the isotopic signature of its sources. Considering that the source of OH most enriched in $\delta^{18}O$ is likely O_3 (following O_3 photolysis, $O(^1D) + H_2O \rightarrow 2OH$), it is therefore a good approximation that the maximum $\delta^{18}O$ of OH in the summer at Summit is -11‰ (e.g., 0.1*(+120‰) + 0.9*(-25‰) = -10.5‰).

In contrast to $\delta^{18}O$, the $\delta^{15}N$ of gas-phase HNO_3 is determined in the box model by nitrogen isotope fractionation associated with NO-NO_2 cycling and by the relative concentrations of NO and NO_2 at Summit. Seasonal changes in nitrate isotopes observed in snowpits sampled at Summit in 2001 are only partially explained by this box model. Clearly, other processes, such as the role of halogen chemistry in oxidant cycling and nitrate formation, changes in source emissions of NO_x, and post-depositional recycling of nitrate, may influence the observed seasonal cycle of nitrate isotopes in the Summit snowpack.

Photolysis of nitrate after deposition has the potential to influence both its $\delta^{15}N$ and $\delta^{18}O$ signatures. The primary product of nitrate photolysis, which occurs at wavelengths between 290 and 345 nm, is NO_2 (Jacobi and Hilker, 2007; Boxe et al., 2006; Cotter et al., 2003; Dubowski et al., 2001). HONO can also be indirectly formed from NO_2^- or NO, which are minor products of nitrate photolysis (Jacobi and Hilker 2007; Cotter et al., 2003; Zhou et al., 2001). Blunier et al. (2005) measured the $^{15}N/^{14}N$ fractionation associated with nitrate photolysis and found that irradiated nitrate in laboratory snow became enriched in ^{15}N by 11.7‰. In a similar experiment, McCabe et al. (2005) found that the $\delta^{18}O$ of nitrate in laboratory ice became depleted in ^{18}O after exposure to UV light. McCabe et al. attributed this finding to the local recombination of photolyzed nitrate products with OH and H_2O, which were depleted in ^{18}O relative to the original nitrate.

3.5.2. Potential Isotopic Fractionation During Collection

Under conditions during which not all of the gas-phase HNO_3 is collected in the mist chambers, isotopic fractionation of HNO_3 is possible. However, numerous studies have used mist chambers to efficiently capture gas-phase HNO_3 from the air (e.g., Dibb et al., 1998; 1994). Our measured gas-phase HNO_3 concentrations are not only in agreement with previous observations at Summit (Honrath et al., 2002; Dibb et al., 1998; 1994), they are also consistent throughout this study despite the different mist chamber setups and flow rates used (see Section 3.4.1). While it is possible that some isotopic fractionation does influence the $\delta^{18}O$ and $\delta^{15}N$ of collected HNO_3, it is unlikely that it would result in the consistent 40‰ difference observed between gas-phase HNO_3 and snow nitrate given the varying flow rates, water volumes, and number of mist chambers. We therefore conclude that the difference in $\delta^{18}O$ between gas-phase HNO_3 and snow nitrate is not a result of isotopic fractionation during HNO_3 collection.

3.5.3. Potential Interference from Filters

One possible explanation for the difference in $\delta^{18}O$ between snow nitrate and gas-phase HNO_3 involves interference from the filters used at the inlet and at the top of the mist chamber samplers. We explore the influence of 1) the presence of particulates on the inlet filters, 2) the contamination of mist chamber samples with particulates from the inlet filters, and 3) the presence of water droplets on the top filters.

First, considerable amounts of nitrite and nitrate were detected on the hydrophobic inlet filters of the mist chamber samplers (total N = nitrate + nitrite = 1.26 to 20.74 μM) and on filter blanks (total N = 1 to 2.5 μM) . Because the inlet filters are not expected to absorb gas-phase HNO_3, any nitrate detected on the filters is likely to have been deposited there either as particulate nitrate or nitrite or as snow containing nitrate. The dominance of nitrite on the filter samples and blanks, equal to 74-78% of the total N, suggests contamination, since measurements at Summit in 2007 showed very low concentrations of particulate nitrite (J. Dibb, personal communication, 2008). Previous studies have also found low concentrations of particulate nitrate at Summit (e.g., Bergin et al., 1995; Dibb et al., 1994).

Furthermore, isotopic measurements of the $\delta^{18}O$ of nitrate on filter samples range from -8‰ to +59‰. Because the $\delta^{18}O$ of filter nitrate is depleted in ^{18}O relative to the snow nitrate, the nitrate or nitrite present on the filters does not account for the 40‰ enrichment in $\delta^{18}O$ of snow nitrate relative to gas-phase HNO_3. Only if the $\delta^{18}O$ of the filter nitrate was enriched relative to the snow nitrate (i.e., filter nitrate $\delta^{18}O$ greater than +80‰) would it be possible for the filters to account for the observed isotopic difference between snow nitrate and gas-phase HNO_3.

Second, it is possible for inlet filter nitrate and/or nitrite, whether a result of particulates or contamination, to have an influence on the $\delta^{18}O$ of gas-phase HNO_3 measured with the mist chambers. Because each inlet filter is exposed for the 48-hour duration of sampling, some particulates collected on the filter may undergo sublimation to the gas phase and become incorporated into the mist chamber sample. For example,

if a small amount of filter nitrate with $\delta^{18}O$ of +10‰ escapes past the filter and into the mist chamber water, it might result in a lower measured value of the $\delta^{18}O$ of gas-phase HNO_3 for that particular sample. However, we note that there is a large variability in the amount of nitrate and nitrite on the filter samples. If filter nitrate did influence the measured $\delta^{18}O$ of mist chamber nitrate, we would expect that this large variability would translate to a large variability in mist chamber nitrate $\delta^{18}O$, which is not observed.

Finally, scattered water droplets were occasionally observed on the hydrophobic filter at the top of each mist chamber, which prevented water vapor from exiting the mist chambers. Of the approximately 20 top filters that were analyzed for nitrate concentration, all contained as much total nitrogen as the inlet filter samples and filter blanks. Isotopic measurements of a select number of filters indicate that the measured $\delta^{18}O$ of nitrate from the top filters are comparable to the $\delta^{18}O$ of nitrate measured in the mist chambers. Thus the presence of nitrate and nitrite on these top filters does not account for the difference in $\delta^{18}O$ of nitrate between mist chamber samples and surface snow samples.

We conclude that interference from filters is not the likely cause of the ~40‰ difference between the $\delta^{18}O$ of snow nitrate and the $\delta^{18}O$ of gas-phase HNO_3.

3.5.4. Photolytic Recycling

Another explanation for the discrepancy between $\delta^{18}O$ of gas-phase HNO_3 and surface snow nitrate is that gas-phase HNO_3 in the near-surface atmosphere at Summit is dominated by recently photolyzed nitrate from the snow surface. It is possible that photolyzed and recombined HNO_3 represents a small portion of the gas-phase HNO_3 in the air column above the snowpack at Summit, yet a large portion of the gas-phase HNO_3 directly above the snow, where our mist chambers were located. We consider this to be a likely scenario given the numerous studies that report large emissions of

NO_x from snow surfaces (e.g., Beine et al., 2002; Honrath et al., 2002; 1999; Jones et al., 2001; 2000) and the short lifetime of NO_2 against conversion to HNO_3.

Once emitted from the snow after nitrate photolysis, NO_2 will cycle rapidly with NO at a rate much faster than NO_2 conversion to HNO_3. Ignoring potential oxygen isotopic fractionations associated with photolytic cycling of NO and NO_2, the $\delta^{18}O$ of NO_2 released from the snowpack upon nitrate photolysis will quickly become dominated by the $\delta^{18}O$ of local oxidants. The subsequent recombination of photolyzed nitrate products with ambient OH (via *R3.1*), which has a negative $\delta^{18}O$ value due to rapid isotopic exchange with water vapor (Grootes and Stuiver, 1997), would lower the $\delta^{18}O$ of recombined HNO_3 from measured surface nitrate values. To explore this idea further, we utilize a box model of HNO_3 air chemistry at Summit, described in Jarvis et al. (submitted, 2008; see Chapter 2) and Kunasek et al. (2008).

Using a range of 90-120‰ in $\delta^{18}O$-O_3 and a summertime $\delta^{18}O$-OH value ranging between -25‰ and -11‰ (see Section 3.5.1.), our box model calculations suggest that the summertime $\delta^{18}O$ of recombined HNO_3 should range between +40 and +55‰. This calculated value of $\delta^{18}O$ of recombined HNO_3 is similar to the range in $\delta^{18}O$ of gas-phase HNO_3 measured in our mist chambers (+25 to +47‰), supporting the idea that the mist chambers predominantly collected recombined HNO_3. The imperfect agreement with the entire range in measured $\delta^{18}O$ of gas-phase HNO_3 may be a result of using a simplified model which does not take into account the potential influence of halogen chemistry (e.g., Morin et al., 2007) or oxygen isotope fractionations during HNO_3 production, which have not yet been fully quantified (e.g., Savarino et al., 2008).

Assuming that the mist chambers collected photolyzed and recombined HNO_3, should we expect to see evidence of this in the $\delta^{15}N$ of snow nitrate and gas-phase HNO_3? Based on the results of Blunier et al. (2005), we expect an 11.7‰ difference between the $\delta^{15}N$ of snow nitrate and that of NO_2, the primary product of nitrate photolysis. Because the average $\delta^{15}N$ of snow nitrate at Summit is -5.5‰ in June (Table 3.1), we assume that the $\delta^{15}N$ of NO_2 emitted from the snow must be 11.7‰ less

than this value, or -17.2‰. This isotope fractionation associated with nitrate photolysis may be partially balanced by the fractionation associated with NO-NO_2 cycling. In a study of NO_x in an urban atmosphere, Freyer et al. (1993) found that as NO_2 cycles with NO, the resulting NO_2 becomes enriched in ^{15}N relative to NO. While relative concentrations of NO, NO_2, OH and O_3 at Summit are very different from urban regions, the effective fractionation factor ($\alpha = 1.018$) measured by Freyer et al. is the only non-laboratory estimate available. Taking this fractionation into account and assuming that, initially, $\delta^{15}N$-NO_x is equal to $\delta^{15}N$-NO_2, box model calculations suggest that the $\delta^{15}N$ of recombined HNO_3 is -9.2‰ in June. This value is more negative than the average observed $\delta^{15}N$ of gas-phase HNO_3 (-3.8‰ ± 0.7; Table 3.1), although it is within the range of our measurements.

It is thus highly probable that the gas-phase HNO_3 collected in the mist chambers originated primarily from recently photolyzed snow nitrate. No other explanation can account for the observed discrepancy in $\delta^{18}O$ between gas-phase HNO_3 and snow nitrate. While we expect photolyzed nitrate products to be depleted in ^{15}N relative to snow nitrate (based on the photolytic fractionation measured by Blunier et al., (2005)), we observe the same $\delta^{15}N$ values in snow nitrate and in gas-phase HNO_3. This suggests two possible scenarios. First, under conditions of 100% recycling of photolyzed nitrate products, the nitrogen isotope fractionation associated with nitrate photolysis must counteract the effective fractionation of local HNO_3 recombination such that we are unable to observe a difference in $\delta^{15}N$ between gas-phase HNO_3 and snow nitrate with these measurements. This scenario requires a small, non-zero fractionation between snow nitrate and locally produced, gas-phase HNO_3 in order for the $\delta^{15}N$ of snow nitrate to remain constant over the diurnal cycle and between snowfall events (as we observe). A second scenario is that the nitrogen isotope fractionation between snow nitrate and gas-phase HNO_3 is large, yet export of photolyzed nitrate products occurs such that we do not observe a difference in $\delta^{15}N$ between snow nitrate and gas-phase HNO_3.

3.5.5. Implications of Photolytic Recycling and Loss

3.5.5.1. $\delta^{18}O$ of Nitrate

With active photolysis incorporating the $\delta^{18}O$ of local oxidants into recombined and redeposited HNO_3, the nitrate isotopes in surface snow may change over time. Here we examine the maximum influence of photolytic recycling and photolytic loss on the $\delta^{18}O$ of snow nitrate.

The burial flux of nitrate in snow (F_{burial}) is a balance between the nitrate deposited to the snow (F_{dep}), the nitrate lost from the snow (F_{lost}), and the nitrate recombined in the air and redeposited to the snow (F_{redep}) (Figure 3.7):

$$F_{burial} = F_{dep} - F_{lost} + F_{redep}$$

Nitrate associated with each of these fluxes has a unique $\delta^{18}O$ signature, such that

$$(\delta^{18}O_{burial} + 1000)*F_{burial} = (\delta^{18}O_{dep} + 1000)*F_{dep} - (\delta^{18}O_{lost} + 1000)*F_{lost} + (\delta^{18}O_{redep} + 1000)*F_{redep}$$

Combining literature estimates of these fluxes with isotope measurements from this study, we determine the expected $\delta^{18}O$ of nitrate buried in snow ($\delta^{18}O_{burial}$) following photolytic recycling of snow nitrate and following photolytic loss of snow nitrate. Our calculation represents the maximum expected change between isotopes of nitrate deposited to snow and isotopes of nitrate buried in snow. We note that this calculation refers only to the uppermost snow layer, and that we ignore the possible influence of changes in the distribution of nitrate after burial. For example, photolysis or volatilization of nitrate at great depths could result in an upward flux of nitrate to the surface layer from below. The importance of such processes will depend on the snow accumulation rate, the e-folding depth of nitrate photolysis in snow, the physical properties of the firn (e.g., density), and the location of nitrate within the snow grains themselves.

To first focus on the effects of photolytic recycling, we assume that 100% of the nitrate lost from snow is redeposited ($F_{lost} = F_{redep}$). Thus the deposition flux of nitrate to snow is equal to the burial flux of nitrate. We calculate the deposition flux of nitrate

to snow using the June average of our field measurements of surface snow nitrate concentration (2.9μM) and assuming a constant snow accumulation of 0.18 cm day^{-1} (Dibb and Fahnestock, 2004) and snow density of 0.24 g cm^{-3}. The June average of our snow nitrate $\delta^{18}O$ values (81‰) represents the $\delta^{18}O$ of deposited nitrate ($\delta^{18}O_{dep}$). The average of our measurements of $\delta^{18}O$ of gas-phase HNO_3 (34‰) represents recombined nitrate, or $\delta^{18}O_{redep}$. The $\delta^{18}O$ of photolyzed nitrate products ($\delta^{18}O_{lost}$) is equal to our snow nitrate measurements ($\delta^{18}O$ = 81‰) assuming no oxygen isotope fractionation during nitrate photolysis. Because McCabe et al. (2005) found ice nitrate to be depleted in ^{18}O after irradiation, any oxygen isotope fractionation, which is expected to enrich the remaining nitrate, must be relatively small. (We note that McCabe et al. (2007) report an oxygen isotopic effect of -3.5‰ for laboratory measurements of nitrate photolysis, but it is not clear if this value, which derives from McCabe et al. (2005), includes some accounting for the recombination of HNO_3 products with water vapor.)

We adjust published measurements of NO_x fluxes at Summit to the measured nitrate concentration in snow during this study. Honrath et al. (2002) measured average NO_x and HONO emissions from the snow surface at Summit in Summer 2000 to be 2.52 x 10^{12} molecules m^{-2} s^{-1} and 4.64 x10^{11} molecules m^{-2} s^{-1}, respectively. Assuming a constant snow accumulation of 0.18 cm day^{-1} (Dibb and Fahnestock, 2004) and snow density of 0.24 g cm^{-3}, this upward flux of NO_x represents 19% of the downward nitrate deposition flux derived from the average surface nitrate concentration measured during the same study. Assuming that this flux ratio of upward NO_x to downward nitrate is relatively constant each year, the concentration of surface snow nitrate in this study and the ratio of NO_x emission to snow nitrate deposition from Honrath et al. (2002) allows us to estimate F_{lost}.

Using these boundary conditions, we solve for the $\delta^{18}O$ of nitrate buried in snow ($\delta^{18}O_{burial}$). For 100% redeposition of photolyzed nitrate products (i.e., photolytic recycling), we calculate that the $\delta^{18}O$ of buried nitrate (+73.6‰) is 7‰ depleted in ^{18}O relative to the $\delta^{18}O$ of deposited nitrate (+81‰).

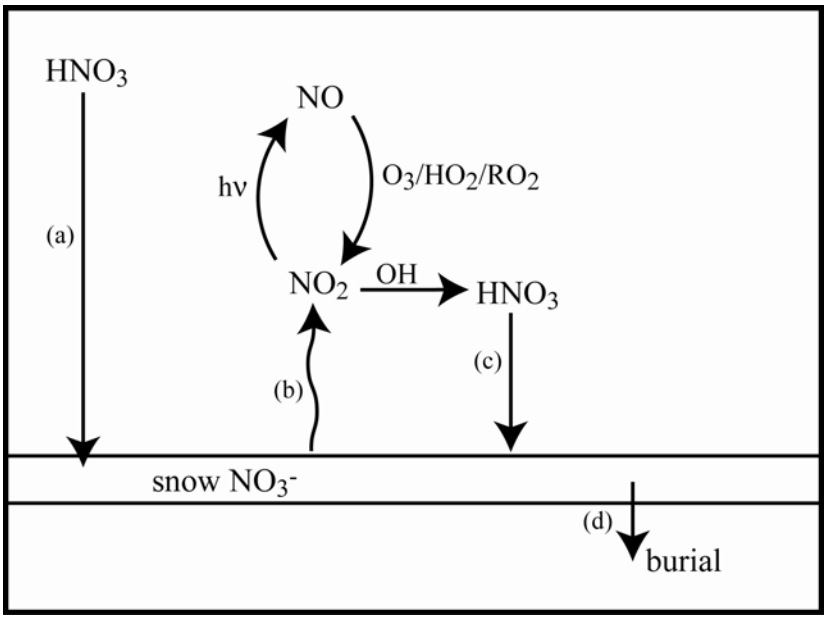

Figure 3.7. A schematic of the general photolytic processes influencing the $\delta^{18}O$ of nitrate in a layer of surface snow. The (d) $\delta^{18}O$ of buried snow nitrate ($\delta^{18}O_{burial}$) is influenced by (a) the deposition of HNO_3 to the snow surface ($\delta^{18}O_{dep}$), (b) the photolysis of nitrate from the snow in the form of NO_2 ($\delta^{18}O_{lost}$), and (c) the recombination and redeposition of HNO_3 from photolyzed nitrate products ($\delta^{18}O_{redep}$).

The redeposition of 100% of NO_x emitted from the surface snow may not be a valid assumption at Summit, especially during the summer months. Honrath et al. (2002) found that upward fluxes of NO_x and HONO exceeded downward fluxes of gas-phase HNO_3. While the difference between these observed fluxes may be negated by snow and fog deposition of HNO_3, the primary source of new nitrate to the snow surface (e.g., Bergin et al., 1995), Honrath et al.'s observations suggest that NO_x may be exported away from Summit. Furthermore, studies of nitrate concentration in snowpits and fresh snow at Summit suggest up to a 7-25% loss of nitrate from surface snow over 1-2 years (Burkhart et al., 2004; Dibb et al., 2007). Therefore we also calculate the $\delta^{18}O$ of buried nitrate if only 10% of photolyzed nitrate is redeposited back to the snow (F_{lost}*0.1 = F_{redep}). This results in a reduced burial flux of nitrate; the burial flux of nitrate is equal to 83% of the deposition flux of nitrate because not all of the photolyzed nitrate is returned to the snow. For this scenario, we calculate that the $\delta^{18}O$ of buried nitrate (+80.1‰) is 0.9‰ depleted relative to the $\delta^{18}O$ of deposited nitrate (+81‰).

Our calculations suggest that the $\delta^{18}O$ of buried snow nitrate should be altered, at most, by 7‰ due to photolytic near-surface recycling with 100% redeposition, and potentially not at all with some amount of export of photolyzed nitrate products away from Summit. We note that these values are dependent on the difference between $\delta^{18}O$ of deposited snow nitrate and that of recombined HNO_3. If we were to increase the difference between the two (i.e., using a $\delta^{18}O$ value of deposited snow nitrate greater than +81‰ or a $\delta^{18}O$ value of recombined HNO_3 less than +34‰), the change in $\delta^{18}O$ of buried snow nitrate due to near-surface photolytic recycling would be greater. Conversely, decreasing the difference between the input $\delta^{18}O$ values would produce a smaller change in $\delta^{18}O$ of buried snow nitrate. A different value of the $\delta^{18}O$ of recombined HNO_3 is possible, given that it is influenced by the $\delta^{18}O$ of the oxidant involved in HNO_3 formation and the isotopic signatures of OH and O_3 are quite different. However, it is unlikely that the $\delta^{18}O$ of locally recombined HNO_3 will change significantly over the summer since the OH oxidation pathway dominates summertime

HNO_3 production at Summit (see Chapter 2). Furthermore, we consistently observe a ~40‰ difference between measured values of $\delta^{18}O$ of gas-phase HNO_3 and snow nitrate. Thus it is unlikely that these estimates of the influence of photolytic loss and photolytic recycling on the $\delta^{18}O$ of buried snow nitrate would change significantly.

3.5.5.2. $\delta^{15}N$ of Nitrate

We follow a similar method to calculate the $\delta^{15}N$ of nitrate buried in snow following photolytic recycling, but we additionally account for the observed nitrogen isotope fractionation associated with nitrate photolysis (α_{photo}). Based on the laboratory experiments of Blunier et al. (2005), we assume that the $\delta^{15}N$ of nitrate photolyzed from snow is 11.7‰ depleted in ^{15}N relative to the deposited snow nitrate ($\delta^{15}N_{lost} = \alpha_{photo} * \delta^{15}N_{dep}$). Because our measured June average $\delta^{15}N$ of snow nitrate and gas-phase HNO_3 agree within the standard errors of the mean (Table 3.1), we use the same value to represent the $\delta^{15}N$ of nitrate deposited to the snow and of recombined HNO_3 redeposited to the snow ($\delta^{15}N_{dep} = \delta^{15}N_{redep} = -5.5‰$).

If 100% of the photolyzed nitrate products are redeposited to the surface snow (i.e., photolytic recycling), we expect the $\delta^{15}N$ of snow nitrate to remain constant, since there is no net loss of nitrogen from snow. However, using the photolytic fractionation factor from Blunier et al. (2005) and our observation that the $\delta^{15}N$ of gas-phase HNO_3 above the snow surface is equal to the $\delta^{15}N$ of snow nitrate, we find that the $\delta^{15}N$ of buried nitrate (-3.6‰) is enriched by 1.9‰ relative to the deposited nitrate (-5.5‰). With 10% redeposition of photolyzed nitrate products, we calculate that the $\delta^{15}N$ of buried snow nitrate (-3.3‰) is 2.2‰ enriched in ^{15}N relative to deposited nitrate (-5.5‰).

The calculated enrichment in $\delta^{15}N$ of buried nitrate following 100% photolytic recycling, as opposed to the expected null effect, highlights the need for a better understanding of the nitrogen isotope fractionation associated with local HNO_3 recombination. If 100% photolytic recycling of nitrate takes place at Summit, our

measurements indicate that the effective fractionation between snow nitrate and gas-phase HNO_3 is smaller than we can observe. If photolytic loss of nitrate takes place at Summit, our measurements indicate that the export of photolyzed nitrate products balances the effective fractionation between snow nitrate and gas-phase HNO_3 such that we do not observe a difference in $\delta^{15}N$ between the species. We note that in either case, our observations suggest a small influence (< ~2‰) on the $\delta^{15}N$ of buried snow nitrate at Summit.

3.5.5.3. Labeled Nitrate

The influence of photolytic recycling at Summit was further explored in the field using labeled nitrate enriched in ^{15}N, which was sprayed on an area of surface snow at Summit. The $\delta^{15}N$ of surface snow nitrate collected from the labeled nitrate region shows a clear decrease over the first three days of sampling (Figure 3.8). The $\delta^{15}N$ decreased ~100‰, from +940‰ to +840‰ vs. VSMOW, not including the last sample, which was collected after fresh snow had fallen. There are no differences in nitrate concentration or $\delta^{18}O$ of nitrate between labeled snow samples and control snow samples (not shown).

We use the framework presented above to model the evolution of $\delta^{15}N$ in a layer of surface snow (1 cm deep, 1 m^2 area) with a starting $\delta^{15}N$ value of +940‰. We account for the nitrogen isotope fractionation associated with nitrate photolysis, but we do not account for any fractionation associated with local recombination of HNO_3. After three days of photolytic recycling with 100% redeposition, the $\delta^{15}N$ of nitrate in the layer of surface snow decreases by 138‰. This modeled decrease occurs because even though snow nitrate is becoming enriched as a result of photolytic loss, we set the $\delta^{15}N$ of deposited nitrate and locally recombined HNO_3 to be equal to our gas-phase HNO_3 measurements, or -5.5‰. The magnitude of the addition of newly deposited snow nitrate is also greater than the magnitude of photolytic loss of nitrate. Thus nitrate in the snow layer becomes depleted in ^{15}N rather quickly. With 10% redeposition, the

$\delta^{15}N$ of snow nitrate decreases by a smaller amount (121‰) because less of the locally recombined HNO_3 is redeposited to the snow.

We note that the observed decrease in $\delta^{15}N$ of nitrate from the labeled snow region is only possible with photolytic recycling, whether it is 10% or 100% of locally photolyzed nitrate products. No new snow deposition occurred over the first three days of sampling, yet the $\delta^{15}N$ of labeled snow nitrate decreased. Because the labeled region is surrounded by natural snow, we expect that redeposited HNO_3 has a $\delta^{15}N$ signature similar to natural snow. Since photolytic loss without redeposition will enrich the snow nitrate, the observed depletion in ^{15}N is indicative of some amount of recycling of photolyzed nitrate products.

The $\delta^{15}N$ of nitrate sampled in 10-cm snowpits from the labeled nitrate and control snow regions is shown in Figure 3.9. We attribute the measured increase in $\delta^{15}N$ of nitrate in the labeled snowpit at 2-4 cm depth to the original labeled nitrate layer. This depth is consistent with ~0.18 cm day^{-1} of snow accumulation (Dibb and Fahnestock, 2004). After 17 days of photolytic recycling, we calculate that the $\delta^{15}N$ in a snow layer starting at +940‰ would decrease to +382‰ with 100% redeposition, and to +412‰ with 10% redeposition of HNO_3. These values are approximately 2.5 to 3 times the $\delta^{15}N$ value measured in the snowpit. Since only enough labeled nitrate was sprayed to thinly coat the snow surface, we expect that the labeled snowpit samples, each of which represent a snow depth of 2 cm, include some mixing of natural snow and labeled snow. Such mixing with natural snow would decrease the $\delta^{15}N$ of measured nitrate. Therefore an exact comparison of $\delta^{15}N$ in the snowpit with $\delta^{15}N$ in the surface snow is difficult, as it is clear that labeled nitrate mixed with natural snow, diffused and/or was redeposited over a depth of ~2 cm of snow.

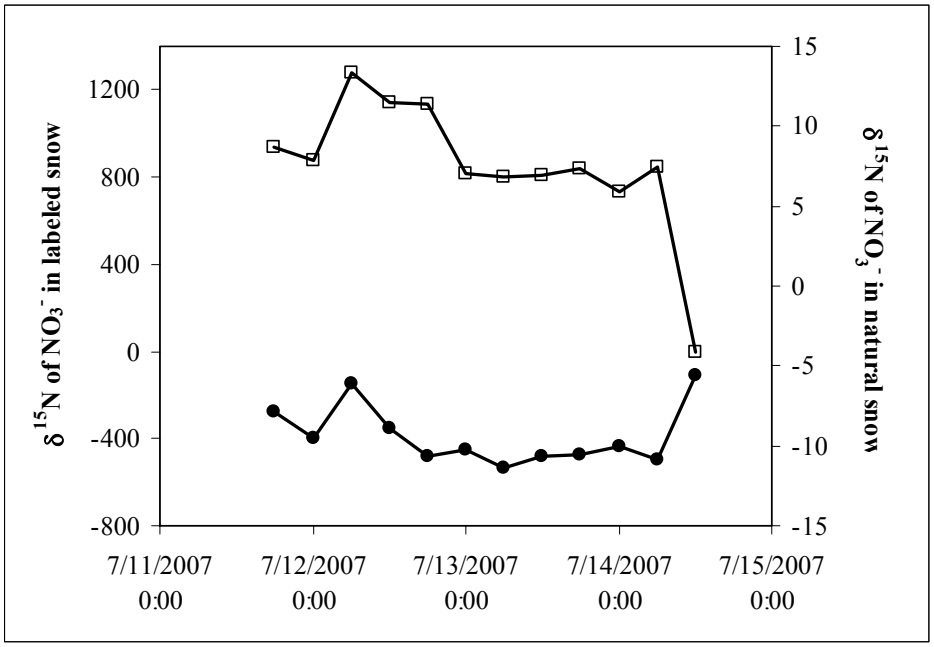

Figure 3.8. The $\delta^{15}N$ of nitrate (‰ vs. N_2) in surface snow sampled from an unaltered control region (filled circles, versus the right axis) and a region sprayed with labeled nitrate (open squares, versus the left axis). Data courtesy of M.G. Hastings.

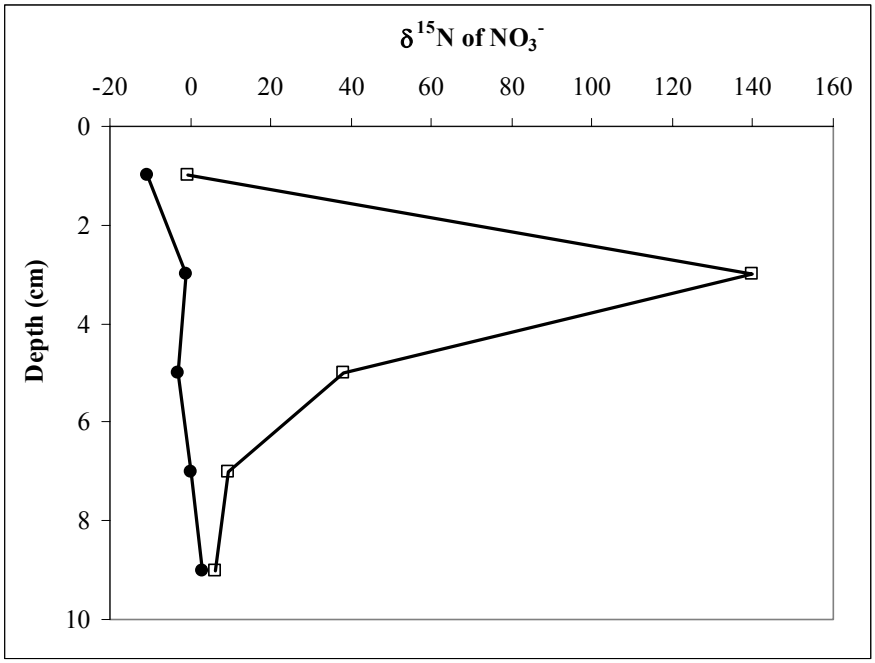

Figure 3.9. The $\delta^{15}N$ (‰ vs. N_2) of nitrate in 10-cm snowpits from the unaltered control region (filled circles) and the labeled nitrate region (open squares), collected 17 days after labeled nitrate enriched in ^{15}N was sprayed on the snow surface in the labeled nitrate region. Data courtesy of M.G. Hastings.

We find that the labeled nitrate experiments confirm the presence of active photolysis in the Summit snowpack, exhibiting a decrease in $\delta^{15}N$ over time. These measurements imply some amount of photolytic recycling at Summit, as an enrichment in $\delta^{15}N$ of labeled nitrate with time, expected with 100% photolytic loss, is not observed.

3.5.6. Seasonal-Annual Changes in Nitrate Isotopes at Summit

The analysis presented in Section 3.5.5 concludes that photolytic recycling and photolytic loss of snow nitrate have different effects on the $\delta^{15}N$ and $\delta^{18}O$ of nitrate preserved in snow at Summit. With photolytic recycling (i.e., 100% redeposition of photolyzed nitrate products), we expect the $\delta^{15}N$ of nitrate buried in snow to remain unchanged from initial values and the $\delta^{18}O$ of snow nitrate to exhibit a depletion of as much as -7‰. This is because the nitrogen isotope composition of snow nitrate is conserved with 100% redeposition, while the oxygen isotope composition of snow nitrate is influenced by the incorporation of local oxidants into redeposited nitrate. With photolytic loss of nitrate (i.e., < 100% redeposition of photolyzed nitrate products), we expect the $\delta^{15}N$ of nitrate buried in snow to exhibit a maximum enrichment of +2.2‰ and the $\delta^{18}O$ of snow nitrate to exhibit a depletion of -0.9‰. In light of the different isotopic influences of photolytic recycling and loss, we examine the temporal changes in our measurements of snowpack nitrate.

We compare seasonal averages of $\delta^{15}N$ and $\delta^{18}O$ of nitrate in surface snow samples from this study with snowpit samples from this study and from Kunasek et al. (2008) (Figure 3.10). For surface snow collected during the periods of July 2005 to March 2006 and August 2006 to March 2007, all samples were analyzed for nitrate concentration yet only a few samples from each season were analyzed for $\delta^{15}N$ and $\delta^{18}O$ of nitrate. Seasonal bins in both snowpits were determined based on the $\delta^{18}O$ of snow, which is known to vary seasonally with temperature (Grootes and Stuiver, 1997). Some variability in nitrate concentration and isotopes is expected due to the spatial variability in snow sampling and snowpit locations. Because a reliable interpretation of

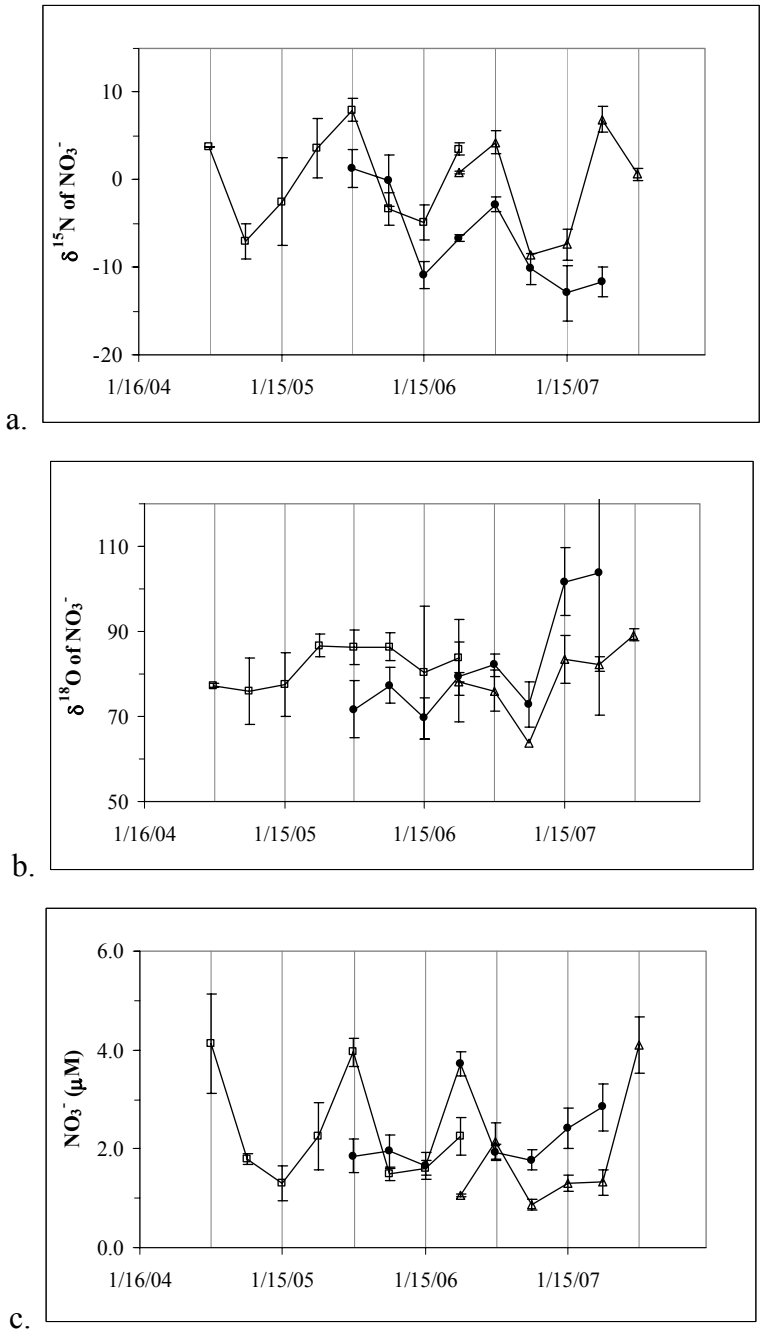

Figure 3.10. A comparison of (a) $\delta^{15}N$ of nitrate (‰ vs. N_2), (b) $\delta^{18}O$ of nitrate (‰ vs. VSMOW), and (c) nitrate concentration (μM) in surface snow (filled circles) and snowpit samples (open triangles: 2007 snowpit; open squares: 2006 snowpit). Vertical lines denote the midpoints of winter and summer seasons. Seasonal bins are reported as averages ±1 standard error of the mean. Nitrate concentrations shown in (c) represent all collected samples, including those not analyzed for isotopes. The 2006 snowpit data is courtesy of S.A. Kunasek and M.G. Hastings.

these data is contingent on how well the limited surface snow measurements represent each season and on how well the snowpit seasonal bins represent the true season of snow deposition, we offer only general observations.

Most notable from this comparison is that seven of the eight overlapping seasons exhibit enriched $\delta^{15}N$ values of snowpit nitrate as compared to surface snow nitrate (Figure 3.10a). This suggests that there may be an enrichment in $\delta^{15}N$ of snow nitrate over time, which is in agreement with previous calculations of the effects of photolytic loss of snow nitrate (Section 3.5.5). However, the maximum expected change in $\delta^{15}N$ enrichment of nitrate in buried snow (+2.2‰) is much smaller than the actual enrichments we observe (as large as +7‰), which either implies the presence of an additional influence on $\delta^{15}N$ of snow nitrate, or reflects significant spatial variability of nitrate isotopes in the snow at Summit. The snowpits were not sampled in the exact same location as the surface snow samples, and it is possible that local spatial variations contribute sampling noise to our measurements of surface snow nitrate isotopes.

We observe no consistent relationship in the $\delta^{18}O$ of nitrate or in nitrate concentration between seasonal bins of surface snow and snowpit samples (Figure 3.10b, c). Seasonal bins of surface snow nitrate are enriched in ^{18}O relative to same-season bins in the 2007 snowpit, yet depleted relative to same-season bins in the 2006 snowpit. The lack of a consistent change in nitrate concentrations between surface snow and snowpit samples is further indication that the $\delta^{15}N$ measurements reflect spatial variability rather than an enrichment over time, as a slight decrease in concentration is expected if $\delta^{15}N$ enrichment is observed.

Finally, we note that the overall seasonal changes in nitrate isotopes measured in surface snow are preserved in the snowpit samples. This suggests that any post-depositional change involving snowpack nitrate at Summit does not influence nitrate isotopes on a scale larger than that of the observed seasonal cycle, which is in agreement with the calculations presented in Section 3.5.5 detailing the isotopic influence of photolytic recycling and loss of nitrate. Quantifying the role of photolytic recycling versus photolytic loss at Summit using these seasonal observations is difficult,

since there is some amount of spatial variability in nitrate concentration and isotopes, as well as some error associated with the designation of snowpit seasonal bins. The analysis of surface snow nitrate over established transects at Summit would help to quantify the spatial variability of nitrate isotopes in snow. In addition, any isotopic effects associated with nitrate volatilization and diffusion in snow must be studied in greater detail.

3.6. Conclusions

We present measurements of the $\delta^{15}N$ and $\delta^{18}O$ of gas-phase HNO_3 and surface snow nitrate from Summit, Greenland. The $\delta^{15}N$ of HNO_3 is similar in surface snow and in air sampled 1.5 meters above the snow surface. The average $\delta^{18}O$ of snow nitrate is ~40‰ greater than the average $\delta^{18}O$ of gas-phase HNO_3. The possibility that this difference in $\delta^{18}O$ is due to oxygen isotope fractionation during HNO_3 collection or to interference from nitrate or nitrite on the inlet filters can be ruled out. We conclude that the gas-phase samples represent locally recombined HNO_3 that originated from photolyzed snow nitrate.

The similarity between $\delta^{15}N$ in gas-phase HNO_3 and snow nitrate samples appears to be at odds with independent observations suggesting that nitrate lost from snow surfaces is depleted in ^{15}N. This suggests that the nitrogen isotope fractionation associated with photolysis and volatilization of snow nitrate may be largely counteracted by the fractionations associated with atmospheric NO-NO_2 cycling and local recombination of HNO_3. Alternatively, it is possible that the similarity between $\delta^{15}N$ in gas-phase HNO_3 and snow nitrate indicates that export removes isotopically light photolyzed nitrate products from the atmosphere above the snow surface.

Taken together, the $\delta^{15}N$ and $\delta^{18}O$ measurements from this study suggest a minimal influence of photolysis on the isotopic composition of nitrate archived in the firn and ice at Summit. With summertime photolytic recycling, we expect no change on the $\delta^{15}N$ of nitrate buried in snow because there is no net loss of nitrate. Since

photolytic recycling incorporates the isotopic signature of local oxidants into the $\delta^{18}O$ of recombined HNO_3, we expect a -7‰ change, at most, in the $\delta^{18}O$ of nitrate buried in snow. With photolytic loss, the amount of recombined HNO_3 returned to snow does not equal the amount of photolyzed nitrate lost from snow, and the $\delta^{15}N$ of buried snow nitrate becomes enriched by a maximum of +2.2‰ while the $\delta^{18}O$ of snow nitrate becomes depleted by -0.9‰.

Previous studies have found little net loss of nitrate from the snow at Summit. Although summertime emissions of NO_x from the snowpack are high, most of the NO_x and gas-phase HNO_3 is recycled back to the snow. Surface snow experiments with labeled nitrate enriched in ^{15}N confirm that significant recycling of nitrate occurs in the surface snow at Summit. We calculate that photolytic recycling with natural snow nitrate accounts for the entire decrease in $\delta^{15}N$ of labeled snow nitrate over a period of 3 days, and a majority of the decrease in $\delta^{15}N$ of labeled snow nitrate over a period of 17 days. As labeled nitrate was lost from the snow surface, it was replaced quickly with nitrate of natural isotopic composition. The remainder of the observed change is likely due to other processes such as diffusion and/or mixing with natural snow.

Quantifying the isotopic effects associated with post-depositional processing of snow nitrate will greatly benefit the study of nitrate isotopes in ice core records from Summit. Further studies are needed to clarify the influence of the spatial variability in nitrate at and around Summit. In addition, measurements of any isotopic effects associated with other post-depositional processes, such as volatilization and diffusion, will help to quantify the degree of post-depositional processing at Summit. Comprehensive isotopic modeling of air chemistry and post-depositional processes at Summit will also aid in our understanding of the preservation of snow nitrate at Summit.

Chapter 4

A Method for the Collection and Nitrogen Isotope Analysis of Atmospheric NO_2 in Remote Environments

4.1. Summary

We present laboratory tests utilizing aqueous triethanolamine bubblers for the collection of gas-phase NO_2. Detailed tests carried out under various laboratory conditions resulted in a standard method for field collection of NO_2 in remote regions. First measurements of the $\delta^{15}N$ of atmospheric NO_2 at Summit, Greenland indicate that the $\delta^{15}N$ of NO_2 ranges between +12.8‰ and -4.6‰ vs. N_2 during early summer 2006. These values are similar to the $\delta^{15}N$ of gas-phase HNO_3 collected during the same period, which implies that the nitrogen isotope fractionation associated with NO_2 oxidation to HNO_3 is small.

4.2. Introduction

It is well known that post-depositional losses of nitrate from snow in Greenland and Antarctica lead to emissions of NO_x (= NO + NO_2) from the surface snow (Beine et al., 2002; Honrath et al., 2002; 1999; Jones et al., 2001; 2000). Once emitted from the snow, NO_2 can be transported away from its emission site (representing post-depositional loss of snow nitrate) or it can be oxidized back to HNO_3 and locally redeposited to the snow surface (representing post-depositional recycling of snow nitrate). Post-depositional loss and post-depositional recycling impact the isotopes of snow nitrate in different ways, as discussed in Chapter 3. Understanding the relationships between the isotopic composition of snow nitrate, emitted NO_2, and recombined HNO_3 is a necessary step towards the quantification of the air-to-snow transfer of nitrate, which, in turn, is vital to the interpretation of ice core records of nitrate. With the goal of characterizing the isotopic composition of NO_2 in the air above

the surface snow at Summit, Greenland, we present laboratory tests of a method for the collection of NO_2 in remote regions for later isotopic analysis.

4.3. Methods

Previous laboratory and field efforts to collect NO_2 have primarily utilized triethanolamine (TEA, $(HOCH_2CH_2)_3$-N), which converts gas-phase NO_2 to nitrite (NO_2^-). Common methods of collection include the use of aqueous solutions of TEA with bubblers, impingers, or flasks (Nonamura et al., 1996; Freyer et al., 1993; Levaggi et al., 1973), molecular sieves impregnated with TEA (Willey et al., 1977; Levaggi et al., 1973), and passive diffusion tubes containing TEA coated stainless steel mesh or filter paper (Gerboles et al., 2005; Hansen et al., 2001; Glasius et al., 1999; Krochmal and Kalina, 1997).

Our choice of an NO_2 sampling method was largely influenced by proven methods of gas collection at Summit, Greenland. Mist chambers, in which water is misted over a fast-flowing stream of sampled air, are commonly used to collect gas-phase HNO_3 and HONO from the air at Summit (Dibb et al., 2002; 1998; 1994), and our work shows that the isotopic composition of the collected gas-phase species can be measured reliably (Chapter 3). Gas-phase NO_2 can be collected in a similar fashion by replacing misting water with an aqueous solution of TEA. During preliminary fieldwork in Greenland in 2005, we tested water and TEA mist chambers for the collection of gas-phase HNO_3 and NO_2 above the snow surface. After early laboratory tests indicated incomplete NO_2 removal using the TEA mist chambers (not shown), we began examining the NO_2 collection efficiency using aqueous TEA bubblers, a technique similar to that used by Nonamura et al., 1996. Sampled air is pulled through two connected bubblers, where NO_2 in the air is captured by reaction with TEA (Figure 4.1). Fine frits (pore size of 4-5.5μm) in each bubbler increase the surface area of interaction of bubbled air with the TEA solution. Filter housing on the top of each bubbler hold hydrophobic filters (Millipore Fluoropore Membrane Filter, 1.0 μm)

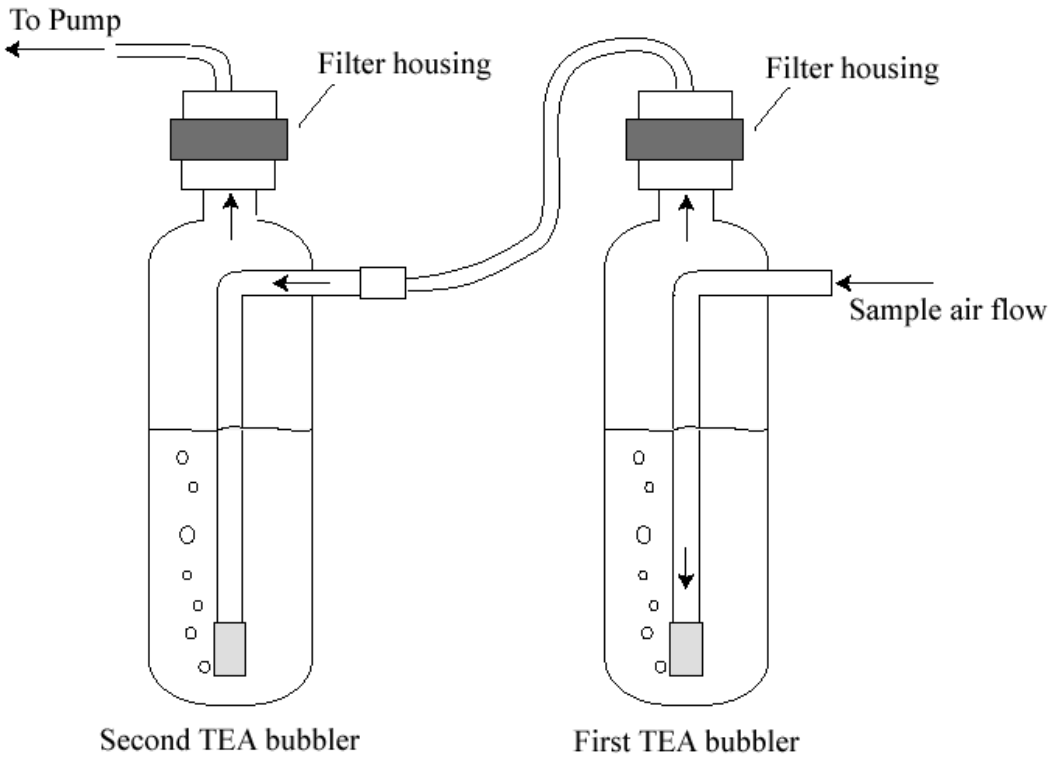

Figure 4.1. Schematic of the TEA bubbler setup in which two bubblers are combined. Arrows denote the flow of air through the bubblers. The filter housing holds hydrophobic filters to prevent TEA solution from exiting the bubblers. For field sampling in Greenland, an inlet filter on the first bubbler prevented gas-phase HNO_3 and particulates from entering the bubblers.

to prevent the TEA solution, which bubbles vigorously in the bubblers, from exiting the sampling chamber.

In laboratory tests, bubblers were connected with Teflon tubing to a pump, which pulled room air through the bubblers at various flows rates. For 60-minute sampling intervals, a flow of NO_2 was directed into the inlet of the first bubbler from a compressed gas cylinder of 5 ppm NO_2 (balance N_2). The flow of NO_2 was limited to 50 and 100 sccm (standard cubic centimeters per minute) using a mass flow meter. A datalogger recorded 1-minute averages of the flow of room air through the bubblers. Flow rates were adjusted such that the expected amount of NO_2 sampled in 60 minutes approximately matched the expected amount of NO_2 collected over 48 hours at Summit, Greenland, where NO_2 concentrations are typically less than 60 pptv (Yang et al., 2002).

For field measurements at Summit, a filter (Whatman filter paper, ashless, Grade 41, 20-25μm pore size) on the sampling inlet of the first bubbler prevented gas-phase HNO_3 and particulates from entering the bubbler chamber. The sampling inlet was located 1.5 meters above the snow surface. The bubblers sampled air continuously for 48-hour intervals, during which time aqueous TEA solution was continually added to the bubblers to maintain a volume of 60-90 mL in each bubbler. Average flow rates through the bubblers were recorded every two minutes and ranged from 5 to 8 LPM.

All laboratory and field samples were stored frozen in amber HDPE containers until the day of analysis. Nitrite and nitrate (NO_3^-) concentrations were measured using a Dionex ion chromatograph with an IonPac AS11-HC column (2x250mm) and an eluent concentration (KOH) of 20mM. The error in nitrate and nitrite concentration measurements is ± 0.2μM and ± 0.05μM, respectively. While the use of suppressed ion chromatography has been shown to give a lower detection limit of nitrite in TEA samples than unsuppressed IC (Krochmal and Kalina, 1997), we find that the nitrite and nitrate peaks in our (suppressed IC) chromatograms are located on the back slope of a large peak which distorts the baseline. The nitrite and nitrate peaks of all samples presented here were integrated in the same manner, although we note the possibility of

variable sample error resulting from the variability in this distorted baseline between samples.

Several studies have explored the stoichiometry of the reaction of TEA with NO_2. Recent work has shown that the reaction of TEA with NO_2 produces NO_2^- in a 1:1 conversion of NO_2 to nitrite (Glasius et al., 1999; Palmes et al., 1976), in contrast to prior studies which suggested that the conversion ratio of NO_2 to nitrite is closer to 2:1 with half of the sampled NO_2 bound up in a TEA complex (Gold, 1977; Levaggi et al., 1972). For proposed TEA complexes of triethanolamine nitrate (Levaggi et al., 1972), triethanoammonium nitrate (Gold, 1977), and nitrosodiethanolamine ($(HOCH_2CH_2)_2$-N-N=O, observed by Aoyama and Yashiro, 1983), the measured concentration of nitrite and nitrate should account for all of the sampled NO_2 (Krochmal and Kalina, 1997). We therefore use the total nitrate and nitrite concentration of each sample to determine the volume of sample required to achieve 10nmol N for isotopic analysis.

The $\delta^{15}N$ of nitrite and nitrate was measured using the denitrifier method (Casciotti et al., 2002; Sigman et al., 2001). Denitrifying bacteria (*Pseudomonas aureofaciens* and *Pseudomonas chlororaphis*) are used to convert nitrite and nitrate to N_2O, which is then analyzed using a continuous flow mass spectrometer. We have no reason to suspect that the denitrifying bacteria used for isotopic analysis will treat the NO_2-TEA complexes differently, as complete conversion of nitrogen oxides to N_2O is expected. The $\delta^{15}N$ of each sample was calibrated to air N_2 using internationally recognized reference standard IAEA-NO-3, which has a $\delta^{15}N$ of +4.7‰ versus N_2 (Böhlke and Coplen, 1995; Gonfiantini et al., 1995). For this study, we assign the 1σ error in $\delta^{15}N$ measurements for a given batch of samples to be equal to the standard deviation in $\delta^{15}N$ of IAEA-NO-3 standards for that batch. The 1σ error for samples presented here ranges from ± 0.1 to 6‰.

4.4. Results and Discussion

Over the course of three years, we completed three separate sets of tests of NO_2 collection using TEA bubblers. In 2006, using only nitrite and nitrate concentration as a measure of bubbler efficiency, we investigated the influences of TEA concentration, volume of aqueous TEA solution, and flow rate on NO_2 collection. For select tests repeated in 2006 and 2007, we analyzed bubbler samples for the $^{15}N/^{14}N$ isotope ratio of nitrite and nitrate. Finally, in 2008, we performed further bubbler tests using a different 5ppm NO_2 gas cylinder.

4.4.1. 2006 Bubbler Tests Using Concentration Measurements

For these initial tests, we report the percent of expected NO_2 collected as a measure of collection efficiency. The expected NO_2 is calculated from the known concentration of the NO_2 tank, the flow of NO_2, and the collection time for a given sampling period.

$$\text{Expected } NO_2 \text{ (nmol)} = [NO_2]_{tank} * NO_2 \text{ flow} * \text{collection time}$$

The collection efficiency for each test is thus calculated from the expected NO_2 and the total measured nitrite and nitrate concentration. For all samples presented here, nitrate accounts for less than 10% of the total nitrite and nitrate concentration.

$$\text{Collection Efficiency (\%)} = \frac{([NO_2^-] + [NO_3^-])_{measured} * \text{volume of sample}}{\text{Expected } NO_2} * 100\%$$

We do not measure or account for potential evaporative losses of the TEA solution during the course of each test. In the event that evaporative losses of TEA solution volume did occur, the NO_2 collection efficiencies reported here overestimate the true NO_2 collection efficiency. However, it is unlikely that the solution volume changed significantly over each 60-minute test.

The flow of room air through the bubblers was choked at the pump using flow control valves, but the exact flow and temporal variations in flow were not recorded for these tests. Thus for the results presented here, we assume that the room air flow during each test was constant and equal to the limit of the flow control valve used. The flow of NO_2 into the bubblers from the tank was held constant at 50 or 100 sccm with a mass flow meter.

4.4.1.1. Concentration of TEA Solution

The standard concentration of TEA solution used in these experiments was calculated to be in excess of 1:1 reaction of TEA with NO_2. Increasing the concentration of the TEA solution resulted in an apparent lower collection efficiency (Table 4.1). This may be due to interference between the large TEA-related peak and the nitrite and nitrate peaks during IC analysis, which may mask the true nitrite and nitrate concentration.

Table 4.1. The percent of expected NO_2 collected in two bubblers inline using two different concentrations of aqueous TEA solution.

[TEA] (mM)	Room air flow (LPM)	NO_2 flow (sccm)	Collection Efficiency (%)
13.4	11.6	100	62.1
			75.4
			76.7
53.6	11.6	100	52.9
			54.9

4.4.1.2. Volume of TEA Solution

The volume of aqueous TEA solution in each bubbler was varied to evaluate the effects of volume on NO_2 collection efficiency (Table 4.2). Variations in TEA volume at two different flow rates of room air show no major increase in the NO_2 collection efficiency.

For tests with 0 LPM room air flow, tubing from the NO_2 gas cylinder was connected directly to the bubbler inlet, effectively forcing NO_2 in N_2 gas to be bubbled through the TEA mixture. These tests show increased NO_2 collection efficiency over tests at 11.6 LPM room air flow. This is to be expected, since 0 LPM room air flow results in an overall lower flow rate of NO_2 through the bubblers, which likely increases the residence time of NO_2 in the TEA solution and allows for more complete reaction. We note that a total flow of 50 or 100 sccm through the bubblers is not realistic for field experiments.

As a result of these tests, and because volumes in excess of 100 mL had a tendency to bubble up into the tubing beyond the top of the bubblers, a standard volume of 80 mL of TEA solution was used for future tests.

Table 4.2. The percent of expected NO_2 collected in two bubblers inline using different volumes of an aqueous TEA solution at two different room air flows. For the first two samples listed at 0 LPM room air flow and 80 mL TEA volume (italicized), a leak between the first and second bubbler likely led to decreased pressure in the first bubbler and a lowered collection efficiency of NO_2.

Volume (mL)	Room air flow (LPM)	NO_2 flow (sccm)	Collection Efficiency (%)
80	0	100	*53.9*
			38.0
			90.8
			88.8
120	0	100	92.5
			91.1
160	0	100	92.7
			97.6
80	11.6	100	62.1
			75.4
			76.7
100	11.6	100	68.1
120	11.6	100	43.2
160	11.6	100	71.7

4.4.1.3. Number of Bubblers

Several tests of NO_2 collection efficiency were conducted using a variable number of bubblers connected inline (Table 4.3). Significantly lower collection efficiencies are measured when only one bubbler is used. We attribute this to a large pressure differential between the bubblers, created when two or more bubblers are connected inline. Such a pressure differential likely results in a longer residence time of sampled air in the first bubbler, thereby increasing the overall collection efficiency for the bubbler set. While these tests indicate that three bubblers connected inline are

preferable, a standard setup of two bubblers was used for future tests due to limited laboratory resources.

Table 4.3. The percent of expected NO_2 collected using 1, 2, and 3 bubblers connected inline.

Number of bubblers inline	Room air flow (LPM)	NO_2 flow (sccm)	Collection Efficiency (%)
1	11.6	100	18.7
			26.9
2	11.6	100	62.1
			75.4
			76.7
3	11.6	100	88.5
			89.8

4.4.1.4. Room Air Flow Rate

Based on the results presented in Table 4.2, which show a higher NO_2 collection efficiency for tests with 0 LPM room air flow, we investigated NO_2 collection efficiency under conditions of variable room air flow rate (Table 4.4). While these tests were conducted without the aid of flow meters and dataloggers to measure and record the total flow, the flow control valves used were expected to choke the room air flow to 3.3, 5.5 and 11.6 LPM STP. We observe the highest collection efficiency at flow rates of 5.5 LPM.

Table 4.4. The percent of expected NO_2 collected under variable room air flow rates.

Room air flow (LPM)	NO_2 flow (sccm)	Collection Efficiency (%)
3.34	100	67.4
5.45	100	87.5
		89.8
11.6	100	62.1
		75.4
		76.7

4.4.2. 2006 and 2007 Bubbler Tests Using $\delta^{15}N$ Measurements

4.4.2.1 Isotopic Fractionation in the First Bubbler

After establishing a standard sampling setup based on the concentration tests discussed in Section 4.4.1. (2 bubblers sampling inline, each with 80 mL of aqueous TEA solution of ~13mM concentration), a select number of bubbler tests were repeated at a variety of flow rates to generate samples for the isotopic analysis of NO_2. For the 20 tests completed in 2006 and the four tests completed in 2007, the flow of NO_2 was held constant at either 50 or 100 sccm while the flow of room air through the bubblers varied from test to test between 3.3 and 13 LPM.

The NO_2 collection efficiency for these tests, calculated from the nitrite and nitrate collected in both bubblers, ranges from 45 to 108% (Figure 4.2). The $\delta^{15}N$ of nitrite/nitrate, shown in Figure 4.3, averaged -52‰ vs. N_2 in the first bubbler and -27‰ vs. N_2 in the second bubbler. That the $\delta^{15}N$ of nitrite/nitrate in the second bubbler is more enriched in ^{15}N than in the first bubbler might be expected, since the collection of NO_2 is, in part, kinetically driven and the lighter isotope is expected to react with TEA faster than the heavier isotope.

The kinetic isotopic fractionation (α_{KIE}) associated with the reaction of NO_2 and TEA can be approximated from the relationship

$$\alpha_{KIE} = k_{15}/k_{14} = (\mu_{14}/\mu_{15})^{1/2} \qquad (4.1)$$

where k_{14} and k_{15} are the rate constants and μ_{14} and μ_{15} are the reduced masses corresponding to the reaction of TEA with $^{14}NO_2$ and $^{15}NO_2$, respectively. The reduced mass (μ) is equal to the quantity $(m_1*m_2)/(m_1+ m_2)$, where m_1 and m_2 correspond to the masses of the reactants. Thus

$$\alpha_{KIE} =((46*149)*(47+149) / (46+149)*(47*149))^{1/2} = 0.9918$$

and

$$\varepsilon_{KIE} = (\alpha_{KIE} - 1)* 1000‰ = -8.2‰.$$

With incomplete collection of NO_2, we therefore expect that NO_2 captured by TEA will be depleted in ^{15}N compared to the NO_2 reservoir from which it was captured.

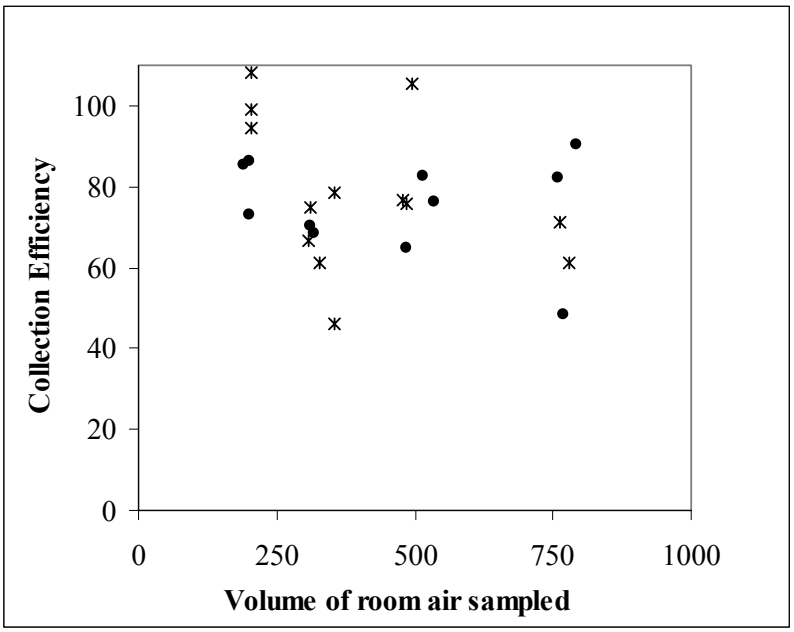

Figure 4.2. The percent of expected NO_2 collected in both bubblers with 100 sccm NO_2 flow (filled circles) and 50 sccm NO_2 flow (stars). The volume of room air sampled (L) is calculated from the recorded 1-minute averages of room air flow rates.

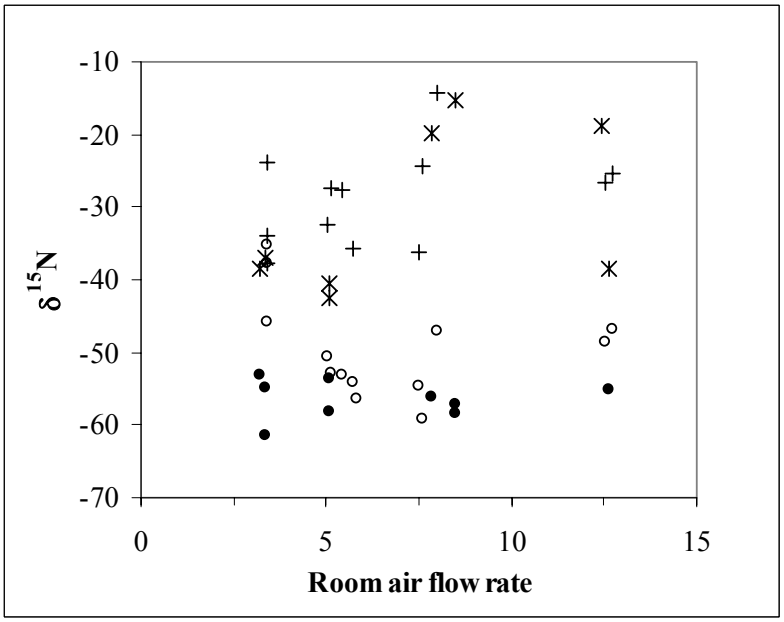

Figure 4.3. The $\delta^{15}N$ (‰ vs. N_2) of nitrite and nitrate collected at various room air flow rates (LPM) with 100 sccm NO_2 flow in the first (solid circles) and second (stars) bubblers and with 50 sccm NO_2 flow in the first (open circles) and second (crosses) bubblers.

In order to use the TEA bubblers to collect atmospheric NO_2 in the field for isotopic analysis, it is imperative that we quantify any isotopic fractionation associated with bubbler collection of NO_2. Despite a rather large range in the fraction of expected NO_2 collected in the first bubbler (Figure 4.4), the $\delta^{15}N$ of nitrite/nitrate is generally between -40 and -60‰ vs. N_2. This small range in $\delta^{15}N$ suggests that the isotopic fractionation associated with NO_2 collection in the first bubbler must be fairly small. We calculate this fractionation and the $\delta^{15}N$ of NO_2(gas) using a Rayleigh relationship,

$$\frac{\delta^{15}N_{Nitrite+Nitrate}}{\delta^{15}N_{NO2(gas)}} = f^{\alpha - 1} \qquad (4.2)$$

where f is the fraction of expected NO_2 collected in the first bubbler, $\delta^{15}N_{Nitrite+Nitrate}$ corresponds to the $\delta^{15}N$ measured in the first bubbler inline, and $\delta^{15}N_{NO2(gas)}$ corresponds to the NO_2 originating from the gas cylinder. This relationship implies that α is the nitrogen isotope fractionation factor associated with NO_2 collection, defined as:

$$\alpha = \frac{\delta^{15}N_{NO2(gas)} + 1000}{\delta^{15}N_{Nitrite+Nitrate} + 1000} \qquad (4.3)$$

A value of α greater than 1.00 implies a depletion in $\delta^{15}N_{Nitrite+Nitrate}$ relative to $\delta^{15}N_{NO2(gas)}$, while a value of α less than 1.00 implies an enrichment in $\delta^{15}N_{Nitrite+Nitrate}$ relative to $\delta^{15}N_{NO2(gas)}$. Rearranging Equation 4.2 into a linear form, a plot of $\ln(\delta^{15}N_{Nitrite+Nitrate})$ versus $\ln(f)$ will yield a straight line with a slope of $(\alpha - 1)$ and a y-intercept of $\ln(\delta^{15}N_{NO2(gas)})$ (Figure 4.5). Using this relationship, we calculate the fractionation associated with NO_2 collection in the first bubbler to be 1.008 (or ε = +8‰) and the $\delta^{15}N$ of the tank to be -49‰ vs. N_2.

Interestingly, the Rayleigh fractionation calculated from the experimental data (using Equation 4.2) and the kinetic isotope fractionation calculated previously from theory (Equation 4.1) are equal in magnitude (8‰). Both suggest that the NO_2 captured in the first bubbler with TEA ($\delta^{15}N_{Nitrite+Nitrate}$) is depleted in ^{15}N relative to $\delta^{15}N_{NO2(gas)}$. From this we conclude that the isotopic fractionation associated with

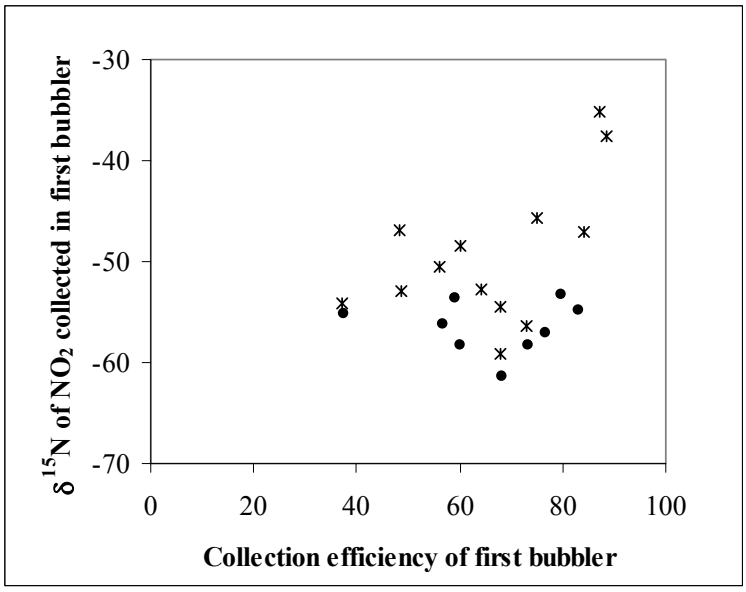

Figure 4.4. The $\delta^{15}N$ (‰ vs. N_2) of nitrite and nitrate collected in the first bubbler with 100 sccm NO_2 flow (filled circles) and 50 sccm NO_2 flow (stars) versus the collection efficiency of NO_2 (%) in the first bubbler.

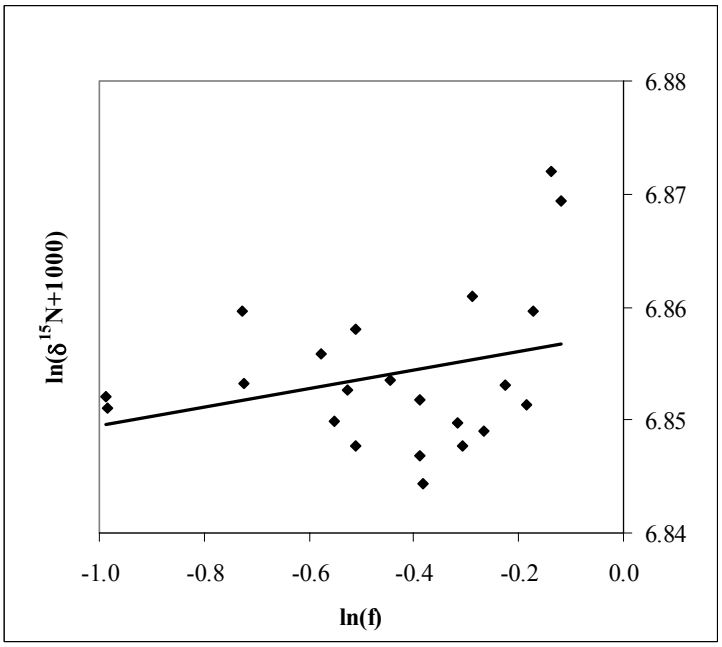

Figure 4. 5. A plot of $\ln(\delta^{15}N_{Nitrite+Nitrate})$ versus $\ln(f)$, where $\delta^{15}N_{Nitrite+Nitrate}$ is the $\delta^{15}N$ of NO_2 collected in the first bubbler and f is the fraction of expected NO_2 collected in the first bubbler. Following the linear form of Equation 4.2, the slope of the line is equivalent to $(\alpha - 1)$ and the y-intercept represents $\ln(\delta^{15}N_{NO2(gas)})$.

NO_2 collection in the first TEA bubbler is due entirely to the kinetic isotope fractionation associated with the reaction of NO_2 and TEA.

4.4.2.2. Isotopic Fractionation in the Second Bubbler

Given that the observed isotopic fractionation of NO_2 collection associated with the first bubbler inline is entirely explained by the 8‰ kinetic fractionation associated with the TEA + NO_2 reaction, it is possible that the same is true for the isotope fractionation associated with NO_2 collection in the second bubbler. To calculate the Rayleigh fractionation associated with the second bubbler, we first account for the amount of NO_2 captured in the first bubbler. Following the linear form of Equation 4.2, we then plot $\ln(\delta^{15}N_{(Nitrite+Nitrate)-2})$ versus $\ln(f_2)$, where $\delta^{15}N_{(Nitrite+Nitrate)-2}$ and f_2 correspond to the $\delta^{15}N$ of NO_2 and the amount of expected NO_2 collected in the second bubbler, respectively. We calculate the isotopic fractionation associated with NO_2 collection in the second bubbler to be 1.005 (or ε = +5‰), where

$$\alpha = \frac{\delta^{15}N_{NO2(gas)\ after\ first\ bubbler} + 1000}{\delta^{15}N_{(Nitrite+Nitrate)-2} + 1000}$$

We calculate that the $\delta^{15}N$ of NO_2(gas) after partial collection in the first bubbler is -23‰. We expect that the NO_2(gas) will be slightly enriched in ^{15}N after passing through the first bubbler, since the first bubbler preferentially collects ^{14}N. However, this calculated value is more enriched than the expected $\delta^{15}N$ of -39‰ ± 4, which is derived from the 8‰ fractionation associated with collection in the first bubbler and from the NO_2 collection efficiencies of the first bubbler. This discrepancy likely reflects the uncertainty associated with these calculations, since isotopic and concentration measurements over several days of bubbler testing are averaged together and the concentrations derived from IC analysis and isotopic analysis differ (discussed in Section 4.4.2.3).

4.4.2.3. Readjusted Concentrations

We note that there is a discrepancy between the total nitrite and nitrate concentration calculated from IC measurements and the total nitrite and nitrate concentration indicated from isotopic measurements. For isotopic analysis with the denitrifier method, the volume of sample analyzed is adjusted such that all samples and standards in a given batch have an equivalent amount (in nmol) of total nitrate and nitrite. Following isotopic analysis, we can calculate the total nitrite and nitrate concentration of each sample by comparing its total peak area to that of a known standard.

On average, we find that concentrations derived from IC analysis are 15% lower than concentrations derived from the peak area on the mass spectrometer. This difference may be attributed to the difficulty in defining nitrite and nitrate IC peaks (discussed in Section 4.3), or may be a indication of the difficulties associated with using bacteria to convert nitrite and nitrate in solutions containing TEA. While isotopic tests of nitrate standards mixed with TEA show good reproducibility of $\delta^{15}N$ (not shown), it is possible that the bacteria process NO_2-TEA complexes and nitrate in TEA solution differently.

Using the readjusted concentration of total nitrate and nitrite for each sample, we calculate the isotopic fractionation associated with NO_2 collection in the first bubbler to be 0.9994 (ε = -0.6‰) and the $\delta^{15}N$ of the gas cylinder to be -52‰. The isotopic fractionation associated with NO_2 collection in the second bubbler is calculated to be 1.005 (ε = +5‰) and the $\delta^{15}N$ of NO_2(gas) after partial collection in the first bubbler is calculated to be -26‰ vs. N_2.

This analysis suggests that NO_2 collected in the first bubbler may be fractionated as little as -0.6‰. While this is entirely possible, we note that there is some uncertainty associated with determining nitrite and nitrate concentrations using the denitrifier method. After readjusting concentrations, nearly one third of the tests return greater than 100% NO_2 collection efficiency for the combined bubblers, with calculated collection efficiencies reaching as high as 136%. This either suggests the presence of NO_2 in the room air sampled or suggests that the gas cylinder contained up to 7 ppm

NO_2 rather than 5 ppm NO_2. These bubbler tests were conducted over several days, and because the room air was not tested for NO_2 each day, it is possible that the observed collection efficiencies greater than 100% are a result of contamination from room air. However, we would expect to see such contamination reflected in the isotopic signature of the sampled NO_2, which we do not.

On the other hand, the NO_2 concentration in the gas cylinder was not certified to 5 ppm, and it is possible that the concentration exceeded 5 ppm. Independent testing of the gas cylinder concentration was inconclusive, but suggested that the NO_2 concentration is actually lower than 5 ppm (D. Reidmiller, personal communication 2007). Because we cannot rule out the possibility that the concentration discrepancy is due to a higher-than-reported NO_2 concentration in the gas cylinder, we conclude that the overall isotopic fractionation associated with NO_2 collection in the first bubbler is between -0.6‰ and +8‰.

4.4.3. 2008 Bubbler Tests Using $\delta^{15}N$ Measurements

The capture and recovery of NO_2 during bubbler tests conducted in 2008 was much worse than in previous experiments in 2006 and 2007. While the earlier tests suggested an average recovery of 77% NO_2, tests conducted in 2008 suggest an average recovery of only 43% NO_2 (Figure 4.6). Furthermore, the $\delta^{15}N$ of NO_2 collected in the first bubbler varied considerably from test to test, ranging -22‰ to -53‰ (Figure 4.7).

There are several reasons we do not have much confidence in the 2008 tests. First, recent column and eluent problems have decreased our ability to accurately measure nitrite and nitrate concentrations using ion chromatography. Second, several variables were altered during the 2008 tests, some of which may have influenced the collection efficiency of the bubblers. For example, a different NO_2 gas cylinder was used in these tests, which were conducted in a different laboratory room near a positive pressure laminar flow hood. Furthermore, a blank sample test, with 0 sccm NO_2 flow from the gas tank, indicated the presence of NO_2 in the room air (with a $\delta^{15}N$ value of -4 ± 0.1‰). We therefore do not further examine the data from the 2008 tests.

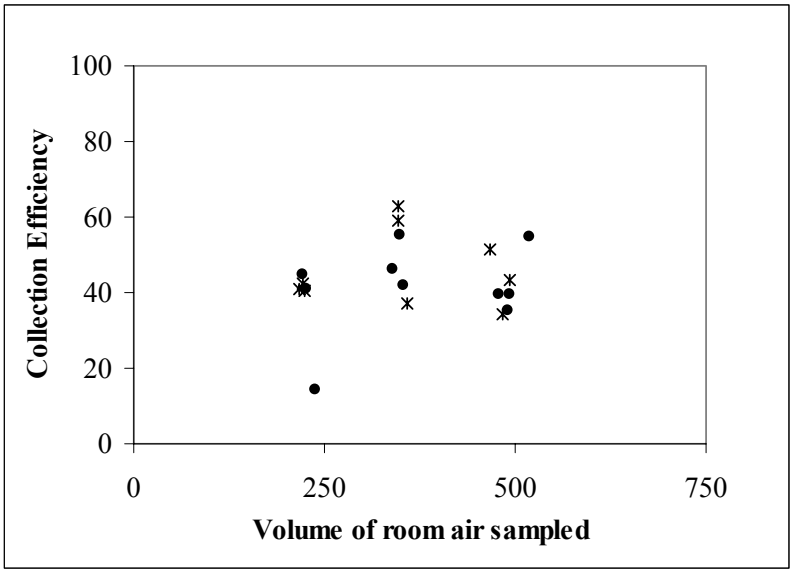

Figure 4.6. The percent of expected NO_2 collected in both bubblers during the 2008 tests with 100 sccm NO_2 flow (filled circles) and 50 sccm NO_2 flow (stars). The volume of room air sampled (L) is calculated from the recorded 1-minute averages of room air flow rates.

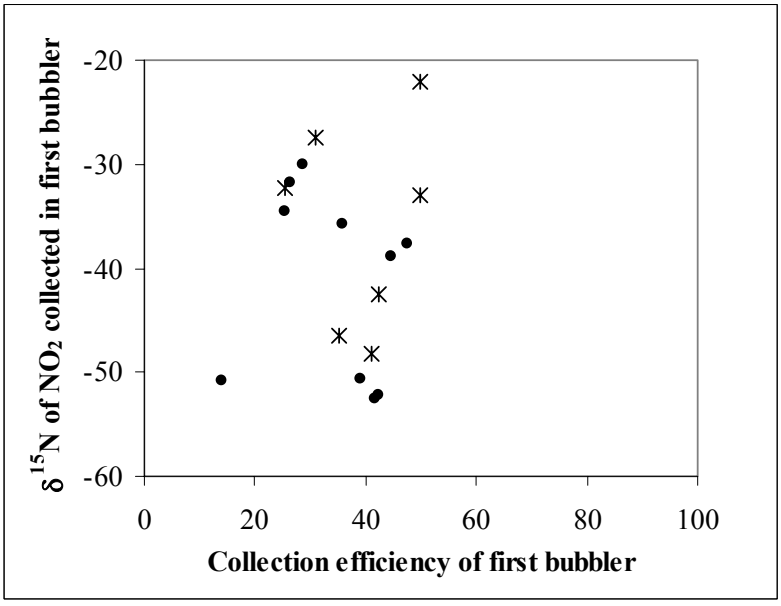

Figure 4.7. The $\delta^{15}N$ (‰ vs. N_2) of nitrite and nitrate collected in the first bubbler during the 2008 tests with 100 sccm NO_2 flow (filled circles) and 50 sccm NO_2 flow (stars) versus the collection efficiency of NO_2 (%) in the first bubbler.

4.4.4. Field Measurements from Summit, Greenland

Field testing of TEA bubblers took place at Summit, Greenland during March-July of 2006. As mentioned previously, each bubbler sample represents 48 continuous hours of sampling, which was necessary to generate enough nitrite and nitrate for isotopic analysis. The concentration of atmospheric NO_2 at Summit in Spring and Summer 2006 derived from bubbler concentrations and flow rates ranged from 48 to 145 pptv (22.4 pptv = 1nmol m^{-3}), slightly greater than previous estimates of NO_2 concentration at Summit which are typically less than 60 pptv (e.g., Honrath et al., 2002; Yang et al., 2002). It is therefore a reasonable assumption that the TEA bubblers exhibited 100% collection efficiency of NO_2 at Summit. We present isotopic measurements of gas-phase NO_2 sampled during four separate periods at Summit (Table 4.5). Sampling took place in the clean air sector at Summit, although we note that the sample collected between 6/06/2006 and 6/08/2006 was affected by camp emissions for approximately one half of the sampling period.

Assuming 100% collection efficiency, we can assume a Rayleigh process to calculate the true $\delta^{15}N$ of NO_2 at Summit ($\delta^{15}N_{NO2\text{-}Summit}$). We utilize the isotopic measurements of NO_2 collected in the first bubbler ($\delta^{15}N_{sample}$) and the fraction of total N collected in the first bubbler (f_{Sample}):

$$\frac{\delta^{15}N_{sample}}{\delta^{15}N_{NO2\text{-}Summit}} = f_{Sample}^{\,\alpha - 1} \qquad (4.4)$$

In Section 4.4.2, we found that the isotopic effect (ε) of NO_2 collection in the first bubbler is between -0.6‰ and +8‰ (α = 0.9994 and 1.008). Using these values of α as end-members of the possible values of isotope fractionation in the first bubbler, we calculate that the $\delta^{15}N$ of NO_2 at Summit ranges from -4.6 to +12.8‰. This is comparable to isotopic measurements of the $\delta^{15}N$ of NO_x sources, which range between -13 and +22‰ (e.g., Savarino et al., 2007; Saurer et al., 2004; Ammann et al., 1999; Heaton, 1990; Hoering, 1957). Furthermore, the measured range in $\delta^{15}N$ of NO_2 at Summit is similar to the $\delta^{15}N$ of gas-phase HNO_3 at Summit over the same time period

(Table 4.6 and Figure 4.8; see Chapter 3 for details on surface snow and gas-phase HNO_3 measurements). This similarity validates the assumption that the $\delta^{15}N$ of HNO_3 reflects the $\delta^{15}N$ of precursor NO_2, which was central to previous box modeling of local atmospheric HNO_3 chemistry at Summit (Chapter 2). Accounting for an isotope fractionation of +8‰ associated with NO_2 collection with the TEA bubblers, we find that the $\delta^{15}N$ of NO_2 at Summit is slightly enriched relative to gas-phase HNO_3. This is in agreement with theoretical calculations of the fractionation between NO_2 and HNO_3, which suggest a small enrichment (3‰) in the $\delta^{15}N$ of HNO_3 formed from NO_2 oxidation (Freyer, 1991).

A detailed interpretation of these data in the context of post-depositional recycling or loss of nitrate at Summit is difficult due to the limited number of measurements. In Figure 4.8., we display measurements of the $\delta^{15}N$ of NO_2 and gas-phase HNO_3 together with $\delta^{15}N$ measurements of surface snow nitrate. During the sampling periods between 5/24/2006 and 5/30/2006, the $\delta^{15}N$ of NO_2 is slightly enriched relative to that of gas-phase HNO_3 and snow nitrate. However, for the sampling periods between 6/02/2006 and 6/08/2006, the $\delta^{15}N$ of NO2 is comparable to gas-phase HNO_3. While we cannot quantify the exact nitrogen isotope fractionation associated with NO_2 oxidation to HNO_3 using these measurements, we can constrain the fractionation to be on the order of or less than 10‰. Additional measurements of the $\delta^{15}N$ of NO_2, concurrent with measurements of HNO_3 in the air and snow, will clarify the influence of post-depositional processing of nitrate at Summit.

Table 4.5. The $\delta^{15}N$ of NO_2 (‰ vs. N_2) collected 1.5 meters above the snow surface at Summit, Greenland during 2006. The error in $\delta^{15}N$ associated with each bubbler sample is equal to the standard deviation of IAEA-NO-3 standards in that sample batch. The samples collected between 5/26 and 5/30 were isotopically analyzed 2+ times, thus the reported error represents the standard error of the mean for those tests. The range of $\delta^{15}N$ of NO_2 at Summit is calculated from the $\delta^{15}N$ of nitrite and nitrate in the first bubbler and the range in isotopic fractionation associated with that bubbler (Equation 4.4).

Sampling period	$\delta^{15}N$ 1st bubbler	$\delta^{15}N$ 2nd bubbler	NO_2 (pptv)	Fraction of total N in 1st bubbler	Calculated range of $\delta^{15}N$-NO_2 at Summit
5/24 18:00 – 5/26 18:00	-1.2 ± 5.9	-4.4 ± 5.9	141	0.44	-1.7 to 5.4
5/26 19:00 – 5/30 20:00	7.0 ± 3.4	9.2 ± 6.5	145	0.49	6.6 to 12.8
6/02 18:00 – 6/06 19:30	-4.2 ± 5.9	-2.8 ± 5.9	65	0.52	-4.6 to 1.0
6/06 20:40 – 6/08 19:30	-3.2 ± 5.9	-5.9 ± 5.9	139	0.41	-3.7 to 4.0

Table 4.6. The $\delta^{15}N$ of gas-phase HNO_3 (‰ vs. N_2) collected 1.5 meters above the snow surface at Summit, Greenland during 2006. Gas-phase HNO_3 was collected using water mist chambers (see Chapter 3 for further details).

Sampling period	$\delta^{15}N$ of gas-phase HNO_3 (single mist chamber)	$\delta^{15}N$ of gas-phase HNO_3 (double mist chamber)	
		1st MC	2nd MC
5/24 18:00 – 5/26 18:00	-	-4.6 ± 4.1	-2.2 ± 3.3
5/26 19:00 – 5/28 19:00	-	-4.1 ± 4.1	-
5/28 20:00 – 5/30 20:00	-5.9 ± 4.1	-5.4 ± 4.1	-1.3 ± 3.3
6/02 18:00 – 6/04 19:00	0.1 ± 1.7	0.9 ± 1.0	-3.5 ± 3.3
6/04 19:50 – 6/06 19:30	-2.2 ± 1.3	-11.4 ± 4.1	-1.0 ± 3.3
6/06 20:40 – 6/08 19:30	0.2 ± 2.6	-3.1 ± 1.0	-1.7 ± 3.3

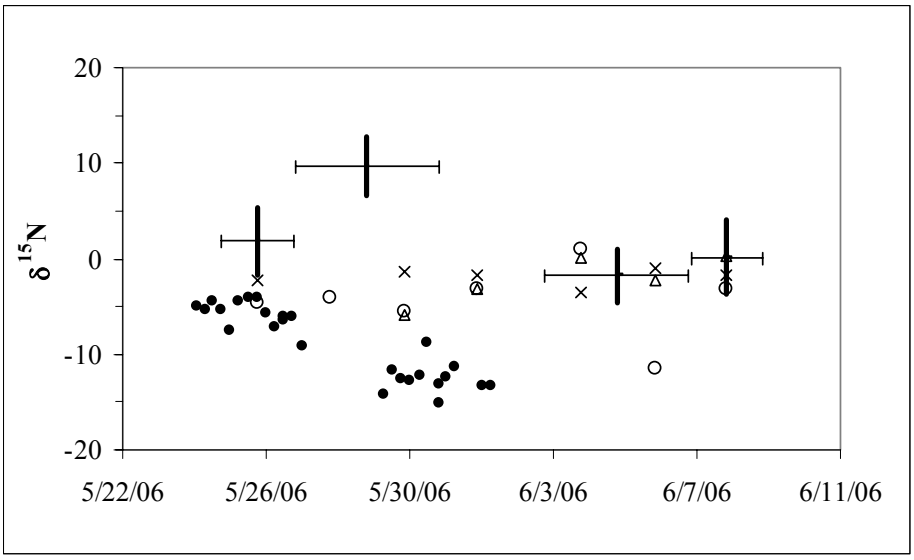

Figure 4.8. The $\delta^{15}N$ (‰ vs. N_2) of surface snow nitrate (solid circles), and gas-phase NO_2 (vertical bars) and HNO_3 (open circles, triangles, and x-marks) collected 1.5 meters above the snow surface at Summit. The horizontal error bars associated with NO_2 data bars represent the length of the sampling period. Gas-phase HNO_3 measurements are plotted at the mid-date of their 48-hour sampling period.

4.5. Conclusions

We present a novel method for the collection of atmospheric NO_2 in remote regions. Detailed laboratory tests carried out under a variety of conditions resulted in an ideal method for field collection of NO_2. First measurements of the $\delta^{15}N$ of atmospheric NO_2 at Summit, Greenland during May-June of 2006 indicate that the $\delta^{15}N$ of NO_2 ranges between +12.8‰ and -4.6‰ vs. N_2, which is similar to concurrent measurements of the $\delta^{15}N$ of gas-phase HNO_3 and surface snow nitrate at Summit. The similarity of these measurements to the $\delta^{15}N$ of gas-phase HNO_3 suggests that the nitrogen isotope fractionation associated with NO_2 oxidation to HNO_3 is small.

Such measurements of the $\delta^{15}N$ of NO_2 in polar regions are central to our understanding of the air-to-snow transfer of nitrogen oxides. Quantifying the $\delta^{15}N$ of NO_2 emitted from different sources and in different environments also has applications to other fields of study. For example, variations in the $\delta^{15}N$ of nitrate in precipitation has been attributed to changes in the source of NO_x to the atmosphere (e.g., Elliott et al., 2007; Heaton et al., 2004; Hastings et al., 2003; Yeatman et al., 2001; Russell et al., 1998). Our ability to interpret seasonal and regional variations in $\delta^{15}N$ of precipitation nitrate is hindered by the lack of specific data regarding the $\delta^{15}N$ of NO_x sources such as soil emissions and biomass burning. Measurements of $\delta^{15}N$ of NO_2 from these sources will aid the interpretation of seasonal trends in precipitation nitrate, and measurements of NO_2 in remote areas can additionally inform studies of source transport and chemistry. Knowledge of the $\delta^{15}N$ of NO_x sources is also fundamental to studies of ice core nitrate, which provide us with the opportunity to learn detailed information about past changes in emissions from these sources. This information is especially valuable because the concentration of NO_x in the atmosphere is increasing (e.g., Galloway et al., 2003).

Chapter 5

Changes in the $\delta^{15}N$ and $\delta^{18}O$ of Nitrate in Ice: A Comparison of Ice Core Records from Greenland and Antarctica

[Jarvis, J.C., M.G. Hastings, E.J. Steig, to be submitted to *Journal of Geophysical Research*]

5.1 Summary

We present measurements of the $\delta^{15}N$ and $\delta^{18}O$ of nitrate in ice cores from Summit, Greenland and South Pole, Antarctica. These cores contain nitrate that was deposited and preserved in very different environments. The $\delta^{15}N$ of nitrate in the Greenland core decreases from a pre-Industrial value of +10‰ vs. N_2 to a present-day value of -1‰. No trend is observed in the $\delta^{18}O$ of nitrate, which varies between 34‰ vs. VSMOW and 89‰. At South Pole, the $\delta^{15}N$ of nitrate exhibits a strong transition at the top of the core, increasing from 98‰ vs. N_2 at 20 meters depth to -4‰ at the surface. Similar to the Greenland core, the $\delta^{18}O$ of nitrate in South Pole ice shows no trend, and varies from 42‰ vs. VSMOW to 94‰. We compare these $\delta^{15}N$ and $\delta^{18}O$ records of nitrate from both regions and explore the influences of post-depositional change and Industrial NO_x emissions on the nitrate record. We find evidence for active post-depositional recycling and loss of nitrate at South Pole. At Summit, we find evidence that the $\delta^{18}O$ of ice nitrate is influenced by post-depositional recycling of nitrate, but that the $\delta^{15}N$ of nitrate is preserved. The trend in $\delta^{15}N$ of nitrate at Summit reflects changes in source emissions of atmospheric NO_x over the past 100 years.

5.2. Introduction

Ice core records of atmospheric species deposited in polar regions have provided valuable information as to how our atmosphere has changed through time. One interesting such record is that of nitrate, which preserves fluctuations in the deposition

of nitric acid (HNO_3) and particulate nitrate ($p\text{-}NO_3^-$), the dominant sinks of atmospheric nitrogen oxides such as NO and NO_2 ($NO + NO_2 = NO_x$). NO_x is emitted to the atmosphere from natural sources such as lightning, stratospheric injection, and biogenic soil emissions, and from anthropogenic sources such as fossil fuel combustion and biomass burning. In studies of Greenland ice, Neftel et al. (1985) and Mayewski et al. (1990; 1986) observed that nitrate concentrations preserved in ice began to sharply increase around the mid-20th century, which they attributed to increasing anthropogenic emissions of NO_x.

While these records provide confirmation of recent changes in atmospheric NO_x, the variability in the ice nitrate record remains difficult to interpret, as subsequent studies have shown that a quantitative interpretation of ice core nitrate is complicated by the reversible deposition of nitrate (e.g., Röthlisberger et al., 2002). Following deposition to snow surfaces, nitrate is released from the snowpack as NO_x and gas-phase HNO_3 through photolysis and volatilization (Grannas et al., 2007; Beine et al., 2002; Honrath et al., 2002; 2000; 1999; Röthlisberger et al., 2002; Jones et al., 2001; 2000). These nitrogen oxides are either transported away or undergo oxidization to HNO_3 and redeposition to the snow. The distinction between export versus redeposition of photolyzed or volatilized nitrate products is important, as the former translates to localized post-depositional *losses* of nitrate from snow, and the latter translates to local post-depositional *recycling* of nitrate in snow. *Loss* and *recycling* have different implications for the interpretation of the nitrate isotope and nitrate concentration record preserved in ice cores.

Several factors influence the deposition, post-depositional loss, and post-depositional recycling of nitrate at a given location. In studies of ice from Antarctica and Greenland, Röthlisberger et al. (2002; 2000) report a relationship between local temperature and nitrate concentration that can be partially attributed to the temperature dependence of depositional processes of nitrate (e.g., the uptake of HNO_3 on ice surfaces). Decreasing temperatures correspond to increasing concentrations of nitrate preserved in ice. At locations with very low accumulation rates (e.g., South Pole, Dome

C), a rapid decrease with depth in snowpit nitrate concentrations is observed, suggesting that the relationship between temperature and nitrate preservation is overwhelmed by the effects of nitrate photolysis and volatilization (e.g., Röthlisberger et al., 2002). Accumulation rate, which is closely tied to temperature, can influence the post-depositional loss and recycling of nitrate by constraining the time during which surface snow is exposed to sunlight and wind. Finally, the presence of other impurities can impact nitrate preservation in ice and snow. For example, nitrate concentrations in Antarctic ice are correlated with Ca^{2+}, which is associated with the deposition of dust (Röthlisberger et al., 2000; Legrand et al., 1999). This correlation likely arises because, by forming $Ca(NO_3)_2$ either before or after deposition to the snow surface, Ca^{2+} inhibits the post-depositional loss of nitrate from snow. Differences in the degree of post-depositional loss or recycling of nitrate at various ice core locations make it difficult to relate fluctuations in ice nitrate concentration to changes in atmospheric sources of NO_x. However, it is well known that atmospheric concentrations of NO_x have increased since the mid-20^{th} century (e.g., Galloway et al., 2003), and that the resulting enhanced nitrogen deposition is observed in Arctic ecosystems (e.g., Wolfe et al., 2006).

Isotopes offer the potential to improve our understanding of post-depositional influences on ice core nitrate and to quantitatively relate ice core nitrate records to NO_x emissions. In this study, we compare ice core records from locations where nitrate is deposited under very different conditions. We present measurements of the $\delta^{15}N$ and $\delta^{18}O$ of nitrate, which contain imprints of variations in the sources of NO_x to the atmosphere and in the chemistry of nitrate formation (Elliott et al., 2007; Hastings et al., 2003; Michalski et al., 2003; Yeatman et al., 2001; Freyer, 1991; Heaton, 1987). Using nitrate isotope records from Summit, Greenland, where the accumulation rate is 22 g cm^{-2} a^{-1} and the average temperature is -26ºC, and South Pole, Antarctica, where the accumulation rate is ~8 g cm^{-2} a^{-1} and the average temperature is -48ºC, we discuss the evidence for post-depositional change in these regions and we evaluate the records in the context of changes in NO_x source emissions over the past 100 years.

5.3. NO_x Chemistry at Summit, Greenland and South Pole, Antarctica

The deposition of nitrate at Summit, Greenland and South Pole, Antarctica occurs under very different conditions. This makes a comparison of ice cores from these locations useful, as we expect depositional and post-depositional processes to influence the isotopes of ice nitrate. At Summit, where the snow accumulation rate is 22 g cm^{-2} a^{-1} (Banta and McConnell, 2007), flux measurements of NO_x, HONO and HNO_3 point towards summertime emission of nitrogen oxides from surface snow (Honrath et al., 2002; 1999; Dibb et al., 1998). In studies of nitrate preservation in snow at Summit, Burkhart et al. (2004) and Dibb et al. (2007) report as much as 7-25% loss of nitrate over 1-2 years. Isotopic measurements of nitrate in the air and snow at Summit indicate that while summertime post-depositional recycling of nitrate does occur, it does not strongly influence the isotopes of nitrate preserved in snow over several seasons (e.g., Chapter 3; Hastings et al., 2004).

Snowpack emissions of nitrogen oxides also occur during summer months at South Pole, as indicated by gradients of HONO and HNO_3 above the snow surface (e.g., Dibb et al., 2004) and elevated atmospheric NO concentrations (e.g., Davis et al., 2001), although the concentration of NO_x in the air above the snow at South Pole is significantly higher than at Summit. During the summers of 1998 and 2000, Davis et al. (2004; 2001) observed NO concentrations between 10 and 600 pptv, nearly six times the concentrations of near-surface NO_x observed at Summit during the summers of 1999 and 2000 (Yang et al., 2002). The concentration of HONO at South Pole is also 3-4 times that at Summit (Chen et al., 2004). Furthermore, elevated OH and ozone concentrations at South Pole suggest that the atmosphere at South Pole is an extremely oxidative environment (Helmig et al., 2008; Wang et al., 2008; Mauldin et al., 2004; 2001; Crawford et al., 2001). The combination of high NO_x emissions and elevated oxidant concentrations results in rapid recycling of nitrogen oxides between the air and snow at South Pole. In fact, Davis et al. (2004) calculate that NO_x emissions from surface snow at South Pole are equal to one half of the annual nitrate deposition to snow. Recent work has also suggested that repeated recycling of near-surface nitric and

pernitric acid (HO_2NO_2, which has not yet been measured at Summit) may occur within a given season at South Pole (Davis et al., 2008; Slusher et al., 2002).

In contrast to snowpit profiles of nitrate concentration at Summit, which remain relatively constant with depth (e.g., Dibb et al., 2007; Burkhart et al., 2004; Hastings et al., 2004), snowpit profiles of nitrate concentration at South Pole exhibit a strong trend. Nitrate concentrations are elevated near the snow surface at South Pole, decreasing with rapidly with depth over the top few meters of snow (McCabe et al., 2007; Dibb et al., 2004; Dibb and Whitlow, 1996; Mayewski and Legrand, 1990).

5.4. Methods

A 100-meter ice core was drilled at Summit, Greenland (72º36'N, 38º30'W, 3200 meters above sea level) in May 2006 and transported to the University of Washington for analysis. The 295-meter South Pole Remote Earth Science and Seismological Observatory (SPRESSO) ice core was drilled near South Pole, Antarctica (89º55'S, 144º23'W, 2900 meters above sea level) in 2002 and was processed at the National Ice Core Laboratory before being transported to the University of Washington. All samples were kept frozen prior to analysis.

Both cores were divided into 1-meter samples that were analyzed for nitrate concentration using a Dionex ion chromatograph with an IonPac AS11-HC column (2x250mm) and a KOH eluent (20mM concentration; loop size and injection size = 100μL). The measurement error in nitrate concentration for the samples presented here is less than ± 0.1 μM (6 ppb). The Greenland core was further subsampled into 3 cm sections which were analyzed for the $\delta^{18}O$ of water in our lab at the University of Washington. The uncertainty in these $\delta^{18}O$-water measurements is less than ±0.1‰.

The $\delta^{15}N$ and $\delta^{18}O$ of nitrate were determined using the denitrifier method, in which denitrifying bacteria (*Pseudomonas aureofaciens* and *Pseudomonas chlororaphis*) convert nitrate to N_2O, which is isotopically analyzed using a continuous flow mass spectrometer (Casciotti et al., 2002; Sigman et al., 2001). Each sample was

calibrated using internationally recognized standards IAEA-NO-3 for $\delta^{15}N$ ($\delta^{15}N$ of +4.7‰, Böhlke and Coplen, 1995 and Gonfiantini et al., 1995) and IAEA-NO-3 ($\delta^{18}O$ of +25.6‰, Böhlke et al., 2003) and USGS35 ($\delta^{18}O$ of +57.5‰, Böhlke et al., 2003) for $\delta^{18}O$. Samples were corrected for blank contribution and oxygen exchange with water following procedures outlined in Kaiser et al. (2007), Hastings et al. (2004), and Casciotti et al. (2002).

Measurements of $\delta^{15}N$ from N_2O are influenced by $\delta^{17}O$, because the isotopomer $^{15}N^{15}N^{17}O$ contributes to the mass 45 signal. Typically, the relationship between $\delta^{17}O$ and $\delta^{18}O$ is mass-dependent and we can assume that $\delta^{17}O \approx 0.52*\delta^{18}O$ and correct $\delta^{15}N$ based on this relationship. However, atmospheric nitrate contains a mass-independent signal, quantified as $\Delta^{17}O$, where $\Delta^{17}O = \delta^{17}O - 0.52*\delta^{18}O \neq 0$ (e.g., Michalski et al., 2003). In this study, values of $\delta^{15}N$ are corrected for the mass-dependent relationship between $\delta^{17}O$ and $\delta^{18}O$. This leads to a possible discrepancy in $\delta^{15}N$ for samples analyzed with both bacteria strains. For samples analyzed using *P. aureofaciens*, very little exchange of oxygen atoms between nitrogen oxides and water is expected during denitrification, while significant exchange is expected for samples analyzed using *P. chlororaphis* (e.g., Casciotti et al., 2002). Thus the $\delta^{18}O$ of samples analyzed using *P. aureofaciens* will reflect the $\delta^{18}O$ (and $\delta^{17}O$) of original nitrate, while the $\delta^{18}O$ of samples analyzed using *P. chlororaphis* will more closely resemble the $\delta^{18}O$ of water. Because water has a mass-dependent relationship between $\delta^{17}O$ and $\delta^{18}O$, the mass-dependent correction to $\delta^{15}N$ will result in a more accurate $\delta^{15}N$ for samples measured with *P. chlororaphis* and an overprediction of the true $\delta^{15}N$ for samples measured with *P. aureofaciens*. This overprediction can be as great as 1-2‰ for atmospheric nitrate samples that have been corrected assuming the mass dependent relationship (Sigman et al., 2001), but is likely less than 1‰ for samples measured with *P. chlororaphis* (Hastings et al., 2004).

Isotopic measurements are reported throughout this text in the δ notation ($\delta_{sample} = (R_{sample}/R_{standard} - 1)*1000‰$, where $R = {}^{15}N/{}^{14}N$ or ${}^{18}O/{}^{16}O$) and are referenced to

atmospheric N_2 for $\delta^{15}N$ and to Vienna Standard Mean Ocean Water (VSMOW) for $\delta^{18}O$. The standard deviation in IAEA-NO-3 standards for a given batch determined the 1σ error for the samples in that batch. For $\delta^{15}N$, the average 2σ error is 5‰ for samples analyzed using *P. aureofaciens* and 1‰ for samples analyzed using *P. chlororaphis*, while for $\delta^{18}O$, the average 2σ error is 6‰. For samples analyzed two or more times, the isotopic value reported here is the average of the analyses ±1 standard error of the mean (standard error = (standard deviation of samples)*(number of samples)$^{-1/2}$).

5.5. Results

5.5.1. Summit, Greenland

Measurements of the $\delta^{15}N$ of nitrate, $\delta^{18}O$ of nitrate, and nitrate concentration throughout the Greenland core are shown in Figure 5.1. The depth-age scale was generated by counting seasonal cycles in the $\delta^{18}O$ of ice (e.g., Figure 5.1), which is known to vary with temperature (Grootes and Stuiver, 1997). Samples presented here represent approximately two years of deposition near the top of the core and three to four years near the bottom of the core. This depth-age relationship compares well with that of the nearby "Sandy" core drilled in 2004 (Banta and McConnell, 2007).

Nitrate concentration increases in the 100-meter core, from an average of 75 ppb prior to the year 1950 to an average of 134 ppb after 1950 (Figure 5.2). The observed increase in nitrate concentration beginning around 1900 and accelerating around 1950 agrees well with increases in nitrate concentration observed in other Greenland ice cores (e.g., Burkhart et al., 2006; Goto-Azuma and Koerner, 2001; Fischer et al., 1998; Freyer et al., 1996; Mayewski et al., 1990; 1986).

The $\delta^{15}N$ of nitrate measured in the Greenland core shows a decrease of 11‰ between pre-1950 ice, where $\delta^{15}N$ of nitrate is approximately equal to +10‰ vs. N_2, and the present day, where $\delta^{15}N$ of nitrate is approximately equal to -1‰. The $\delta^{18}O$ of nitrate shows no apparent trend throughout the core, ranging from +34 to +89‰ vs.

VSMOW. The standard deviation of the $\delta^{18}O$ of nitrate, based on averaging samples over 9- to 10-year periods, is 7.9‰.

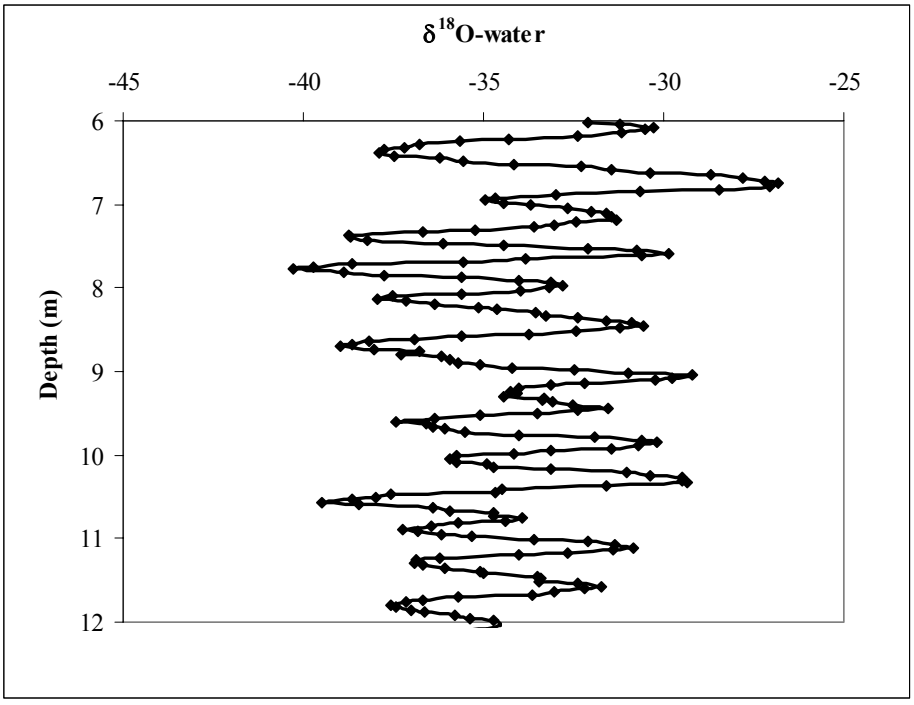

Figure 5.1. The $\delta^{18}O$ of water (‰ versus VSMOW) from a section of the Greenland ice core.

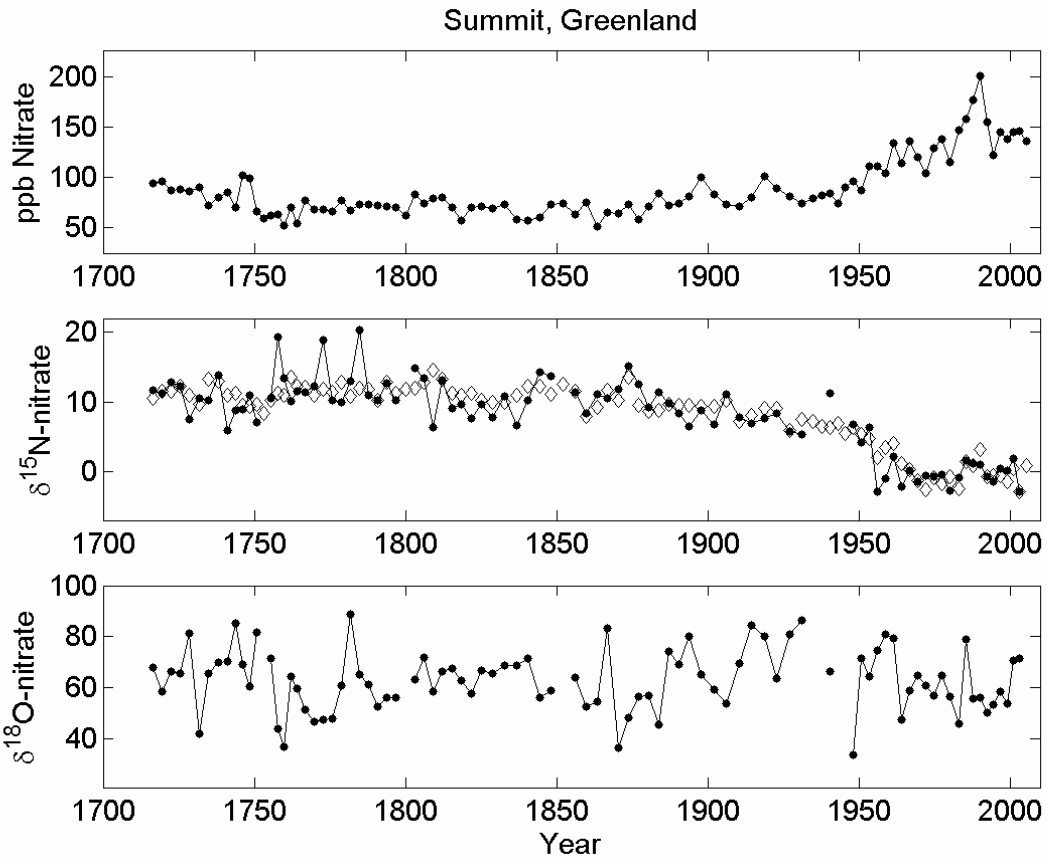

Figure 5.2. The (a) nitrate concentration (ppb), (b) $\delta^{15}N$ of nitrate (‰ versus N_2) and (c) $\delta^{18}O$ of nitrate (‰ versus VSMOW) in an 100-meter ice core drilled at Summit, Greenland in 2006. The age-depth relationship was generated using measurements of $\delta^{18}O$-water. For $\delta^{15}N$ of nitrate, measurements using both *Pseudomonas chlororaphis* (open diamonds; average 2σ error is 1‰) and *Pseudomonas aureofaciens* (closed circles; average 2σ error is 5‰) are shown. The average 2σ error for $\delta^{18}O$ of nitrate is 6‰.

5.5.2. South Pole, Antarctica

Measurements of nitrate concentration and the $\delta^{15}N$ and $\delta^{18}O$ of nitrate from the top 110 meters of the SPRESSO core are shown in Figure 5.3. For the top 10 meters of ice, the $\delta^{15}N$ and $\delta^{18}O$ of nitrate in 1-meter long samples were measured using both *Pseudomonas chlororaphis* and *Pseudomonas aureofaciens*. One-meter long samples were also analyzed for the $\delta^{15}N$ and $\delta^{18}O$ of nitrate for odd meters between 10 and 110 meters depth. The age-depth relationship for the SPRESSO core was determined stratigraphically (D. Meese, personal communication, 2008). Although this timescale is preliminary, it should be accurate to the decade and is therefore adequate for the analyses presented here. Samples presented here represent approximately 5 years of deposition near the top of the core and ~12 years near 100 m depth.

Nitrate concentration near the top of the SPRESSO core (440 ppb in the top two meters) is significantly larger than throughout the rest of the core (~100 ppb for all samples below 6 meters depth) (Figure 5.3). This large change in near-surface nitrate concentration is similar to previous observations of snowpack nitrate at South Pole (e.g., McCabe et al., 2007; Dibb et al., 2004; Dibb and Whitlow, 1996; Mayewski and Legrand, 1990).

The $\delta^{15}N$ of nitrate exhibits a strong trend over the top 20 meters of core, which represent the last ~120 years, increasing from -4‰ vs. N_2 at the surface to +98‰ at 20 m depth. The $\delta^{18}O$ of nitrate ranges from +42 to +94‰ vs. VSMOW. The standard deviation of the $\delta^{18}O$ of nitrate is 8.3‰, based on averaging samples over approximately 10-year periods.

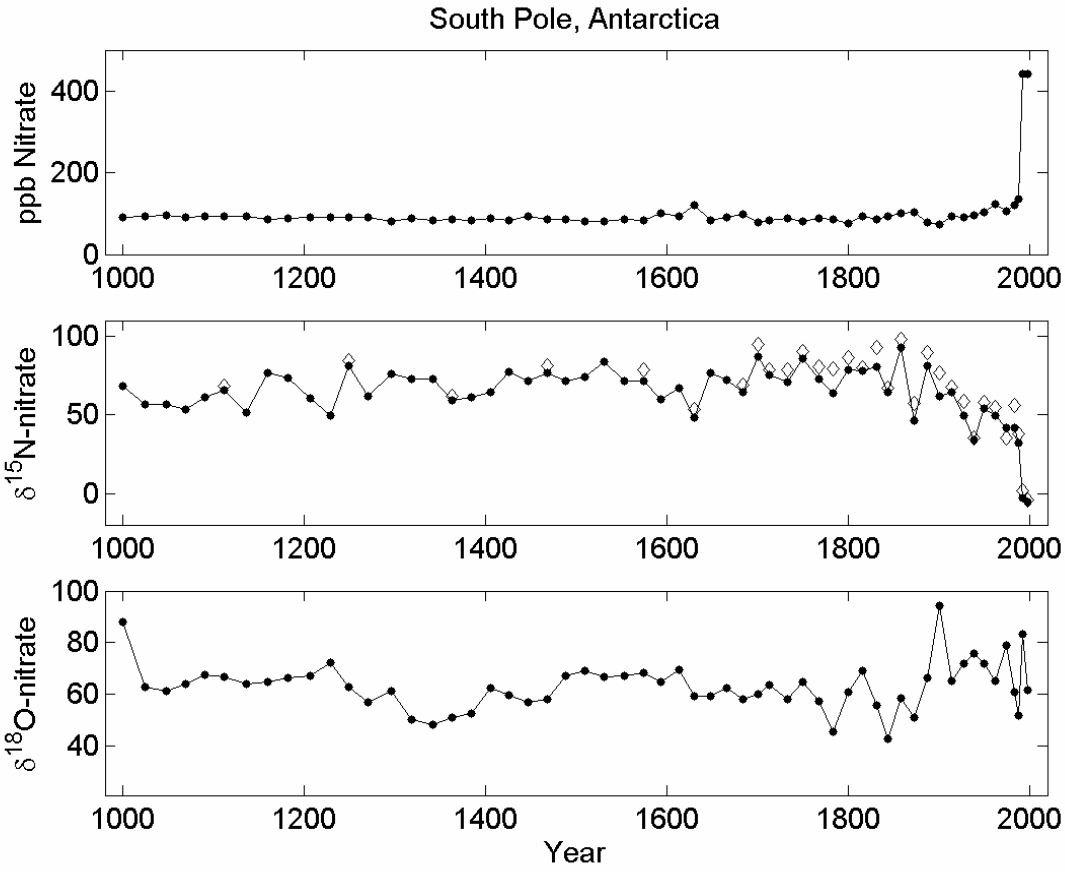

Figure 5.3. The (a) nitrate concentration (ppb), (b) $\delta^{15}N$ of nitrate (‰ versus N_2), and (c) $\delta^{18}O$ of nitrate (‰ versus VSMOW) in the top 110 meters of a 300-meter ice core drilled at South Pole, Antarctica in 2002. For $\delta^{15}N$ of nitrate, measurements using both *Pseudomonas chlororaphis* (open diamonds; average 2σ error is 1‰) and *Pseudomonas aureofaciens* (closed circles; average 2σ error is 5‰) are shown. The average 2σ error for $\delta^{18}O$ of nitrate is 6‰. The time scale shown was developed stratigraphically.

5.6. Discussion

5.6.1. Role of Post-depositional Processing at South Pole

The $\delta^{15}N$ of nitrate in ice from Summit and South Pole exhibit remarkably different ranges which can be attributed to differences in post-depositional processing at each ice core site and the preservation of NO_x source signals at Summit. At Dome C, Antarctica, where annual snow accumulation (2.7 g cm^{-2} a^{-1}, Röthlisberger et al., 2000) is much lower than at South Pole (~8 g cm^{-2} a^{-1}, Mosley-Thompson et al., 1999), Blunier et al. (2005) found significant changes in nitrate concentration and $\delta^{15}N$ of nitrate in the upper 15 cm of snow. Using a simple Rayleigh fractionation calculation, Blunier et al. determined the isotopic effect (ε) of post-depositional loss of nitrate to be -54‰ (ε is equal to the quantity (α-1)*1000‰, where α represents the effective isotope fractionation factor for loss).

A Rayleigh description of the process of post-depositional loss accounts for a change in size of the reservoir in question. For example, post-depositional losses may include both the loss of nitrate from surface snow (e.g., via nitrate photolysis or volatilization) and the rearrangement of nitrate within the snowpack and/or firn (e.g., via nitrate diffusion). These processes change the amount of nitrate in a given layer of snow. As nitrate is lost from the snow, the rate of change of the isotopic composition of remaining snow nitrate increases as the fraction of remaining nitrate decreases. This relationship is represented by

$$\frac{\delta^{15}N_f + 1000}{\delta^{15}N_0 + 1000} = f^{(\alpha-1)} \qquad (5.1)$$

where $\delta^{15}N_f$ represents the $\delta^{15}N$ of the fraction of remaining nitrate (*f*) and $\delta^{15}N_0$ represents the $\delta^{15}N$ of the initial snow nitrate prior to post-depositional loss. Although different loss processes may have different fractionation factors (α), using an effective "bulk" fractionation factor to describe the loss provides a useful first-order assessment

of the degree of influence of post-depositional losses on the final isotope signature of nitrate in snow.

Following Blunier et al. (2005), we apply a Rayleigh fit to our measurements of the $\delta^{15}N$ of nitrate in South Pole ice. Rearranging Equation 5.1 into a linear form and substituting $f = C_f/C_0$, where C_0 is the initial snow nitrate concentration prior to post-depositional loss and C_f is the concentration of remaining nitrate, we obtain

$$\ln(\delta^{15}N_f + 1000) = (\alpha\text{-}1)^* \ln(C_f) - (\alpha\text{-}1)^* \ln(C_0) + \ln(\delta^{15}N_0 + 1000). \quad (5.2)$$

We calculate α from the slope of a linear fit to a plot of $\delta^{15}N$ of nitrate ($\delta^{15}N_f$) versus nitrate concentration (C_f) measured in the South Pole ice core (Figure 5.4). This analysis does not require knowledge of the initial nitrate concentration (C_0) and isotopes ($\delta^{15}N_0$), but allows us to determine a rough estimate of the magnitude of α at South Pole. While the measurements of Blunier et al. (2005) focused on the top 15 cm of snow, we are limited by the 1 m sampling resolution of SPRESSO. We thus calculate the isotopic effect of post-depositional loss to two different depths. Considering the top 5 m and 20 m of ice, we calculate isotopic effects of -32‰ and -38‰, respectively. Although we expect post-depositional losses to occur primarily in the upper 0-10 m of ice, we calculate an isotopic effect to 20 m depth to allow for the inclusion of more data points and the possibility that some loss may occur at depths greater than 10 m under extreme conditions.

To evaluate how well these calculated isotopic effects explain the change in $\delta^{15}N$ of nitrate throughout the entire core, we recreate the $\delta^{15}N$ of nitrate in the South Pole core. Here, we solve Equation 5.1 for $\delta^{15}N_f$ at each measurement depth of the core, using a range of effective isotope fractionation factors (α). We take the measurements from the top meter of ice to be representative of the initial conditions ($\delta^{15}N_0$ and C_0), and we use the measured nitrate concentrations throughout the core to calculate the fraction of remaining nitrate, *f*, at each depth. Figure 5.5 clearly shows that an isotopic effect between -40‰ and -50‰ explains a majority of the observed variation in $\delta^{15}N$ throughout the core. Above ~20 m depth, an isotopic effect smaller than -40‰ is

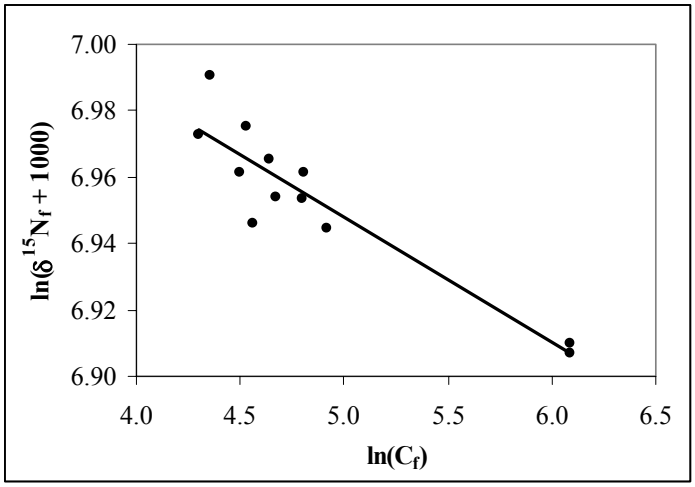

Figure 5.4. A linear fit to a plot of $\ln(\delta^{15}N_f + 1000)$ and $\ln(C_f)$ over the top 20 m of the South Pole ice core. Values of $\delta^{15}N_f$ and C_f represent our measurements of the $\delta^{15}N$ of nitrate (‰ versus N_2) and nitrate concentration (ppb), respectively. Following Equation 5.2, the effective isotope fractionation factor associated with post-depositional loss of nitrate at South Pole (α) is calculated from the slope of the linear fit.

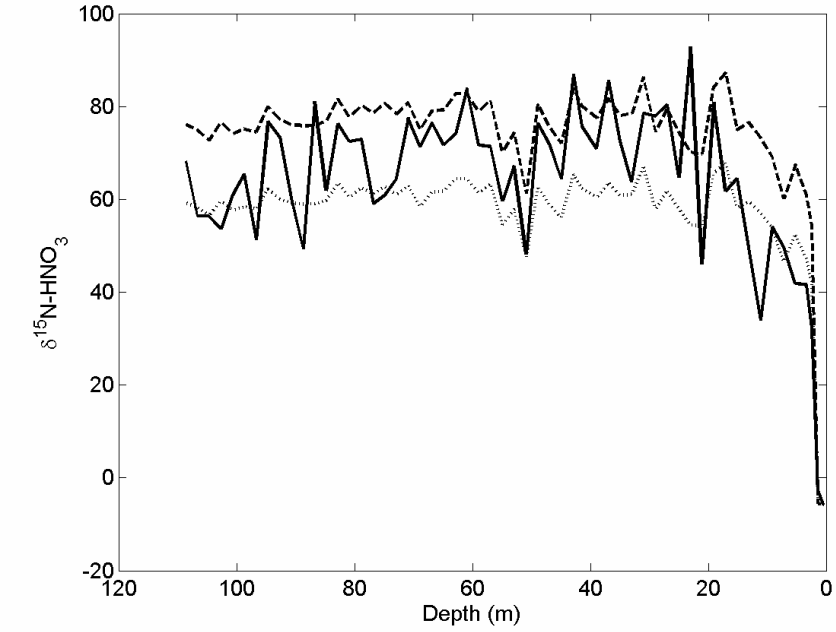

Figure 5.5. The measured $\delta^{15}N$ of nitrate (‰ versus N_2) in the SPRESSO ice core from South Pole, Antarctica (solid black line) versus depth. Dashed lines represent profiles of $\delta^{15}N$ of nitrate calculated from the measured concentration profile of nitrate, the measured value of $\delta^{15}N$ of nitrate in the top meter of the ice core, and a Rayleigh fractionation of -40‰ (gray dotted line) or -50‰ (black dashed line)

needed to better match the observed $\delta^{15}N$ of nitrate. This calculation assumes that present-day surface conditions at South Pole are representative of typical conditions. Since this may not be an accurate assumption, our calculation of α should be considered an estimate.

Because laboratory measurements indicate that the photolysis of nitrate enriches the $\delta^{15}N$ of remaining snow nitrate by 11.7‰ (Blunier et al., 2005), the large isotopic effect we observe in South Pole ice cannot solely be attributed to photolytic post-depositional loss. This is in agreement with the conclusions of Blunier et al. (2005) for Dome C snow and with Wolff et al. (2002), who found that only about 40% of near-surface nitrate loss from snow at low accumulation sites in Antarctica is due to nitrate photolysis. Therefore the large isotope effect we observe at South Pole is most likely due to a combination of nitrate photolysis in the upper tens of centimeters of snow, volatilization and loss of nitrate in the upper portion of firn, and volatilization and diffusion of nitrate throughout the firn. To our knowledge, any isotopic effects associated with nitrate volatilization and diffusion in ice have not yet been measured directly. The similarity between our -40‰ to -50‰ isotope effect and that observed by Blunier et al. (2005) at Dome C (-54‰) suggests that the ratio of photolytic loss to other loss processes (e.g., volatilization) is comparable at South Pole and Dome C. We also cannot rule out the possibility that some part of the large change in $\delta^{15}N$ at South Pole is a result of variations in the source of nitrate transported to South Pole, although we note that this may be unlikely given the distance to dominant NO_x sources (excluding the surrounding snowpack), the lifetime of NO_x against deposition, and the evidence for active post-depositional loss of nitrate from snow at South Pole (e.g., Davis et al., 2008; 2004).

While the near-surface trends in nitrate concentration and $\delta^{15}N$ of nitrate measured in the South Pole ice core are indicative of large post-depositional losses, the $\delta^{18}O$ of nitrate does not show a comparable change. This is possibly because the oxygen isotopic effect associated with post-depositional losses of nitrate is not as large as the nitrogen isotopic effect. From measurements of $\delta^{18}O$ of nitrate in the top 18 cm

of snow at South Pole, McCabe et al. (2007) observed a depletion in ^{18}O of 6.8‰ with depth, which is larger than their reported value for the depletion associated with nitrate photolysis alone (3.5‰). McCabe et al (2005) attribute the observed depletion in $\delta^{18}O$ of laboratory ice nitrate following photolysis to the recombination of photolyzed nitrate products with local oxidants. Considering the sharp near-surface trend in nitrate concentration in the South Pole core, and assuming a Rayleigh-like process, an oxygen isotopic fractionation of 6.8‰ or 3.5‰ would result in a decreasing trend in $\delta^{18}O$ of nitrate with depth, which we do not observe with 1 m sample resolution.

A second explanation for the lack of near-surface trend in $\delta^{18}O$ of nitrate is that a significant amount of nitrate lost from surface snow at South Pole through photolysis and volatilization is recycled back to the snow, incorporating the isotopic signature of local oxidants into the $\delta^{18}O$ of redeposited nitrate. In fact, taking into account the elevated concentrations of atmospheric oxidants at South Pole and the short lifetime of HNO_3 and HO_2NO_2, Davis et al. (2004) calculate that it takes less than one day for NO_x emitted from South Pole snow to be redeposited to the snowpack as nitrate. This vigorous recycling of nitrogen oxides in the air and snow would result in a close resemblance between the $\delta^{18}O$ of nitrate and the $\delta^{18}O$ of local oxidants. This implies that the $\delta^{18}O$ of nitrate in South Pole ice may record long-term variations in local oxidants, since the $\delta^{18}O$ of OH and HO_2 are expected to be very different from the $\delta^{18}O$ of tropospheric O_3 (Grootes and Stuiver, 1997; Johnston and Thiemens, 1997; Krankowsky et al., 1995). While variations in local oxidants have been shown to be preserved in the $\Delta^{17}O$ of nitrate at South Pole (McCabe et al., 2007; $\Delta^{17}O \approx \delta^{17}O - 0.52*\delta^{18}O$), we note that a similar analysis of oxidant change using the $\delta^{18}O$ of nitrate is complicated by the large sampling resolution of the SPRESSO measurements, as well as potential mass-dependent isotopic effects which would impact the preserved $\delta^{18}O$ while not affecting the $\Delta^{17}O$. Furthermore, calculating the influence of changes in local oxidants on the $\delta^{18}O$ of nitrate at South Pole may also require understanding the $\delta^{18}O$ of locally produced ozone, the concentration of which is closely related to changes in the

emission rate of NO_x from the snowpack (e.g., Jones and Wolff, 2003; Crawford et al., 2001).

We conclude that both post-depositional loss of nitrate and post-depositional recycling of nitrate occurs at South Pole. An isotopic effect between -40‰ and -50‰ describes the trend in $\delta^{15}N$ of nitrate in the South Pole core, which encompasses the effects of nitrate photolysis in the upper tens of centimeters of snow, volatilization and loss of nitrate in the upper portion of firn, and volatilization and diffusion of nitrate throughout the firn. Variations in the $\delta^{18}O$ of nitrate are related to active recycling of nitrate in South Pole snow, which incorporates the various isotopic signatures of local oxidants into the $\delta^{18}O$ of nitrate. The influence of post-depositional recycling on the $\delta^{18}O$ of nitrate indicates that any oxygen isotopic effect associated with post-depositional loss must not be as large as the nitrogen isotopic effect. Clearly, the combination of $\delta^{15}N$ and $\delta^{18}O$ nitrate records imply losses of nitrate from the upper snowpack at South Pole, followed by export away from South Pole (i.e., loss) or redeposition to the snow (i.e., recycling). Here we note that migration of nitrate within the snowpack, which may contribute to the sharp decrease in nitrate concentration with depth observed at South Pole, would have the same isotopic effect on remaining nitrate as a loss process.

5.6.2. Role of Post-depositional Processing at Summit

While it is clear that post-depositional recycling and loss of nitrate at South Pole strongly influences the nitrate isotopes preserved in ice, we do not expect to observe a similarly strong influence of post-depositional loss on nitrate isotopes in ice and snow at Summit. High snow accumulation rates limit the time during which nitrate is influenced by post-depositional processes. For example, photolytic production of NO_x from snow nitrate occurs in the upper few tens of centimeters of snowpack (Galbavy et al., 2007; Qiu et al., 2002; King and Simpson, 2001). Because the annual snow accumulation rate is much greater at Summit than at South Pole, nitrate deposited to the

snow at Summit is exposed to photolysis for less time and will therefore be influenced to a smaller degree than nitrate in South Pole snow.

At Summit, we cannot attribute the enrichment in $\delta^{15}N$ of nitrate with depth observed in the Greenland core to post-depositional loss of nitrate. There are two reasons for this. First, there is no obvious mechanism by which post-depositional loss of nitrate can occur to such great depths. The change in $\delta^{15}N$ of nitrate in the Greenland core occurs over a depth of 40 m, whereas post-depositional losses of nitrate due to photolysis and volatilization only occur in the top several centimeters to meters of snow. Other than diffusion of nitrate in ice, which occurs at a rate less than 1 cm per thousand years (Thibert and Dominé, 1998), we know of no other physical mechanism that could account for this loss.

Second, in Greenland ice, the onset of the rapid increase in nitrate concentration consistently occurs in ice deposited between 1940 and 1950, despite differences in the year during which each core was drilled (e.g., Burkhart et al., 2006; Goto-Azuma and Koerner, 2001; Fischer et al., 1998; Freyer et al., 1996; Mayewski et al., 1990; 1986). If the strong trend were due to the degree of post-depositional loss, the profile of change in nitrate concentration would be constant with depth, regardless of the year the ice core was sampled. Furthermore, Freyer et al. (1996) report a transition in the $\delta^{15}N$ of nitrate measured in an ice core drilled at Summit, Greenland in 1989, and although the resolution is lower than in our core, the essential results are the same. The $\delta^{15}N$ of nitrate in ice deposited prior to 1950 (+12 to +18‰, n ~ 5) is ~10-20‰ larger than the $\delta^{15}N$ of nitrate in ice deposited after 1950 (+5 to -5‰, n ~ 6-14). We therefore conclude that, while post-depositional processing of nitrate at Summit does occur (e.g., see Chapter 3), the observed change in $\delta^{15}N$ since ~1950 in the Greenland core is not a result of post-depositional loss of nitrate.

While we conclude that post-depositional loss is not important at Summit, the large interannual variability in $\delta^{18}O$ of nitrate in the Greenland core, which is comparable to the seasonal variation in $\delta^{18}O$ of snow nitrate measured in previous studies at Summit (see Chapter 3 and Hastings et al., 2004), does suggest post-

depositional recycling of nitrate. Furthermore, the variability in $\delta^{18}O$ of nitrate in the Greenland core is as great as in the South Pole core. It is possible that changes in atmospheric conditions enhance or deplete the recycling of nitrate in snow. For example, Honrath et al. (2002) attribute differences in the diurnal cycle of NO_x above the surface snow at Summit during 1999 and 2000 to enhanced vertical mixing in the atmosphere in 2000. A similar conclusion was reached for differences between NO_x measurements during fieldwork in 1998 and 2000 at South Pole: Davis et al. (2004) attribute changes in NO_x concentration to changes in the height of the planetary boundary layer and thus to changes in vertical mixing. These types of atmospheric changes can influence the variability in $\delta^{18}O$ of snow nitrate by altering the amount of nitrate recycling in snow. For example, reduced vertical mixing will lead to a buildup of NO_x above the snow surface, which influences local production of O_3 and HNO_3. Our work has suggested that photolytic recycling (i.e., 100% redeposition of photolyzed nitrate products) will not significantly alter the $\delta^{15}N$ of snow nitrate, but can alter the $\delta^{18}O$ of nitrate by as much as 7‰ given an initial $\delta^{18}O$ value of 81‰ for snow nitrate and 34‰ for recycled, recombined nitrate (see Chapter 3). Variations in the degree of recycling that occurs each year can therefore impact the seasonal or annual variability of the $\delta^{18}O$ of nitrate. Furthermore, variations in the concentration and isotope signatures of local oxidants within a given season may also influence the $\delta^{18}O$ of nitrate recycled back to the snowpack. For example, recent studies at Summit have detected high levels of BrO, which is involved in both the formation of HNO_3 and the destruction of O_3 (Huey et al., 2007; Morin et al., 2007), while the decrease in stratospheric O_3 at South Pole has been shown to influence surface O_3 levels and the photolytic production of NO_2 from snow nitrate (Jones and Wolff, 2003). Further measurements and detailed isotopic modeling of these processes may provide more insight into the range in $\delta^{18}O$ of nitrate observed in the Greenland and South Pole ice cores.

5.6.3. Influence of Changing NO_x Emissions on Nitrate in Greenland Ice

Since the enrichment with depth in $\delta^{15}N$ of nitrate in Greenland ice is not a result of post-depositional losses, we look to recent changes in NO_x source emissions. The relationship between an observed increase in nitrate concentration in Greenland ice and the recent increase in atmospheric NO_x has been noted and discussed in several previous studies (e.g., Burkhart et al., 2006; Goto-Azuma and Koerner, 2001; Fischer et al., 1998; Mayewski et al., 1990; 1986). Measurements of the $\delta^{15}N$ of ice nitrate allow for a more detailed analysis of the relationship between Greenland nitrate and atmospheric NO_x emissions. Several studies have shown that the $\delta^{15}N$ of nitrate is influenced by the $\delta^{15}N$ of precursor NO_x, which has both anthropogenic and natural emission sources (Elliott et al., 2007; Heaton et al., 2004; Hastings et al., 2003; Yeatman et al., 2001; Russell et al., 1998; Freyer, 1991; Heaton, 1987). Heaton (1990) measured the $\delta^{15}N$ of NO_x emitted from coal-fired boilers to be +6‰ to +9‰ (Figure 5.6). The $\delta^{15}N$ of NO_x from vehicle exhaust was found to be -13‰ to -2‰ (Heaton, 1990), although measurements of NO_x in a forest near a busy highway found $\delta^{15}N$ values between -2‰ and +9‰, with lower values for NO (Ammann et al., 1999). A subsequent study of tree ring $\delta^{15}N$ at the same highway location calculated that the $\delta^{15}N$ of NO_2 emissions from vehicles traversing the highway ranged from +1.3‰ to +6.4‰ (Saurer et al., 2004). Hoering (1957) measured the $\delta^{15}N$ of NO_x associated with electrical discharge, which is comparable to lightning, to be -0.5‰ to +1.4‰. The $\delta^{15}N$ of NO_x associated with biomass burning, stratospheric NO_x, and biogenic soil emissions have not yet been measured, although Savarino et al. (2007) calculate the $\delta^{15}N$ of stratospheric NO to be +19 ± 3‰.

To explore the link between nitrate concentrations and NO_x emissions, we compare our Greenland ice core record of nitrate with an historical record of NO_x emissions. We utilize the Edgar-Hyde 1.3 dataset (Van Aardenne et al., 2001), which is composed of source- and region-specific anthropogenic emission estimates for decadal time steps between 1890 and 1990. The increase in nitrate concentration we observe in

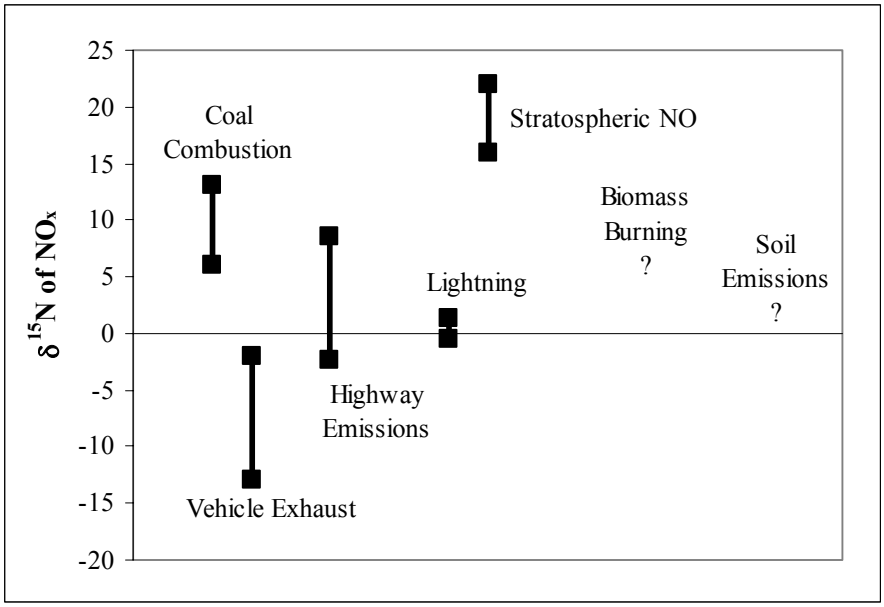

Figure 5.6. The $\delta^{15}N$ of NO_x sources (‰ versus N_2) (Savarino et al., 2007; Saurer et al., 2004; Ammann et al., 1999; Heaton, 1990; Hoering, 1957).

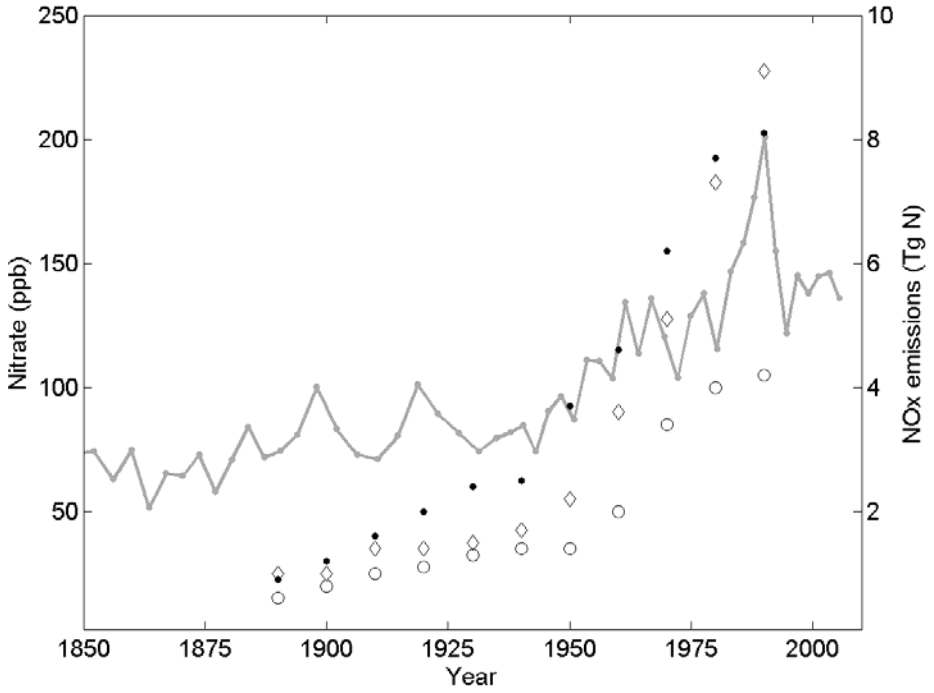

Figure 5.7. The concentration of nitrate (ppb) in an ice core from Summit, Greenland (gray line, vs. left axis) and estimates of global NO_x emissions from the Edgar-Hyde 1.3 dataset (Van Aardenne et al., 2001) (data points, vs. right axis). Regional emissions data include North America (USA and Canada; black circles), OECD Europe (open circles), and Asia (former USSR, China, Japan, and East Asia; open diamonds). Note that the emissions data and nitrate concentration data from the Greenland core are scaled the same.

the ice core from Summit, Greenland compares well with the recent increase in world-wide emissions of NO_x (Figure 5.7). In a study of six Greenland ice cores, Burkhart et al. (2006) find a strong correlation between NO_x emissions data and ice core nitrate concentrations. We find a similarly strong correlation ($r = 0.97$, $p < 0.05$) between nitrate concentration in our Greenland ice core and global NO_x emissions. The correlation between ice nitrate concentration and combined NO_x emissions from the USA, Canada, and OECD Europe is equally strong ($r = 0.96$, $p < 0.05$), which is to be expected given that air masses at Summit originate primarily from North America, with influences from Asian and European source regions (Kahl et al., 1997).

We compare decadal averages of the $\delta^{15}N$ of nitrate in the Greenland ice core with source-specific NO_x emissions estimates from the Edgar-Hyde 1.3 dataset (Figure 5.8). Fossil fuel combustion clearly accounts for the majority of the global increase in NO_x emissions since 1930, rapidly increasing between 1940 and 1980 while all other sources remain relatively unchanged. During this same period, the decadally-averaged $\delta^{15}N$ of nitrate decreases considerably, from +6.1‰ to -0.2‰. Taking the values of $\delta^{15}N$ of nitrate in Greenland ice to be representative of the $\delta^{15}N$ of atmospheric NO_x in 1940 and 1980 ($\delta^{15}N_{1940\_Nitrate}$ and $\delta^{15}N_{1980\_Nitrate}$), we use a simple mass balance to calculate the $\delta^{15}N$ of NO_x ($\delta^{15}N_{\Delta NOx}$) associated with the change in NO_x emissions between 1940 and 1980 (Δ_{NOx}),

$$\delta^{15}N_{1940\_Nitrate} * NO_{x\_1940} + \Delta_{NOx} * \delta^{15}N_{\Delta NOx} = \delta^{15}N_{1980\_Nitrate} * NO_{x\_1980}$$

where NO_{x_19XX} refers to global NO_x emissions in 1940 or 1980 (in Tg N).

We calculate a $\delta^{15}N$ of -3.8‰ accounts for the effects of the change in NO_x emissions on the $\delta^{15}N$ of Greenland nitrate. Since fossil fuel combustion accounts for 73% of the increase in global NO_x emissions between 1940 and 1980, this suggests that fossil fuel combustion NO_x has an overall negative $\delta^{15}N$ value. While the Edgar-Hyde 1.3 dataset does not quantify the source contributions to fossil fuel combustion (e.g., from vehicle emissions, coal combustion, etc.), available emissions estimates from the U.S. indicate that NO_x emissions in 1940 originated primarily from on-road vehicles

and industrial fuel combustion (U.S. Environmental Protection Agency, 2000). By 1970, on-road vehicles accounted for 47% of total U.S. NO_x emissions, far exceeding all other sources (EPA National Emissions Inventory (NEI) Air Pollutant Emissions Trends Data (1970-2006); http://epa.gov/ttn/chief/trends/). Given that the $\delta^{15}N$ of NO_x associated with vehicle exhaust is negative (Heaton, 1990), we conclude that the $\delta^{15}N$ of nitrate in Greenland ice is recording these changes in source emissions of NO_x.

Further evidence of the relationship between NO_x sources and the $\delta^{15}N$ of nitrate in Greenland ice is the trend spanning 1970-2000. Burkhart et al. (2006) observe a slight decrease since 1990 in nitrate concentration in Greenland ice cores, which they attribute to a decrease in U.S. NO_x emissions since the 1980s and in European NO_x emissions since 1990. The decrease in U.S. and European NO_x emissions continues between 1997 and 2005 (Stavrakou et al., 2008), although an increase in emissions from China is observed over the same period. From measurements of our Greenland core, we also observe a decrease in nitrate concentration since the early 1990s, as well as a slight increase and a leveling of $\delta^{15}N$ values (Figure 5.2). In Figure 5.9, source-specific NO_x emissions from the U.S. (from EPA NEI Air Pollutant Emissions Trends Data (1970-2006)) are plotted with the decadally-averaged $\delta^{15}N$ of nitrate from the Greenland core. The decrease in U.S. NO_x emissions since the 1980s is due primarily to on-road vehicle emissions (which have a negative $\delta^{15}N$ signature (Heaton, 1990)), while an increase is observed in emissions from electrical utilities fuel combustion (which includes coal combustion with a positive $\delta^{15}N$ signature (Heaton, 1990)). During the same period, the decadal average of $\delta^{15}N$ of nitrate in the Greenland core slightly increases, which further suggests that nitrate isotopes in the Greenland core are recording changes in NO_x sources. Further analysis of this trend requires better estimates of the $\delta^{15}N$ of sources, as well as higher resolution sampling of Greenland ice.

Finally, we note that the $\delta^{15}N$ of nitrate in the Greenland core is clearly positive prior to the mid-20th century increase in fossil fuel combustion emissions. Measurements from the base of the core (e.g., +8 to +13‰ during the early 1700s)

agree well with the average of pre-Industrial Holocene nitrate ($\delta^{15}N = +9.7‰$) measured in the GISP2 ice core (Hastings et al., 2005). This implies that natural sources of NO_x likely have positive $\delta^{15}N$ values.

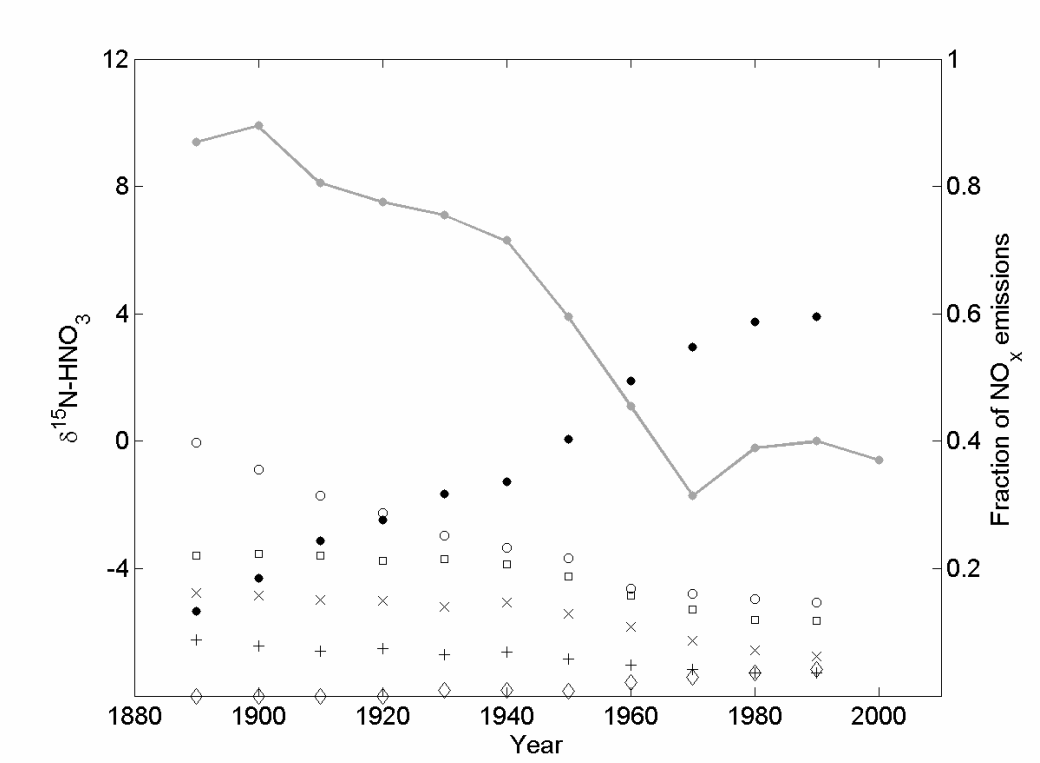

Figure 5.8. Decadal averages of the $\delta^{15}N$ of nitrate (‰ versus N_2) in Greenland ice from this study (gray line, vs. left axis) and the fraction of global NO_x emissions from Van Aardenne et al. (2001) (data points, vs. right axis). Emissions sources include fossil fuel combustion (black circles), agriculture (open circles), biomass burning (open squares), agricultural waste burning (x marks), biofuel consumption (+ marks), and industrial processes (open diamonds). Biomass burning emissions include savannah burning and deforestation. Decadal averages of $\delta^{15}N$ are plotted at the start of the 10-year periods they represent.

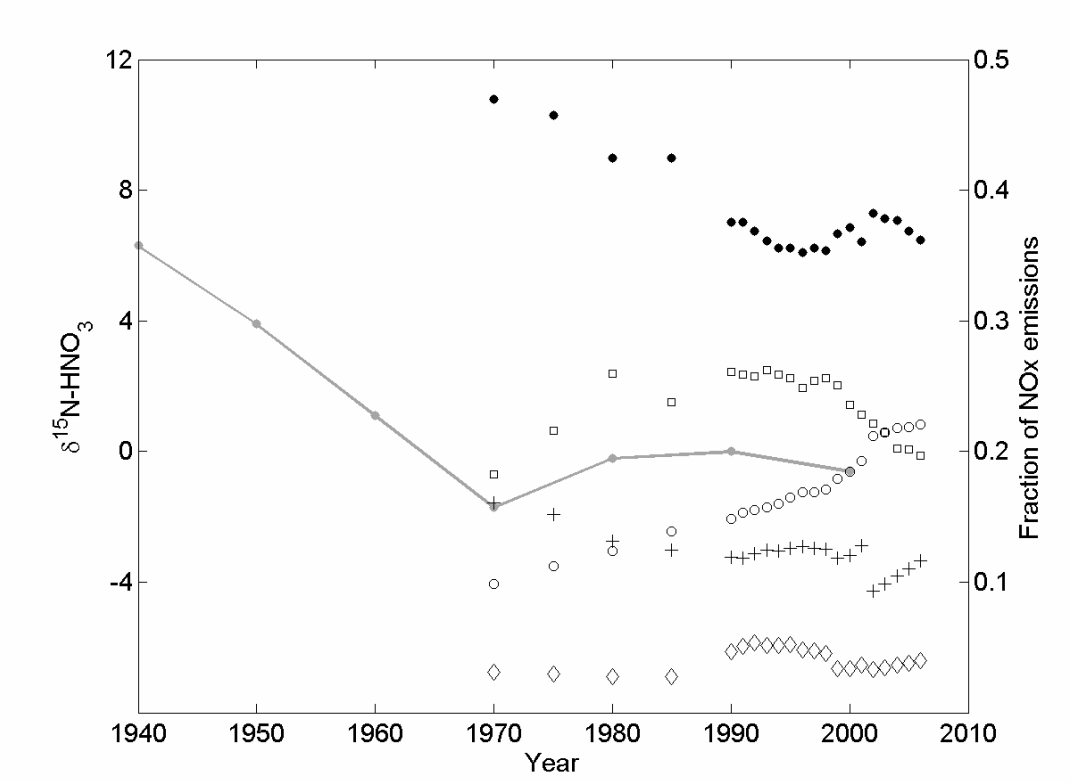

Figure 5.9. Decadal averages of the $\delta^{15}N$ of nitrate (‰ versus N_2) in Greenland ice from this study (gray line, vs. left axis) and the fraction of source-specific U.S. NO_x emissions from EPA NEI Air Pollutant Emissions Trends (data points, vs. right axis). Sources include on-road vehicles (black circles), off-road vehicles (open circles), fuel combustion – electrical utilities (open squares), fuel combustion – industrial (+ marks), and fuel combustion – other (open diamonds). Additional sources (e.g., metals processing, waste disposal and recycling, petroleum and related industries) together account for less than 7% of the total NO_x emissions for the years shown.

5.7. Conclusions

Measurements of the $\delta^{15}N$ and $\delta^{18}O$ of nitrate in ice cores from Summit, Greenland and South Pole, Antarctica show remarkably different ranges of values. These cores contain nitrate that was deposited and preserved in very different environments. We compare the $\delta^{15}N$ and $\delta^{18}O$ records of nitrate from both regions and explore the influences of post-depositional change and NO_x emissions on the nitrate record.

We attribute the large near-surface trend in $\delta^{15}N$ of nitrate in South Pole ice to post-depositional losses of nitrate. Assuming a Rayleigh fit, we calculate that an isotopic effect between -40‰ and -50‰ describes the trend in $\delta^{15}N$ of nitrate. This is comparable to the isotopic effect observed by Blunier et al. (2005) at Dome C, Antarctica (-54‰), and likely includes the influences of nitrate photolysis, volatilization, and/or diffusion in ice.

The $\delta^{18}O$ of nitrate in South Pole ice shows no distinct trend with depth, indicating that the oxygen isotopic effect associated with post-depositional loss is overwhelmed by the influence of local oxidants involved in nitrate recycling in the air and snow at South Pole. This implies that the oxygen isotopic effect associated with post-depositional loss of nitrate is smaller than the nitrogen isotopic effect. These records of the $\delta^{15}N$ and $\delta^{18}O$ of ice nitrate provide evidence for active nitrate recycling at South Pole, in agreement with previous observations (e.g., Dibb et al., 2004; Davis et al., 2004; 2001), and imply a loss of nitrate from the snowpack followed by export away from South Pole and/or redeposition of locally recombined HNO_3 to the snow.

Changes in the $\delta^{15}N$ of nitrate in the Greenland core also exhibit an enrichment in ^{15}N with depth, although to a lesser degree than at South Pole. We do not attribute this enrichment to post-depositional losses of nitrate since the trend occurs over a depth of 40 m and we know of no mechanism for post-depositional loss of nitrate that can occur to such a great depth. Furthermore, because the trends in $\delta^{15}N$ and nitrate concentration correspond temporally to similar trends observed in a core drilled nearly

two decades earlier at Summit (Freyer et al., 1996), we conclude that the $\delta^{15}N$ enrichment with depth is not a result of post-depositional loss.

We attribute the trend in $\delta^{15}N$ in Greenland nitrate to recent changes in source emissions of NO_x. A comparison of nitrate concentration in the Greenland core with historical NO_x emissions estimates exhibits a strong correlation, similar to observations in other Greenland ice cores (Burkhart et al., 2006). Comparing the Greenland record of $\delta^{15}N$ to historical NO_x emissions estimates from Van Aardenne et al. (2001) and to U.S. source-specific NO_x emissions, we conclude that the depletion in $\delta^{15}N$ of nitrate from 1940 to 1980 is related to the influence of vehicle emissions of NO_x. The trend in $\delta^{15}N$ of nitrate in Greenland ice deposited between 1980 and 2000 can be qualitatively explained by source changes in U.S. NO_x emissions from vehicles and fuel combustion, suggesting that the Greenland $\delta^{15}N$ record is preserving changes in source emissions of atmospheric NO_x. Finally, our measurements imply that the $\delta^{15}N$ signature of natural NO_x sources is positive.

Future work will further quantify the relationship between nitrate isotopes in polar ice and local post-depositional processing of nitrate versus changes in NO_x emissions. Detailed isotopic modeling of post-depositional recycling of nitrate will clarify the influence of recycling on the $\delta^{18}O$ of nitrate in Greenland. Quantification of any nitrogen isotopic effect associated with nitrate volatilization and diffusion are needed. In addition, measurements of the $\delta^{15}N$ of NO_x sources will further aid our understanding of the extent of influence of NO_x emissions on records of environmental change. Finally, higher resolution sampling of snow nitrate over the last 20-30 years may further elucidate the effects of the recent decrease in U.S. and European NO_x emissions on the $\delta^{15}N$ of nitrate in Greenland ice.

Chapter 6

Summary and Future Directions

6.1. Summary

This dissertation is comprised of four different studies which contribute towards the goal of understanding controls on nitrate isotopes preserved in polar ice.

In Chapter 2, a box model is used to explore the influence of local photochemistry on the $\delta^{15}N$ and $\delta^{18}O$ of atmospheric HNO_3 at Summit, Greenland. These model results identify the importance of known influences on HNO_3 isotopes and suggest additional processes that may also influence nitrate isotopes in Greenland. Previous measurements of the $\delta^{15}N$ and $\delta^{18}O$ of nitrate in snowpits at Summit exhibited a strong seasonal cycle, with enriched $\delta^{18}O$ and depleted $\delta^{15}N$ during the winter months, and depleted $\delta^{18}O$ and enriched $\delta^{15}N$ during the summer months (Hastings et al., 2004). Photochemical box modeling discussed in Chapter 2 suggests that seasonal changes in the local ratio of NO to NO_2, combined with the nitrogen isotope fractionation associated with NO-NO_2 cycling, explains less than one third of the observed seasonal cycle in $\delta^{15}N$ of snowpit nitrate. The seasonal range observed in $\delta^{15}N$ of snowpit nitrate must therefore be influenced by additional processes, such as seasonal changes in NO_x sources, a significantly larger NO-NO_2 isotopic fractionation than previously measured, or isotopic fractionations associated with NO_y cycling that have yet to be quantified.

The seasonal cycle in $\delta^{18}O$ of snowpit nitrate observed at Summit is smaller than predicted by seasonal changes in HNO_3 formation chemistry and the different isotopic compositions of OH and O_3. The discrepancy between modeled $\delta^{18}O$ of HNO_3 and observed $\delta^{18}O$ of snowpit nitrate may be related to seasonal variations in the $\delta^{18}O$ of NO_x or HNO_3 transported to Summit, post-depositional processing of nitrate in surface snow, or the influence of halogen chemistry on HNO_3 formation.

Chapter 3 explores the role of post-depositional processing of nitrate in snow at Summit, Greenland. Gas-phase HNO_3, surface snow nitrate, and snowpit nitrate collected between 2005 and 2007 were analyzed for the $\delta^{15}N$ and $\delta^{18}O$ of nitrate. A large difference between the $\delta^{18}O$ of snow nitrate and gas-phase HNO_3 (40‰) implies that mist chamber sampling of gas-phase HNO_3 near the snow surface collected recombined photolyzed nitrate products. This is an important result, as it implies that NO_x emitted from the snow surface through photolysis can quickly recombine with local oxidants to produce HNO_3 just above the snow surface. Local production of HNO_3 suggests that not all emitted nitrogen oxides are permanently lost from the snow.

Concurrent measurements of the $\delta^{15}N$ of snow nitrate and gas-phase HNO_3 are quite similar, which implies that the isotopic fractionation associated with photolytic loss of snow nitrate counteracts the isotopic fractionations associated with atmospheric NO-NO_2 cycling and HNO_3 recombination. Calculations using these measurements indicate that the maximum influence of summertime photolytic loss and recycling on the isotopes of nitrate in buried snow is +2.2‰ for $\delta^{15}N$ and -7‰ for $\delta^{18}O$ of nitrate. Additional measurements of surface snow labeled with nitrate enriched in ^{15}N confirm that significant recycling of nitrate occurs at Summit. Thus photolytic recycling and loss of nitrate in Summit snow has a small influence on the nitrate isotopes preserved in firn and ice.

Chapter 4 describes a technique to capture atmospheric NO_2 in remote regions for later isotopic analysis. Measurements of the $\delta^{15}N$ of NO_2 at Summit, Greenland, which are the first such measurements, show similarities between NO_2 and HNO_3. This similarity validates the assumption that the $\delta^{15}N$ of HNO_3 reflects the $\delta^{15}N$ of precursor NO_2, which was central to the box modeling work of Chapter 2. Furthermore, it implies that the nitrogen isotope fractionation associated with the oxidation of NO_2 to HNO_3, which has not yet been measured, must be small.

Chapter 5 describes ice core measurements of the $\delta^{15}N$ and $\delta^{18}O$ of nitrate from Summit, Greenland and South Pole, Antarctica, which clearly exhibit the importance of understanding post-depositional processing of nitrate and the way in which it differs

between locations. The nitrate isotope record from South Pole shows evidence of active post-depositional recycling and loss of nitrate. A large near-surface trend in the $\delta^{15}N$ of nitrate is observed and can be described with post-depositional losses that produce an isotopic effect between -40‰ and -50‰. This is comparable to the isotopic effect observed in the top 15 cm of snow at Dome C, Antarctica.

The $\delta^{18}O$ of nitrate in South Pole ice shows no distinct trend with depth, indicating that the oxygen isotopic effect associated with post-depositional loss is overwhelmed by the influence of local oxidants involved in nitrate recycling in the air and snow at South Pole. This implies that the oxygen isotopic effect associated with post-depositional loss of nitrate is smaller than the nitrogen isotopic effect. These records both indicate active nitrate recycling at South Pole, in agreement with the findings of prior studies, and imply a loss of nitrate from the snowpack followed by export away from South Pole and/or redeposition to the snow.

Changes in the $\delta^{15}N$ of nitrate in the Greenland core also exhibit an enrichment in ^{15}N with depth, which can be attributed to recent changes in source emissions of NO_x. A comparison of the Greenland $\delta^{15}N$ record to historical NO_x emissions estimates from the Edgar-Hyde 1.3 dataset shows that the $\delta^{15}N$ of NO_x emissions between 1940 and 1980, which are dominated by fossil fuel combustion, must be -3.8‰. The agreement between this value and estimates of the $\delta^{15}N$ of NO_x in vehicle exhaust suggests that the Greenland $\delta^{15}N$ record is preserving changes in source emissions of atmospheric NO_x. This also implies that the average $\delta^{15}N$ value of natural NO_x sources is positive.

6.2. Future Directions

These findings point to several possible avenues of future work. The initial modeling work in Chapter 2 highlights how little is known about isotopic fractionations associated with atmospheric cycling of nitrogen oxides. Quantification of the fractionations associated with HNO_3 formation, as well as isotopic measurements or

modeling of oxidants at Summit will help to refine models such as the one presented here. In addition, the role of halogens and PAN at Summit is not well understood; measurements of the isotopic composition of these compounds in the air and snow at Summit will help to determine their influence on nitrate isotopes in snow.

Detailed modeling of nitrate isotopes in the air and snow at Summit, including the effects of post-depositional processes, can enhance our understanding of seasonal and annual trends in snow nitrate. The seasonal comparison of nitrate isotopes in surface snow and snowpit samples presented in Chapter 3 brings up additional questions regarding the spatial variability of nitrate isotopes in snow at Summit and how this may relate to variability in post-depositional processing.

Clearly, post-depositional processing of nitrate in polar snow is an important process at Summit and at South Pole. However, there is much more to be learned about these processes and how they influence ice core records of nitrate. For example, what is the isotopic fractionation associated with nitrate volatilization and diffusion? How important are post-depositional losses of nitrate at other low accumulation sites in Antarctica? Can models of post-depositional recycling explain the variability in the $\delta^{18}O$ of nitrate in the Greenland and South Pole ice cores?

Finally, the connection between atmospheric NO_x sources and the $\delta^{15}N$ of nitrate in Greenland ice, discussed in Chapter 5, suggests that there is significant potential to learn more about our atmosphere from further studies of ice nitrate isotopes. Measurements of the $\delta^{15}N$ of NO_x sources by methods similar to that presented in Chapter 4 will enhance our understanding of the influence of NO_x emissions on the isotopes of nitrate in rain and snow. High resolution sampling of snow nitrate deposited over the last 20-30 years in Greenland may further elucidate the effects of the recent decrease in U.S. and European NO_x emissions on the $\delta^{15}N$ of nitrate in Greenland ice.

LIST OF REFERENCES

Alexander, B., J. Savarino, K.J. Kreutz, and M.H. Thiemens, (2004), Impact of preindustrial biomass burning emissions on the oxidation pathways of tropospheric sulfur and nitrogen, *Journal of Geophysical Research*, *109* (D08303), doi:10.1029/2003JD004218.

Ammann, M., R. Siegwolf, F. Pichlmayer, M. Suter, M. Saurer, and C. Brunold, (1999), Estimating the uptake of traffic-derived NO_2 from ^{15}N abundance in Norway spruce needles, *Oecologia*, *118*, 124-131.

Aoyama, T. and T. Yashiro, (1983), Analytical study of low-concentration gases. IV. Investigation of the reaction by trapping nitrogen dioxide in air using the triethanolamine method, *Journal of Chromatography*, *265*, 69-78.

Banta, J. R. and J. R. McConnell, (2007), Annual accumulation over recent centuries at four sites in central Greenland, *Journal of Geophysical Research*, *112*, D10114, doi:10110.11029/12006JD007887.

Begun, G.M. and C.E. Melton, (1956), Nitrogen isotopic fractionation between NO and NO_2 and mass discrimination in mass analysis of NO_2, *Journal of Chemical Physics*, *25*, 1292-1293.

Beine, H., D. Jaffe, J. Herring, J. Kelly, T. Krognes, and F. Stordal, (1997), High-latitude springtime photochemistry. Part I: NO_x, PAN and ozone relationships, *Journal of Atmospheric Chemistry*, *27*, 127-153.

Beine, H. J., R. E. Honrath, F. Domine, W. R. Simpson, and J. D. Fuentes, (2002), NO_x during background and ozone depletion periods at Alert: Fluxes above the snow surface, *Journal of Geophysical Research*, *107* (D21), doi:10.1029/2002JD002082.

Bergin, M. H., J.-L. Jaffrezo, C. I. Davidson, J. E. Dibb, S. N. Pandis, R. Hillamo, M. Maenhaut, H. D. Kuhns, and T. Makela, (1995), The contributions of snow, fog, and dry deposition to the summer flux of anions and cations at Summit, Greenland, *Journal of Geophysical Research*, *100* (D8), 16275-16288.

Bey, I., D.J. Jacob, R.M. Yantosca, J.A. Logan, B.D. Field, A.M. Fiore, Q. Li, H.Y. Liu, L.J. Mickley, and M.G. Schultz, (2001), Global modeling of tropospheric chemistry with assimilated meterology: Model description and evaluation, *Journal of Geophysical Research*, *106* (D19), 23,073-23,095.

Blunier, T., G. L. Floch, H.-W. Jacobi, and E. Quansah, (2005), Isotopic view on nitrate loss in Antarctic surface snow, *Geophysical Research Letters*, *32* (L13501), doi:10.1029/2005GL023011.

Böhlke, J. K. and T. B. Coplen, (1995), Interlaboratory comparison of reference materials for nitrogen-isotope-ratio measurements, in *Reference and intercomparison materials for stable isotopes of light elements, Tech. Doc. 825*, 51-66, International Atomic Energy Agency, Vienna.

Böhlke, J. K., S.J. Mroczkowski, and T. B. Coplen, (2003), Oxygen isotopes in nitrate: New reference materials for ^{18}O:^{17}O:^{16}O measurements and observations on nitrate-water equilibration, *Rapid Communications in Mass Spectrometry, 17*, 1835-1846.

Bottenheim, J.W., L.A. Barrie, and E. Atlas, (1993), The partitioning of nitrogen oxides in the lower Arctic troposphere during spring 1988, *Journal of Atmospheric Chemistry*, *17*, 15-27.

Boxe, C. S., A. J. Colussi, M. R. Hoffmann, I. M. Perez, J. G. Murphy, and R. C. Cohen, (2006), Kinetics of NO and NO_2 evolution from illuminated frozen nitrate solutions, *Journal of Physical Chemistry A*, *110*, 3578-3583.

Burkhart, J. F., M. Hutterli, R. C. Bales, and J. R. McConnell, (2004), Seasonal accumulation timing and preservation of nitrate in firn at Summit, Greenland, *Journal of Geophysical Research*, *109* (D19302), doi:19310.11029/12004JD004658.

Burkhart, J. F., R. C. Bales, J. R. McConnell, and M. A. Hutterli, (2006), Influence of North Atlantic Oscillation on anthropogenic transport recorded in northwest Greenland ice cores, *Journal of Geophysical Research*, *111* (D22309), doi:10.1029/2005JD006771.

Casciotti, K. L., D. M. Sigman, M. G. Hastings, J. K. Böhlke, and A. Hilkert, (2002), Measurement of the oxygen isotopic composition of nitrate in seawater and freshwater using the denitrifier method, *Analytical Chemistry*, *74*, 4905-4912.

Chen, G., D. Davis, J. Crawford, L. M. Hutterli, L. G. Huey, D. Slusher, L. Mauldin, F. Eisele, D. Tanner, J. Dibb, M. Buhr, J. McConnell, B. Lefer, R. Shetter, D. Blake, C. H. Song, K. Lombardi, and J. Arnoldy, (2004), A reassessment of HO_x South Pole chemistry based on observations recorded during ISCAT 2000, *Atmospheric Environment*, *38*, 5451-5461.

Cotter, E. S. N., A. E. Jones, E. W. Wolff, and S. J.-B. Bauguitte, (2003), What controls photochemical NO and NO_2 production from Antarctic snow? Laboratory investigation assessing the wavelength and temperature dependence, *Journal of Geophysical Research*, *108* (D4), doi:10.1029/2002JD002602.

Crawford, J.H., D.D. Davis, G. Chen, M. Buhr, S. Oltmans, R. Weller, L. Mauldin, F. Eisele, R. Shetter, B. Lefer, R. Arimoto, and A. Hogan, (2001), Evidence for photochemical production of ozone at the South Pole surface, *Geophysical Research Letters*, *28* (19), 3641-3644.

Davis, D., J. B. Nowak, G. Chen, M. Buhr, R. Arimoto, A. Hogan, F. Eisele, L. Mauldin, D. Tanner, R. Shetter, B. Lefer, and P. McMurry, (2001), Unexpected high levels of NO observed at South Pole, *Geophysical Research Letters*, *28* (19), 3625-3628.

Davis, D., G. Chen, M. Buhr, J. Crawford, D. Lenschow, B. Lefer, R. Shetter, F. Eisele, L. Maudlin, and A. Hogan, (2004), South Pole NO_x chemistry: an assessment of factors controlling variability and absolute levels, *Atmospheric Environment*, *38*, 5375-5388.

Davis, D. D., J. Seelig, G. Huey, J. Crawford, G. Chen, Y. Wang, M. Buhr, D. Helmig, W. Neff, D. Blake, R. Arimoto, and F. Eisele, (2008), A reassessment of Antarctic plateau reactive nitrogen based on ANTCI 2003 airborne and ground based measurements, *Atmospheric Environment*, *42*, 2831-2848.

Dibb, J. E., R. W. Talbot, and M. H. Bergin, (1994), Soluble acidic species in air and snow at Summit, Greenland, *Geophysical Research Letters*, *21*, 1627-1630.

Dibb, J. E. and S. I. Whitlow, (1996), Recent climate anomalies and their impact on snow chemistry at South Pole, 1987-1994, *Geophysical Research Letters*, *23* (10), 1115-1118.

Dibb, J. E., R. W. Talbot, J. W. Munger, D. J. Jacob, and S. M. Fan, (1998), Air-snow exchange of HNO_3 and NO_y at Summit, Greenland, *Journal of Geophysical Research*, *103* (D3), 3475-3486.

Dibb, J.E., M. Arsenault, M.C. Peterson, and R.E. Honrath, (2002), Fast nitrogen oxide photochemistry in Summit, Greenland snow, *Atmospheric Environment*, *36*, 2501-2511.

Dibb, J.E. and M. Fahnestock, (2004), Snow accumulation, surface height change, and firn densification at Summit, Greenland: Insights from 2 years of in situ observation, *Journal of Geophysical Research*, 109 (D24113), doi:10.1029/2003JD004300.

Dibb, J. E., L. G. Huey, D. L. Slusher, and D. J. Tanner, (2004), Soluble reactive nitrogen oxides at South Pole during ISCAT 2000, *Atmospheric Environment*, *38*, 5399-5409.

Dibb, J. E., S. I. Whitlow, and M. Arsenault, (2007), Seasonal variations in the soluble ion content of snow at Summit, Greenland: Constraints from three years of daily surface snow samples, *Atmospheric Environment*, *41*, 5007-5019.

Dominé, F. and P.B. Shepson, (2002), Air-snow interactions and atmospheric chemistry, *Science*, *297* (5586), 1506-1510.

Dubey, M.K., R. Mohrschladt, N.M. Donahue, and J.G. Anderson, (1997), Isotope specific kinetics of hydroxyl radical (OH) with water (H_2O): Testing models of reactivity and atmospheric fractionation, *Journal of Physical Chemistry A*, *101*, 1494-1500.

Dubowski, Y., A. J. Colussi, and M. R. Hoffmann, (2001), Nitrogen dioxide release in the 302 nm band photolysis of spray-frozen aqueous nitrate solutions. Atmospheric implications, *Journal of Physical Chemistry A*, *105*, 4928-4932.

Elliott, E.M., C. Kendall, S.D. Wankel, D.A. Burns, E.W. Boyer, K. Harlin, D.J. Bain, and T.J. Butler, (2007), Nitrogen isotopes as indicators of NO_x source contributions to atmospheric nitrate deposition across the midwestern and northeastern United States, *Environmental Science and Technology*, *41*, 7661-7667.

Fischer, H., D. Wagenbach, and J. Kipfstuhl, (1998), Sulfate and nitrate firn concentrations on the Greenland ice sheet 2. Temporal anthropogenic deposition changes, *Journal of Geophysical Research*, *103* (D17), 21,935-21,942.

Ford, K.M., B.M. Campbell, P.B. Shepson, S.B. Bertman, R.E. Honrath, M. Peterson, and J.E. Dibb, (2002), Studies of Peroxyacetyl nitrate (PAN) and its interaction with the snowpack at Summit, Greenland, *Journal of Geophysical Research*, *107* (D10), doi:10.1029/2001JD000547.

Freyer, H.D., (1991), Seasonal variation of $^{15}N/^{14}N$ in atmospheric nitrate species, *Tellus, Ser. B*, *43*, 34-44.

Freyer, H.D., D. Kley, A. Volz-Thomas, and K. Kobel, (1993), On the interaction of isotopic exchange processes with photochemical reactions in atmospheric oxides of nitrogen, *Journal of Geophysical Research*, *98*, 14,791-14,796.

Freyer, H. D., K.Kobel, R. J. Delmas, D. Kley, and M. R. Legrand, (1996), First results of $^{15}N/^{14}N$ ratios in nitrate from alpine and polar ice cores, *Tellus*, *48B*, 93-105.

Galbavy, E. S., C. Anastasio, B. Lefer, and S. Hall, (2007), Light penetration in the snowpack at Summit, Greenland: Part 2 Nitrate photolysis, *Atmospheric Environment*, *41*, 5091-5100.

Galloway, J. N., J. D. Abner, J. W. Erisman, S. P. Seitzinger, R. W. Howarth, E. B. Cowling, and B. J. Cosby, (2003), The Nitrogen Cascade, *Bioscience*, *53*, 341-356.

Gerboles, M., D. Buzica, and L. Amantini, (2005), Modification of the Palmes diffusion tube and semi-empirical modelling of the uptake rate for monitoring nitrogen dioxide, *Atmospheric Environment*, *39*, 2579-2592.

Glasius, M., M. F. Carlsen, T. S. Hansen, and C. Lohse, (1999), Measurements of nitrogen dioxide on Funen using diffusion tubes, *Atmospheric Environment*, *33*, 1177-1185.

Gold, A., (1977), Stoichoimetry of nitrogen dioxide determination in triethanolamine trapping solution, *Analytical Chemistry*, *49*, 1448-1450.

Gonfiantini, R., W. Stichler, and K. Rozanski, (1995), Standards and intercomparison materials distributed by the International Atomic Energy Agency for stable isotope measurements, *IAEA-TECDOC-825*, International Atomic Energy Agency, Vienna.

Goto-Azuma, K. and R. M. Koerner, (2001), Ice core studies of anthropogenic sulfate and nitrate trends in the Arctic, *Journal of Geophysical Research*, *106* (D5), 4959-4969.

Grannas, A. M., A. E. Jones, J. Dibb, M. Ammann, C. Anastasio, H. J. Beine, M. Bergin, J. Bottenheim, C. S. Boxe, G. Carver, G. Chen, J. H. Crawford, F. Dominé, M. M. Frey, M. I. Guzman, D. E. Heard, D. Helmig, M. R. Hoffmann, R. E. Honrath, L. G. Huey, M. Hutterli, H. W. Jacobi, P. Klan, B. Lefer, J. McConnell, J. Plane, S. Sander, J. Savarino, P. B. Shepson, W. R. Simpson, J. R. Sodeau, R. von Glasow, R. Weller, E. W. Wolff, and T. Zhu, (2007), An overview of snow photochemistry: evidence, mechanisms, and impacts, *Atmospheric Chemistry and Physics*, *7*, 4329-4373.

Grootes, P.M. and M. Stuiver, (1997), Oxygen 18/16 variability in Greenland snow and ice with 10^3 to 10^5 year time resolution, *Journal of Geophysical Research*, *102*, 26,455-26,470.

Hansen, T. S., M. Kruse, H. Nissen, M. Glasius, and C. Lohse, (2001), Measurements of nitrogen dioxide in Greenland using Palmes diffusion tubes, *Journal of Environmental Monitoring*, *3*, 139-145.

Hastings, M.G., D.M. Sigman, and F. Lipschultz, (2003), Isotopic evidence for source changes of nitrate in rain at Bermuda, *Journal of Geophysical Research*, *108* (D24), doi:10.1029/2003JD003789.

Hastings, M.G., E.J. Steig, and D.M. Sigman, (2004), Seasonal variations in N and O isotopes of nitrate in snow at Summit Greenland: Implications for the study of nitrate in snow and ice cores, *Journal of Geophysical Research*, *109* (D20306), doi:10.1029/2004JD004991.

Hastings, M. G., D. M. Sigman, and E. J. Steig, (2005), Glacial/interglacial changes in the isotopes of nitrate from the Greenland Ice Sheet Project (GISP2) ice core, *Global Biogeochemical Cycles*, *19* (GB4024), doi:4010.1029/2005GB002502.

Heaton, T.H.E., (1987), $^{15}N/^{14}N$ ratios of nitrate and ammonium in rain at Pretoria, South Africa, *Atmospheric Environment*, *21*, 843-852.

Heaton, T. H. E., (1990), $^{15}N/^{14}N$ ratios of NO_x from vehicle engines and coal-fired power stations, *Tellus*, *42B*, 304-307.

Heaton, T.H.E., P. Wynn, and A.M. Tye, (2004), Low $^{15}N/^{14}N$ ratios for nitrate in snow in the High Arctic (79N), *Atmospheric Environment*, *38*, 5611-5621.

Helmig, D., B. Johnson, S.J. Oltmans, W. Neff, F. Eisele, and D.D. Davis, (2008), Elevated ozone in the boundary layer at South Pole, *Atmospheric Environment*, *42*, 2788-2803.

Hoering, T., (1957), The isotopic composition of ammonia and nitrate ion in rain, *Geochimica Cosmochimica Acta*, *12*, 97-102.

Honrath, R. E., M. C. Peterson, S. Guo, J. E. Dibb, P. B. Shepson, and B. Campbell, (1999), Evidence of NO_x production within or upon ice particles in the Greenland snowpack, *Geophysical Research Letters*, *26*, 695-698.

Honrath, R. E., S.Guo, M. C. Peterson, M. P. Dziobak, J. E. Dibb and M. A. Arsenault, (2000), Photochemical production of gas phase NO_x from ice crystal NO_3^-, *Journal of Geophysical Research*, *105* (D19), 24183-24190.

Honrath, R.E., Y. Lu, M.C. Peterson, J.E. Dibb, M.A. Arsenault, N.J. Cullen, and K. Steffen, (2002), Vertical fluxes of NO_x, HONO, and HNO_3 above the snowpack at Summit, Greenland, *Atmospheric Environment*, *36*, 2629-2640.

Huey, L.G., J. Dibb, J. Stutz, S. Brooks, R. von Glasow, B. Lefer, G. Chen, S. Kim, and D. Tanner, (2007), Observations of Halogens at Summit, Greenland, *Eos Trans. AGU, 88* (52), Fall Meeting Supplement, Abstract A42B-05.

Jacobi, H.-W. and B. Hilker, (2007), A mechanism for the photochemical transformation of nitrate in snow, *Journal of Photochemistry and Photobiology A: Chemistry*, *185*, 371-382.

Johnston, J.C. and M.H. Thiemens, (1997), The isotopic composition of tropospheric ozone in three environments, *Journal of Geophysical Research*, *102* (D21), 25,395-25,404.

Jones, A. E., R. Weller, E. W. Wolff, and H.-W. Jacobi, (2000), Speciation and rate of photochemical NO and NO_2 production in Antarctic snow, *Geophysical Research Letters*, *27*, 345-348.

Jones, A. E., R. Weller, P. S. Anderson, H.-W. Jacobi, E. W. Wolff, O. Schrems, and H. Miller, (2001), Measurements of NOx emissions from the Antarctic snowpack, *Geophysical Research Letters*, *28*, 1499-1502.

Jones, A. E. and E. W. Wolff, (2003), An analysis of the oxidation potential of the South Pole boundary layer and the influence of stratospheric ozone depletion, *Journal of Geophysical Research*, *108* (D18), 4565, doi:4510.1029/2003JD003379.

Kahl, J. D. W., D. A. Martinez, H. Kuhns, C. I. Davidson, J.-L. Jaffrezo, and J. M. Harris, (1997), Air mass trajectories to Summit, Greenland: A 44-year climatology and some episodic events, *Journal of Geophysical Research*, *102* (C12), 26861-26875.

Kaiser, J., M. G. Hastings, B. Z. Houlton, T. Rockmann, and D. M. Sigman, (2007), Triple oxygen isotope analysis of nitrate using the denitrifier method and thermal decomposition of N_2O, *Analytical Chemistry*, *79*, 599-607.

King, M. D. and W. R. Simpson, (2001), Extinction of UV radiation in Arctic snow at Alert, Canada (82ºN), *Journal of Geophysical Research*, *106* (D12), 12499-12507.

Krankowsky, D., D. Bartecki, G.G. Klees, K. Mauersberger, K. Schellenbach, and J. Stehr, (1995), Measurement of heavy isotope enrichment in tropospheric ozone, *Geophysical Research Letters*, *22*, 1713-1716.

Krochmal, D. and A. Kalina, (1997), A method of nitrogen dioxide and sulphur dioxide determination in ambient air by use of passive samplers and ion chromatography, *Atmospheric Environment*, *31* (20), 3473-3479.

Kunasek, S.A., B. Alexander, M.G. Hastings, E.J. Steig, D.J. Gleason, and J.C. Jarvis, (in review, 2008), Measurements and modeling of $\Delta^{17}O$ of nitrate in snowpits from Summit, Greenland, *Journal of Geophysical Research.*

Legrand, M., E. Wolff, and D. Wagenbach, (1999), Antarctic aerosol and snowfall chemistry: implications for deep Antarctic ice-core chemistry, *Annals of Glaciology*, *29*, 66-72.

Levaggi, D. A., W. Siu, M. Feldstein, and E. L. Kothny, (1972), Quantitative separation of nitric oxide from nitrogen dioxide at atmospheric concentration ranges, *Environmental Sciences Technology*, *6*, 250-252.

Levaggi, D. A., W. Siu, and M. Feldstein, (1973), A new method for measuring average 24-hour nitrogen dioxide concentrations in the atmosphere, *Journal of the Air Pollution Control Association*, *23*, 30-33.

Levy, H., W.J. Moxim, A.A. Klonecki, and P.S. Kasibhatla, (1999), Simulated tropospheric NO_x: Its evaluation, global distribution and individual source contributions, *Journal of Geophysical Research*, *104*, 26,279-26,306.

Lyons, J. R., (2001), Transfer of mass-independent fractionation in ozone to other oxygen-containing radicals in the atmosphere, *Geophysical Research Letters*, *28*, 3231-3234.

Mauldin, R. L., F. L. Eisele, D. J. Tanner, E. Kosciuch, R. Shetter, B. Lefer, S. R. Hall, J. B. Nowak, M. Buhr, G. Chen, P. Wang, and D. Davis, (2001), Measurements of OH, H_2SO_4, and MSA at the South Pole during ISCAT, *Geophysical Research Letters*, *28* (19), 3629-3632.

Mauldin, R.L., E. Kosciuch, B. Henry, F.L. Eisele, R. Shetter, B. Lefer, G. Chen, D. Davis, G. Huey, and D. Tanner, (2004), Measurements of OH, $HO_2 + RO_2$, H_2SO_4, and MSA at the South Pole during ISCAT 2000, *Atmospheric Environment*, *38*, 5423-5437.

Mayewski, P. A., W. B. Lyons, M. J. Spencer, M. Twickler, W. Dansgaard, B. Koci, C. I. Davidson, and R. E. Honrath, (1986), Sulfate and nitrate concentrations from a South Greenland ice core, *Science*, *232*, 975-977.

Mayewski, P. A., W. B. Lyons, M. J. Spencer, M. S. Twickler, C. F. Buck, and S. Whitlow, (1990), An ice core record of atmospheric response to anthropogenic sulphate and nitrate, *Nature*, *346*, 554-556.

Mayewski, P. A. and M. R. Legrand, (1990), Recent increase in nitrate concentration of Antarctic snow, *Nature*, *346*, 258-260.

McCabe, J. R., C. S. Boxe, A. J. Colussi, M. R. Hoffmann, and M. H. Thiemens, (2005), Oxygen isotopic fractionation in the photochemistry of nitrate in water and ice, *Journal of Geophysical Research*, *110* (D15310), doi:10.1029/2004JD005484.

McCabe, J. R., M. H. Thiemens, and J. Savarino, (2007), A record of ozone variability in South Pole Antarctic snow: role of nitrate oxygen isotopes, *Journal of Geophysical Research*, *112* (D12303), doi:10.1029/2006JD007822.

Michalski, G., Z. Scott, M. Kabiling, and M.H. Thiemens, (2003), First measurements and modeling of $\Delta^{17}O$ in atmospheric nitrate, *Geophysical Research Letters*, *30* (16), doi:10.1029/2003GL017015.

Morin, S., J. Savarino, S. Bekki, S. Gong, and J.W. Bottenheim, (2007), Signature of Arctic surface ozone depletion events in the isotope anomaly ($\Delta^{17}O$) of atmospheric nitrate, *Atmospheric Chemistry and Physics*, *7*, 1451-1469.

Mosley-Thompson, E., J.F. Paskievitch, A.J. Gow, and L.G. Thompson, (1999), Late 20^{th} Century increase in South Pole snow accumulation, *Journal of Geophysical Research*, *104* (D4), 3877-3886.

Moxim, W.J., H. Levy, II, and P.S. Kasibhatla, (1996), Simulated global tropospheric PAN: Its transport and impact on NO_x, *Journal of Geophysical Research*, *101* (D7), 12,621-12,638.

Munger, J.W., D.J. Jacob, S.-M. Fan, A.S. Colman, and J.E. Dibb, (1999), Concentrations and snow-atmosphere fluxes of reactive nitrogen at Summit, Greenland, *Journal of Geophysical Research*, *104* (D11), 13,721-13,724.

Neftel, A., J. Beer, H. Oeschger, F. Zurcher, and R. C. Finkel, (1985), Sulphate and nitrate concentrations in snow from South Greenland 1895-1978, *Nature*, *314*, 611-613.

Nonomura, M., T. Hobo, E. Kobayashi, T. Murayama, and M. Satoda, (1996), Ion chromatographic determination of nitrogen monoxide and nitrogen dioxide after collection in absorption bottles, *Journal of Chromatography A*, *739*, 301-306.

Palmes, E. D., A. F. Gunnison, J. DiMattio, and C. Tomczyk, (1976), Personal sampler for nitrogen dioxide, *American Industrial Hygiene Association Journal*, *37*, 570-577.

Qiu, R., S. A. Green, R. E. Honrath, M. C. Peterson, Y. Lu, and M. Dziobak, (2002), Measurements of J_{NO3^-} in snow by nitrate-based actinometry, *Atmospheric Environment*, *36*, 2563-2571.

Röthlisberger, R., M. A. Hutterli, S. Sommer, E. W. Wolff, and R. Mulvaney, (2000), Factors controlling nitrate in ice cores: Evidence from the Dome C deep ice core, *Journal of Geophysical Research*, *105* (D16), 20565-20572.

Röthlisberger, R., M. A. Hutterli, E. W. Wolff, R. Mulvaney, H. Fischer, M. Bigler, K. Goto-Azuma, M. E. Hansson, U. Ruth, M.-L. Siggaard-Andersen, and J. P. Steffensen, (2002), Nitrate in Greenland and Antarctic ice cores: a detailed description of post-depositional processes, *Annals of Glaciology*, *35*, 209-216.

Russell, K.M., J.N. Galloway, S.A Macko, J.L. Moody, and J.R. Scudlark, (1998), Sources of nitrogen in wet deposition to the Chesapeake Bay region, *Atmospheric Environment*, *32*, 2453-2465.

Saurer, M., P. Cherubini, M. Ammann, B. D. Cinti, and R. Siegwolf, (2004), First detection of nitrogen from NO_x in tree rings: a $^{15}N/^{14}N$ study near a motorway, *Atmospheric Environment*, *38*, 2779-2787.

Savarino, J., J. Kaiser, S. Morin, D. M. Sigman, and M. H. Thiemens, (2007), Nitrogen and oxygen isotopic constraints on the origin of atmospheric nitrate in coastal Antarctica, *Atmospheric Chemistry and Physics*, *7*, 1925-1945.

Savarino, J., S.K. Bhattacharya, S. Morin, M. Baroni, and J.-F. Doussin, (2008), The $NO+O_3$ reaction: A triple oxygen isotope perspective on the reaction dynamics and atmospheric implications for the transfer of the ozone isotope anomaly, *Journal of Chemical Physics*, *128*, 194303.

Sigman, D. M., K. L. Casciotti, M. Andreani, C. Barford, M. Galanter, and J. K. Böhlke, (2001), A bacterial method for the nitrogen isotopic analysis of nitrate in seawater and freshwater, *Analytical Chemistry*, *73*, 4145-4153.

Sjostedt, S.J., L.G. Huey, D.J. Tanner, J. Peischl, G. Chen, J.E. Dibb, B. Lefer, M.A. Hutterli, A.J. Beyersdorf, N.J. Blake, D.R. Blake, D. Sueper, T. Ryerson, J. Burkhart, and A. Stohl (2007), Observations of hydroxyl and the sum of peroxy radicals at Summit, Greenland during summer 2003, *Atmospheric Environment*, *41*, 5122-5137.

Slusher, D. L., L. G. Huey, D. J. Tanner, G. Chen, D. D. Davis, M. Buhr, J. B. Nowak, F. L. Eisele, E. Kosciuch, R. L. Mauldin, B. L. Lefer, R. E. Shetter, and J. E. Dibb, (2002), Measurements of pernitric acid at the South Pole during ISCAT 2000, *Geophysical Research Letters*, *29* (21), 2011, doi:2010.1029/2002GL015703.

Stavrakou, T., J.-F. Müller, K. F. Boersma, I. D. Smedt, and R. J. van der A, (2008), Assessing the distribution and growth rates of NO_x emission sources by inverting a 10-year record of NO_2 satellite columns, *Geophysical Research Letters*, *35* (L10801), doi:10.1029/2008GL033521.

Thibert, E. and F. Dominé, (1998), Thermodynamics and kinetics of the solid solution of HNO3 in ice, *Journal of Physical Chemistry B*, *102*, 4432-4439.

U.S. Environmental Protection Agency, (2000), National Air Pollutant Emission Trends, 1900-1988, *Report EPA-454/R-00-002*, Office of Air Quality Planning and Standards, Research Triangle Park, N.C.

Van Aardenne, J. A., F. J. Dentener, J. G. J. Olivier, C. G. M. K. Goldewijk, and J. Lelieveld, (2001), A 1ºx1º resolution data set of historical anthropogenic trace gas emissions for the period 1890-1990, *Global Biogeochemical Cycles*, *15*, 909-928.

Wang, Y., J.A. Logan, and D.J. Jacob, (1998), Global simulation of tropospheric O3-NOx-hydrocarbon chemistry 2. Model evaluation and global ozone budget, *Journal of Geophysical Research*, *103* (D9), 10,727-10,755.

Wang, Y., Y. Choi, T. Zeng, D. Davis, M. Buhr, L. G. Huey, and W. Neff, (2008), Assessing the photochemical impact of snow NO_x emissions over Antarctica during ANTCI 2003, *Atmospheric Environment*, *42*, 2849-2863.

Willey, M. A., J. C. S. McCammon, and L. J. Doemeny, (1977), A solid sorbent personal sampling method for the simultaneous collection of nitrogen dioxide and nitric oxide in air, *American Industrial Hygiene Association Journal*, *38*, 358-363.

Wolfe, A. P., C. A. Cooke, and W. O. Hobbs, (2006), Are current rates of atmospheric nitrogen deposition influencing lakes in the Eastern Canadian Arctic?, *Arctic, Antarctic, and Alpine Research*, *38*, 465-476.

Wolff, E. W., A. E. Jones, T. J. Martin, and T. C. Grenfell, (2002), Modelling photochemical NO_x production and nitrate loss in the upper snowpack of Antarctica, *Geophysical Research Letters*, *29* (20), doi:10.1029/2002GL015823.

Yang, J., R.E. Honrath, M.C. Peterson, J.E. Dibb, A.L. Sumner, P.B. Shepson, M. Frey, H.-W. Jacobi, A. Swanson, and N. Blake, (2002), Impacts of snowpack emissions on deduced levels of OH and peroxy radicals at Summit, Greenland, *Atmospheric Environment*, *36*, 2523-2534.

Yeatman, S.G., L.J. Spokes, P.F. Dennis, and T.D. Jickells, (2001), Comparisons of aerosol nitrogen isotopic composition at two polluted coastal sites, *Atmospheric Environment*, *35*, 1307-1320.

Zhou, X., H.J. Beine, R.E. Honrath, J.D. Fuentas, W. Simpson, P.B. Shepson, and J.W. Bottenheim, (2001), Snowpack photochemical production of HONO: A major source of OH in the Arctic boundary layer in springtime, *Geophysical Research Letters*, *28* (21), 4087-4090.

Appendix A

Additional Snowpit Measurements - West Antarctica

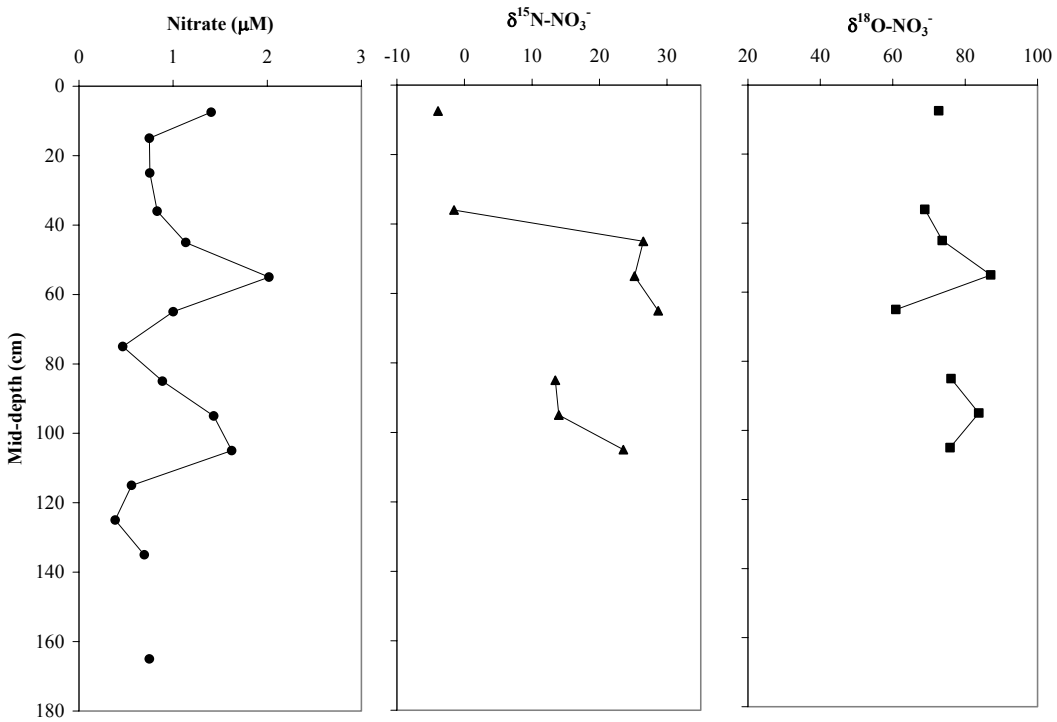

Figure A.1. Nitrate concentration (μM), $\delta^{15}N$ of nitrate (‰ vs. N_2), and $\delta^{18}O$ of nitrate (‰ vs. VSMOW) from a snowpit sampled at Site F of the 2000-2001 ITASE Traverse (124.00ºW, 77.41ºS; 1833 m elevation).

Table A.1. Data corresponding to Figure A.1.: nitrate concentration (μM), $\delta^{15}N$ of nitrate (‰ vs. N_2), and $\delta^{18}O$ of nitrate (‰ vs. VSMOW) from a snowpit sampled at Site F of the 2000-2001 ITASE Traverse.

Mid-depth (cm)	Depth range (cm)	Nitrate (μM)	$\delta^{15}N$ of NO_3^- (‰ vs. N_2)	$\delta^{18}O$ of NO_3^- (‰ vs. VSMOW)
1.5	0-3	-	-	-
7.5	5-10.5	1.41	-3.9	72.7
15	10.5-20	0.75	-	-
25	20-31	0.75	-	-
36	31-41	0.83	-1.5	68.9
45	41-50	1.13	26.5	73.7
55	50-60	2.02	25.2	87.1
65	60-70	1.00	28.7	60.9
75	70-80	0.47	-	-
85	80-91	0.89	13.5	76.1
95	91-100	1.43	14.0	83.8
105	100-110	1.62	23.5	75.9
115	110-120	0.46	-	-
125	120-130	0.39	-	-
135	130-140	0.69	-	-
145	140-150	-	-	-
155	150-160	-	-	-
165	160-170	0.75	-	-

Table A.2. Nitrate concentration (μM), $\delta^{15}N$ of nitrate (‰ vs. N_2), and $\delta^{18}O$ of nitrate (‰ vs. VSMOW) from a snowpit sampled at Site E of the 2000-2001 ITASE Traverse (120.05ºW, 78.05ºS; 1690 m elevation).

Mid-depth (cm)	Depth range (cm)	Nitrate (μM)	$\delta^{15}N$ of NO_3^- (‰ vs. N_2)	$\delta^{18}O$ of NO_3^- (‰ vs. VSMOW)
1.5	0-3	1.10	-2.3	72.3
5	0-10	0.76		
15	10-20	0.73		
25	20-30	0.43		
35	30-40	0.46		
45	40-50	0.55		
55	50-60	0.56		
65	60-70	0.85		
75	70-80	1.05	16.6	75.8
85	80-90	0.86		
95	90-100	0.98		
105	100-110	0.89		
120	115-125	0.47		
130	125-135	0.36		
140	135-145	1.86		
150	145-155	0.80		
160	155-165	0.58		
170	165-175	0.53		
180	175-185	0.45		

Appendix B

Ice Core Measurements - Byrd Station, Antarctica

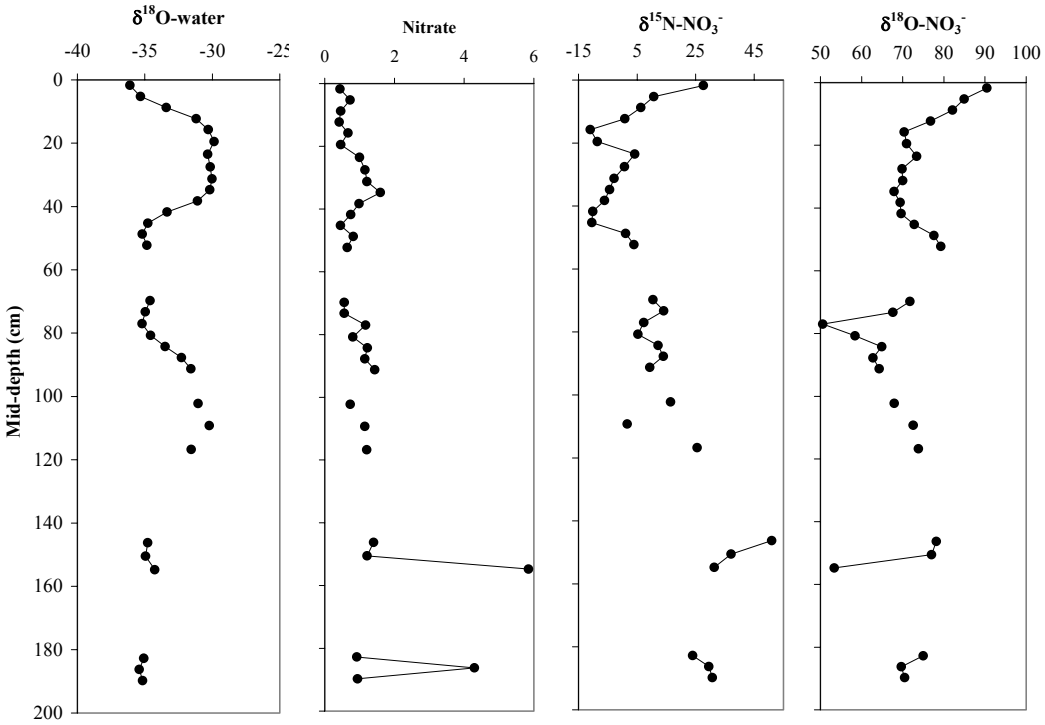

Figure B.1. The $\delta^{18}O$ of water (‰ vs. VSMOW), nitrate concentration (μM), $\delta^{15}N$ of nitrate (‰ vs. N_2), and $\delta^{18}O$ of nitrate (‰ vs. VSMOW) from the top 2 m of a 20 m ice core drilled at Byrd Station, Antarctica. The nitrate isotope measurements are corrected using the Princeton spreadsheet correction scheme.

Table B.1. Data corresponding to Figure B.1.: the $\delta^{18}O$ of water (‰ vs. VSMOW), nitrate concentration (μM), $\delta^{15}N$ of nitrate (‰ vs. N_2), and $\delta^{18}O$ of nitrate (‰ vs. VSMOW) from a 20 m ice core drilled at Byrd Station, Antarctica. The nitrate isotope measurements are corrected using the Princeton spreadsheet correction scheme.

Mid-Depth (cm)	$\delta^{18}O$-water (‰ vs. VSMOW)	Nitrate (μM)	$\delta^{15}N$ of NO_3^- (‰ vs. N_2)	$\delta^{18}O$ of NO_3^- (‰ vs. VSMOW)
1.75	-36.11	0.44	27.67	90.46
5.25	-35.33	0.73	10.69	84.95
8.75	-33.41	0.46	6.30	82.10
12.25	-31.20	0.41	0.80	76.80
15.75	-30.31	0.67	-10.98	70.37
19.5	-29.87	0.46	-8.57	70.95
23.5	-30.34	1.00	4.20	73.42
27.5	-30.16	1.15	0.65	69.85
31.25	-30.02	1.21	-2.83	70.01
34.75	-30.18	1.60	-4.41	67.90
38.25	-31.10	0.99	-6.13	69.40
41.75	-33.35	0.75	-10.13	69.62
45.25	-34.78	0.46	-10.48	72.79
48.75	-35.19	0.82	1.07	77.59
52.25	-34.85	0.65	3.98	79.24
69.75	-34.62	0.56	10.43	71.77
73.25	-34.97	0.56	14.10	67.62
77.00	-35.21	1.17	7.26	50.56
80.75	-34.58	0.81	5.25	58.41
84.25	-33.49	1.22	12.14	64.92
87.75	-32.28	1.15	13.97	62.77
91.25	-31.59	1.43	9.32	64.31
102.25	-31.05	0.73	16.44	67.97
109.25	-30.22	1.15	1.65	72.57
116.75	-31.56	1.21	25.48	73.81
146.25	-34.79	1.40	51.02	78.14
150.5	-34.95	1.22	37.15	77.04
154.75	-34.26	5.85	31.39	53.38
182.75	-35.08	0.92	23.98	74.99
186.25	-35.41	4.30	29.51	69.64
189.75	-35.17	0.94	30.68	70.47

VITA

Julia C. Jarvis is originally from Bloomington, Illinois. In 2001, she completed a Bachelor of Arts in Chemistry at Carleton College in Northfield, Minnesota, where she was involved in aerosol chemistry research. After Carleton, Julia moved to New Mexico and spent a year working at Los Alamos National Laboratory. Her research there focused on the electrochemical properties of anhydrous ionic liquids (fused salts). Julia arrived in Seattle in 2002 to begin her Ph.D. work at the University of Washington. As part of her dissertation research, she spent two field seasons at the Summit research station on top of the Greenland ice sheet. In addition to her scientific and academic pursuits, Julia enjoyed her years in Seattle where she was able to take advantage of the numerous outdoor recreational activities as well as other activities unique to the Pacific Northwest, including hand building a traditional Aleutian skin-on-frame kayak. In 2008, Julia completed her Ph.D. from the Department of Earth and Space Sciences at the University of Washington.